18th International Workshop on Inelastic Ion-Surface Collisions (IISC-18)

Gatlinburg, Tennessee USA
September 26 – October 1, 2010

Book of Abstracts

Edited by

C. O. Reinhold, P. S. Krstić and F. W. Meyer

Conference Chair

C. O. Reinhold – Chair P. S. Krstić – Co-Chair F. W. Meyer – Co-Chair

International Scientific Committee

F Aumayr (Austria)
R. Hoekstra (The Netherlands)
I. Juaristi (Spain)
K. Kimura (Japan)
T. Koshikawa (Japan)
H. Lebius (France)
C. Linsmeier (Germany)
M. Martiarena (Argentina)
C. O. Reinhold (USA)
P. Roncin (France)
M. Schleberger (Germany)
H. Winter (Germany)
Y. Yamazaki (Japan)

Local Organizing Committee

J. P. Allain (Purdue)
M. E. Bannister (ORNL)
M. J. Dadras
P. R. Harris (ORNL)
C. C. Havener (ORNL)
F. M. Ownby (ORNL)
D. R. Schultz (ORNL)
L. H. Saddiq (ORNL)
C. E. Sosolik (Clemson)
C. R. Vane (ORNL)

Sponsors

Office of Fusion Energy Sciences
Excellent Science Attractive Energy
Physics ORNL
Office of Basic Energy Sciences
Serving the Present, Shaping the Future
CSM Computer Science and Mathematics
Computing and Computational Sciences Directorate
NEC NATIONAL ELECTROSTATICS CORP.
THE WORLD LEADER IN MEGAVOLT ACCELERATOR TECHNOLOGY
RoentDek Handels GmbH
PFEIFFER VACUUM
OAK RIDGE National Laboratory
DREBIT Electron & Ion Beam Technologies
OXFORD INSTRUMENTS
LDS-VACUUM.COM
BEAM IMAGING SOLUTIONS

HISTORY OF IISC

IISC	Year	Location	Country	Organizer
1.	1976	Bell Labs, Murray Hill, NJ	USA	N. Tolk
2.	1978	McMaster Univ., Hamilton	Canada	R. Kelly
3.	1980	Feldkirchen-Westerham	Germany	E. Taglauer, W. Heiland
4.	1982	Hindsgavl Manor, Middelfart	Denmark	P. Sigmund
5.	1984	Gold Canyon Ranch, AZ	USA	P. Williams
6.	1986	Argonne Nat'l Laboratory, IL	USA	D. Gruen
7.	1988	Jagellonian Univ., Krakow	Poland	M. Szymonski
8.	1990	Wiener Neustadt	Austria	G. Betz, P. Varga
9.	1992	Aussois	France	M. Bernheim, J.P. Gauyacq
10.	1994	Grand Targhee, WY	USA	N. Tolk
11	1996	Island of Wangerooge	Germany	W. Heiland
12.	1998	South Padre Island, TX	USA	J.W. Rabalais, P. Nordlander
13.	2000	San Carlos di Bariloche	Argentina	M. Martiarena
14.	2002	Island of Ameland	Netherlands	R. Hoekstra, P. Zeijlman v. E.
15.	2004	Ise-Shima	Japan	K. Morita, T. Koshikawa
16.	2006	Hernstein	Austria	F. Aumayr
17.	2008	Porquerolles	France	H. Lebius, B. Ban d'Etat
18.	2010	Gatlinburg, TN	USA	C.O. Reinhold, P.S. Krstić, F.W. Meyer

High Performance
to the smallest Detail

©BICOM_10483.02 0.07.2010

TURBOLAB 80
compact and ready-to-operate high vacuum systems for laboratories

UNIVEX 300 bell jar coating and experimentation systems for research and pilot production

Vacuum solutions for research, development and pilot production.

Applications from analytics, large physics laboratories like particle accelerators, storage rings, or space simulation chambers require reliable and maintenance-free vacuum components. Oerlikon Leybold Vacuum components and system solutions have shown their benefits in major research centers worldwide.

Get the details at oerlikon.com/leyboldvacuum

Oerlikon Leybold Vacuum USA, Inc.
5700 Mellon Road
Export, PA USA
T 1-800-764-5369
F 1-800-215-7782
info.vacuum.ex@oerlikon.com
www.oerlikon.com/leyboldvacuum

œrlikon
leybold vacuum

18th International Workshop on Inelastic Ion-Surface Collisions (IISC-18)

Gatlinburg, Tennessee USA
September 26 – October 1, 2010

Time Schedule

Sunday, September 26, 2010

2:00 – 6:00 pm	**Registration**
7:00 – 9:00 pm	**Welcome Reception & Dinner** (Location - Outside Garden) C. O. Reinhold, P. S. Krstić, and F. W. Meyer

Monday, September 27, 2010

8:30 – 8:45 am	**Carlos O. Reinhold,** *Oak Ridge National Laboratory, Oak Ridge, TN* – Welcome and Opening Remarks	
	Session Chair: **Friedrich Aumayr**	
8:45 – 9:30 am	**Henning Lebius**, *CIMAP, Caen, France* **[P]** Creation of surface nanostructures by swift heavy ion irradiation under grazing incidence	p. 3
9:30 – 10:00 am	**Robert Ritter**, *Inst. of Applied Physics, TU Wien, Austria* **[R]** Nanostructures formed on surfaces due to the impact of slow highly charged ions	p. 4
10:00 – 10:30 am	**Coffee Break**	
	Session Chair: **Kenji Kimura**	
10:30 – 11:00 am	**Orkhan Osmani,** *University of Duisburg-Essen, Germany* **[R]** Track formation processes in swift heavy ion irradiated dielectrics	p. 5
11:00 – 11:30 am	**Raquel Giulian**, *Australian National University, Australia* **[R]** Swift heavy ion irradiation of embedded metal nanoparticles	p. 6
11:30 – 12:00 noon	**Kaoru Nakajima,** *Kyoto University, Japan* **[R]** Secondary ion emission from a KCl(001) by grazing-angle incidence of swift heavy ions	p. 7
12:00 – 12:20 pm	**Juergen Scheer**, *University of Bern, Switzerland* **[S]** Ionization at insulating surfaces – A review about a successful technique to measure energetic neutral particles (ENA) in space	p. 8
12:20 – 2:20 pm	**Lunch** (location – Garden View C,D,E)	
	Session Chair: **Chad Sosolik**	
2:20 – 2:50 pm	**Yasushi Yamauchi**, *National Institute for Materials Science, Japan* **[R]** Spin polarization of organic molecules on magnetic surfaces probed by a metastable helium beam	p. 9
2:50 – 3:10 pm	**Peter Varga**, *Vienna University of Technology, Austria* **[S]** Ion-beam induced magnetic nanostructures	p. 10
3:10 – 3:40 pm	**Detlef Diesing**, *University of Duisburg-Essen, Germany* **[R]** Ion-induced "internal" electron emission studied by thin film junctions	p. 11
3:40 – 4:00 pm	**Joshua Pomeroy**, *National Inst. of Standards & Technology, USA* **[S]** Highly charged ion interactions with thin insulating films	p. 12

Monday, September 27 (contd)

4:00 – 4:30 pm	**Coffee Break**	
	Session Chair: **Iñaki Juaristi**	
4:30 – 5:00 pm	**Peter Bauer**, *Johannes Kepler University, Linz, Austria* **[R]** Electronic interactions of very slow ions at solid surfaces	p. 13
5:00 – 5:30 pm	**Arkady Krasheninnikov**, *University of Helsinki, Finland* **[R]** Irradiation-induced phenomena in carbon and boron-nitride nanostructures	p. 14
5:30 – 5:50 pm	**Marika Schleberger**, *University of Duisburg-Essen, Germany* Light emission from ion-irradiated $SrTiO_3$ **[S]**	p. 15
5:50 – 6:10 pm	**Maria Luz Martiarena**, *Centro Atomico Bariloche, Argentina* **[S]** Li^+ ion neutralization on Au(111), Ag(111) and Ag layers grown on Au(111)	p. 16

Tuesday, September 28

	Session Chair: **Ronnie Hoekstra**	
8:30 – 9:15 am	**Kai Nordlund**, *University of Helsinki, Finland* **[P]** Atomistic simulations of particle-surface interactions	p. 19
9:15 – 9:45 am	**Stephan Wethekam**, *Humboldt University of Berlin, Germany* **[R]** Interactions of fullerenes during grazing scattering from surfaces	p. 20
9:45 – 10:05 am	**Andreas Wucher**, *University of Duisburg-Essen, Germany* **[S]** Sputtered neutral Si_xC_y clusters as a monitor for carbon implantation during C_{60}^+ bombardment of silicon	p. 21
10:05 – 10:30 am	**Coffee Break**	
	Session Chair: **María Silvia Gravielle**	
10:30 – 11:00 am	**Zoran Miskovic**, *University of Waterloo, Canada* [**R**] Ion interactions with carbon nano-structures	p. 22
11:00 – 11:30 am	**Erwin Bodewits,** *University of Groningen, The Netherlands* [**R**] HCI-induced secondary electron yields from thin films of C_{60}	p. 23
11:30 – 11:50 am	**Kristin Krantzman**, *College of Charleston, USA* **[S]** Molecular dynamics simulations of multi-impact bombardment of Si with 20 keV C_{60} with applications to depth profiling experiments	p. 24

<u>Tuesday, September 28</u> (contd)

11:50 – 2:00 pm **Lunch** (location – Garden View C,D,E)

Session Chair: **Helmut Winter**

2:00 – 2:20 pm **Purushottam Chakraborty**, *Saha Inst. of Nuclear Physics, India* **[S]** p. 25
Large third-order optical nonlinearity of metal-colloids in silica glasses synthesized by ion implantation

2:20 – 2:40 pm **Jory Yarmoff**, *University of California-Riverside, USA* **[S]** p. 26
Multi-electron effects in low energy Sr^+ ion scattering

2:40 – 3:40 pm **Poster Introduction**

The oral introduction (maximum of 2 minutes each) should attract attention to the posters

Surface nanostructuring of $SrTiO_3$ single crystals by slow highly charged ions and swift heavy ions – **Friedrich Aumayr**, *Vienna University of Technology, Austria* p. 29

Molecular dynamics simulations to explore the effects of Si-C chemistry in 20-keV C_{60} bombardment of Si **– Clarissa Briner**, *College of Charleston*, USA p. 30

Low-energy Ne^+ scattering by III-V compound semiconductors – **Nenad Bundaleski**, *Tecnologia Universidade Nova de Lisboa, Caparica, Portugal* p. 31

A statistical analysis of the lateral displacement of Si atoms in molecular dynamics simulations of successive bombardment with 20-keV C_{60} projectiles – **Edward Cook**, *College of Charleston, USA* p. 32

Chemical sputtering of deuterated amorphous carbon at various surface temperatures **–** **Jonny Dadras**, *University of Tennessee*, *USA* p. 33

Electron transmission through a microsize tapered glass capillary **– Buddhika Dassanayake**, *Western Michigan University, USA* p. 34

Bombarding of graphene by light atoms: change of chemistry, induced defects, and quantum electron transport through damaged graphene **– Chris Ehemann**, *Middle Tennessee State University, USA* p. 35

Calculation of Auger-neutralization probabilities for He^+-ions in LEIS **– Dominik Goebl**, *Johannes Kepler Universität Linz, Austria* p. 36

Diffraction of swift N atoms from Ag(111) surfaces **– Maria Silvia Gravielle**, *Instituto de Astronomía y Física del Espacio (IAFE), Argentina* p. 37

Photoelectron emission from LiF surfaces by ultrashort pulses **– Maria Silvia Gravielle**, *Instituto de Astronomía y Física del Espacio (IAFE), Argentina* p. 38

Tuesday, September 28 (contd)

Surface State Effects in Electron Emission from Beryllium Surfaces – **Maria Silvia Gravielle**, *Instituto de Astronomía y Física del Espacio (IAFE), Argentina* p. 39

Deuterium ion-surface interactions of lithium thin films on micro-porous molybdenum substrates – **Bryan Heim**, *Purdue University, USA* p. 40

Kinetic excitation of solids induced by energetic particle bombardment: latest results and new approaches – **Christian Heuser**, *University of Duisburg-Essen, Germany* p. 41

Time-dependent quantum mechanical simulations of electrons in carbon nanomaterials research – **Jacek Jakowski**, *University of Tennessee, USA* p. 42

Scattering of low energy N_2 molecules from the W(110) surface using different exchange correlation functionals – **Inaki Juaristi,** *Facultad de Quimicas, UPV/EHU, Spain* p. 43

Auger neutralization in the scattering of He^+ ions from a polycrystalline Cu surface – **Karima Khalal-Kouache,** *Université des Sciences et de la Technologie Houari Boumediene (USTHB), Algeria* p. 44

Internal excitation of slow C_{60}^+ ions during grazing angle scattering at a KCl(001) surface – **Kenji Kimura**, *Kyoto University, Japan* p. 45

Ion-induced beryllium nitride formation and its influence on deuterium retention – **Christian Linsmeier,** *Max-Planck-Institut für Plasmaphysik, Garching, Germany* p. 46

Sulphur induced reconstruction of Ag(111) surfaces – **Maria Luz Martiarena**, *Centro Atómico Bariloche, Argentina* p. 47

The role of substrate vacancies in the structuring of methylthiolate monolayers on Ag(111) – **Maria Luz Martiarena**, *Centro Atómico Bariloche, Argentina* p. 48

Sputtering of lunar regolith simulant by protons and multicharged heavy ions at solar wind energies – **Fred W. Meyer**, *Oak Ridge National Laboratory, USA* p. 49

Influence of screening length modification on the scattering cross section in LEIS – **Daniel Primetzhofer**, *Johannes Kepler Universität, Austria* p. 50

A multi-element organic compound studied by high-resolution Rutherford backscattering spectrometry – **Daniel Primetzhofer**, *Johannes Kepler Universität, Austria* p. 51

Directed irradiation synthesis and *in-situ* characterization of self-assembled nanostructures in the particle and radiation interaction with hard and soft matter (PRIHSM) facility – **Dan Rokusek,** *Purdue University, USA* p. 52

Charge exchange of He^+ ions on aluminum surfaces – **Stefanie Rund**, *Johannes Kepler Universität, Austria* p. 53

Mechanisms for electron emission in collisions of slow ions with insulators **– Raul Baragiola** *University of Virginia, USA* p. 54

Tuesday, September 28 (contd)

H(1s) angular distributions calculations for H^+ impinging on Al(111) at grazing incidences – **Herve Jouin**, *Université Bordeaux 1, France* p. 55

Correlated double electron capture by slow helium ions above transition metal surfaces – **Christian Tusche,** *Max-Planck-Institut für Mikrostrukturphysik, Halle, Germany* p. 56

Influence of projectile charge state on the ionization probability of sputtered particle – **Boris Weidtmann**, *University Duisburg-Essen, Germany* p. 57

Study on oxidation of NiAl(110) via electron emission during grazing surface scattering of fast He atoms – **Helmut Winter**, *Humboldt University of Berlin, Germany* p. 58

Development of new MD potentials for metal walls: Li-C-H – **Eric Yang**, *Purdue University, USA* p. 59

Alkali ion scattering from metal nanoclusters on TiO_2(110) – **Jory Yarmoff**, *University of California-Riverside, USA* p. 60

The formation of luminescing SiC nanoclusters within ion-implanted SiO_2 films – **Anatoly Zatsepin**, *Ural Federal University, Russia* p. 61

3:40 – 7:00 pm **Posters and Refreshments** (location – Ballroom 2)

Wednesday, September 29

Session Chair: : **Marika Schleberger**

8:30 – 9:15 am **Joachim Burgdörfer**, *Vienna University of Technology, Austria* **[P]** p. 65
Guiding of ions and electrons through nano-capillaries

9:15 – 9:45 am **Walter Meissl**, *RIKEN, Japan* **[R]** p. 66
Closed-tip tapered glass capillaries as a novel tool for micro-irradiation of living cells by MeV ion beams

9:45 – 10:05 am **Buddhika Dassanayake**, *Western Michigan University, USA* **[S]** p. 67
Transmission of electrons through a single glass macro-capillary: energy and time dependence

10:05 – 10:30 am **Coffee Break**

Session Chair: **Kristin D. Krantzman**

10:30 – 10:50 am **Friedrich Aumayr**, *Vienna University of Technology, Austria* **[S]** p. 68
Controlling the guiding properties of mesoscopic glass capillaries for slow highly charged ions

Wednesday, September 29 (contd)

10:50 – 11:20 am	**Takanori Koshikawa**, *Osaka Electro-Communication Univ., Japan* **[R]** Surface study with MEIS and LEEM/PEEM	p. 69
11:20 – 11:50 am	**Cristina Díaz**, *Univ. Autonoma de Madrid, Spain* **[R]** Computing dissociative adsorption probabilities from grazing incidence collisions of light molecules with metal surfaces	p. 70
11:50 – 1:00 pm	**Lunch** (location – Garden View C,D,E)	
1:00 – 6:30 pm	**Break and Conference Excursions**	
7:30 – 9:00 pm	**Conference Dinner** (location – Garden View C,D,E) **Jack C. Wells**, *Oak Ridge National Laboratory, USA* Advanced computing for scalable electrochemical energy storage	

Thursday, September 30

Session Chair: **Christian Linsmeier**

8:30 – 9:15 am	**Russ Doerner**, *University of California-San Diego, USA* **[P]** Multi-component plasma interactions with elemental and mixed-material surfaces	p. 73
9:15 – 9:45 am	**Pedro Zeijlmans van Emmichoven**, *FOM-Inst. for Plasma Phys. Rijnhuizen*, *The Netherlands* **[R]** Hydrogenic retention in tungsten exposed to high-flux plasmas	p. 74
9:45 – 10:15 am	**Martin Oberkofler**, *Max-Planck-Institut für Plasmaphysik, Garching, Germany* **[R]** Retention and release mechanisms of deuterium implanted into beryllium as a fusion first wall material	p. 75
10:15 – 10:45 am	**Coffee Break**	

Session Chair: **Daniel Primetzhofer**

10:45 – 11:15 am	**Jean Paul Allain**, *Purdue University, USA* **[R]** In-situ elemental and chemical state characterization of lithiated surfaces under energetic singly-charged particle bombardment	p. 76
11:15 – 11:45 am	**Thomas Schwarz-Selinger**, *Max-Plank-Institut für Plasmaphysik*, *Garching, Germany* **[R]** Studying synergistic effects in chemical sputtering using dual beam irradiation	p. 77

Thursday, September 30 (contd)

11:45 – 12:05 pm	**Peter Harris**, *Oak Ridge National Laboratory, USA* **[S]** Molecular size effect in the chemical sputtering of a-C:H thin films by low energy H^+, H_2^+, and H_3^+ ions	p. 78
12:05 – 12:25 pm	**Marek Rubel**, *Royal Institute of Technology, Sweden* **[S]** An overview of nuclear micro-probe applications for characterization of plasma-facing materials from tokamaks	p. 79
12:25 – 2:30 pm	**Lunch** (location – Outside Garden)	
	Session Chair: **Peter Varga**	
2:30 – 3:00 pm	**Nenad Bundaleski**, *Universidade Nova de Lisboa, Portugal* **[R]** Decoherence in fast atom diffraction from surfaces	p. 80
3:00 – 3:20 pm	**Maria Silvia Gravielle**, *Instituto de Astronoma y Fisica del Espacio*, *Argentina* **[S]** He-LiF surface interaction potential from fast atom diffraction	p. 81
3:20 – 3:40 pm	**Helmut Winter**, *Humboldt University Berlin, Germany* **[S]** Recent progress in studies on fast atom diffraction during grazing surface scattering	p. 82
3:40 – 4:00 pm	**Paul Tiwald**, *Vienna University of Technology, Austria* **[S]** Atom-Al surface scattering potentials from *ab-initio* calculations	p. 83
4:00 – 4:30 pm	**Coffee Break**	
	Session Chair: **Purushottam Chakraborty**	
4:30 – 4:50 pm	**Dennis Neufeld**, *Rice University, USA* **[S]** Probing stray electric fields at surfaces with Rydberg atoms	p. 84
4:50 – 5:10 pm	**Marcel Fallet**, *Clemson University, USA* **[S]** Evolution of carbon-based surfaces using deuterium bombardment: characteristics of the steady state	p. 85
5:10 – 5:30 pm	**Russell Lake**, *Clemson University, USA* **[S]** Electronic interaction of highly charged ions with dielectric covered metal surfaces	p. 86
7:00 pm	**Conference Dinner** (location – Ballroom 3) IISC 18 Remarks: C. O. Reinhold IISC 19 Preview: C. Linsmeier	
	Donald L. Hillis, *Oak Ridge National Laboratory, USA* Energy from heaven in an environment from hell: challenges in materials research for fusion energy development	

Friday, October 1

	Session Chair: **Henning Lebius**	
8:30 – 9:15 am	**Thomas Orlando**, *Georgia Institute of Technology, USA* **[P]** Particle-induced surface processes in the solar system	p. 89
9:15 – 9:35 am	**Nasser, Barghouty**, *NASA-Marshall Space Flight Center, USA* **[S]** Solar wind sputtering of lunar surface materials: role and some possible implications of potential sputtering	p. 90
9:35 – 10:05 am	**Michio Okada**, *Osaka University, Japan* **[R]** Stereodynamical control of surface chemistry with oriented molecular beams	p. 91
10:05 – 10:30 am	**Coffee Break**	
	Session Chair: **Jean Paul Allain**	
10:30 – 10:50 am	**Gunther Andersson**, *Flinders University, Australia* **[S]** Determining concentration depth profiles in thin foam films with neutral impact collision ion scattering spectroscopy	p. 92
10:50 – 11:20 am	**Robert D. Kolasinski**, *Sandia National Laboratory, USA* **[R]** Characterization of surface structure in real space using low energy ion scattering and recoil maps	p. 93
11:20 – 11:50 pm	**Torgny Gustafson**, *Rutgers State University, USA* **[R]** Structure and composition of high-k materials on novel substrates	p. 94
11:50 – 12:00 noon	**Closing**	
12:00 noon	**Lunch** (location – Ballroom 2)	
Departure		

* * * * * * * * * * * * *

Index p. 96

List of Participants p. 99

Monday, September 27, 2010

RoentDek

Handels GmbH

Fast Position Sensitive Delay-Line Detectors
Multi-Hit Detection
Imaging Systems for Multifragment Processes
in Atoms, Molecules and on Surfaces

http://roentdek.com/

CREATION OF SURFACE NANOSTRUCTURES BY SWIFT HEAVY ION IRRADIATION UNDER GRAZING INCIDENCE

H. Lebius[1,*], *and M. Schleberger*[3]

[1] CIMAP (CEA, CNRS, ENSICAEN, UCBN), rue Claude Bloch, 14070 Caen, France
[2] Universität Duisburg-Essen, Inst. f. Exp. Physik, Lotharstr., 47057 Duisburg, Germany

1. INTRODUCTION

Grazing angle irradiation is a relatively new field. First, experiments were done with surfaces covered with clusters, measuring the strength of a shock wave stemming from an ion traversing a surface at shallow depth.

We decided to look at the structuring of a surface due to grazing impact with swift heavy ions. The main excitation process is due to electronic stopping, the interaction of the projectile ion with the electrons in the target. This initial electronic excitation is very similar to the electronic excitation of very slow, highly charged ions. The main difference lies in the depth, up to which electronic excitation is occurring. With slow, highly charged ions this depth is very shallow, accounting for several nm. For swift heavy ions, the depth can reach to several µm. In order to diminish the depth difference, grazing angles can be chosen, allowing the projectile to travel for long distances at a very small penetration depth. This grazing angle projects the track to the surface, allowing us to study the track with surface sensitive methods, like atomic force microscopy.

Ions at around 100 MeV kinetic energy were used, the target was a single crystal of $SrTiO_3$. The striking result of these studies is the creation of a line of repeating hillocks. One line is generated typically by one incident ion. The individual distances between the hillocks are constant over one line or one incident ion, respectively. The overall length of the line as well as the distance between the hillocks, is a geometric function of the incidence angle. This lead to the following model description: the electron density is oscillating when the projectile penetrates into the target, therefore the deposited energy is also oscillating. At regions of high energy deposition hillocks are formed, up until a maximal depth, from which surface modifications are no more possible. In order to quantitatively describe the processes involved, the thermal spike model was enhanced and expanded to a full 3-D calculation.

The above-mentioned lines of hillocks can be seen for a large group of materials, from insulators to conductors and from single crystals to amorphous materials.

As it is quite common for modifications due to stopping, a threshold energy loss can be found, both in measurements as well as in the enhanced thermal spike model. Experiments at the surface (topology by means of atomic force microscopy) as well as in the bulk (crystallinity by means of translational electron microscopy) yield the same threshold.

In order to better understand the processes involved, we started using films on top of the support. Our material of choice was Graphene, a single layer of Graphite on several different supports. While showing the above-mentioned lines of hillocks, the layer of grapheme is torn apart and shows unique folding patterns, strongly dependent on the incident angle.

[*] E-mail: lebius@ganil.fr

NANOSTRUCTURES FORMED ON SURFACES DUE TO THE IMPACT OF SLOW HIGHLY CHARGED IONS

R. Ritter[1,*], *G. Kowarik*[1], *C. Vasko*[1], *R. Ginzel*[2], *L. Maunoury*[3], *M. Toulemonde*[3], *C. Dufour*[3], *H. Lebius*[3], *R. M. Papaléo*[4], *W. Rupp*[5], *Q. Shen*[6], *C. Teichert*[6], *J. R. Crespo López-Urrutia*[2], *J. Ullrich*[2], *and F. Aumayr*[1]

[1] Institute of Applied Physics, TU Wien - Vienna University of Technology, 1040 Vienna, Austria, EU
[2] Max-Planck Institut für Kernphysik, 69029 Heidelberg, Germany, EU
[3] CIMAP, ENSICAEN, CEA, CNRS, Univ.Caen, 14070 Caen, France, EU
[4] Faculty of Physics, Catholic University of Rio Grande do Sul, 90619-900 Porto Alegre, Brazil
[5] IMS Nanofabrication AG, 1020 Vienna, Austria, EU
[6] Institute of Physics, Montanuniversität Leoben, 8700 Leoben, Austria, EU

1. INTRODUCTION

As demonstrated recently [1], slow (keV) highly charged ions (HCI) are able to induce stable, topographic and non-erasable nano-structures (hillocks) on a CaF_2 surface. Although very similar surface modifications can also be obtained by swift (up to GeV) heavy ion irradiation, slow HCI have the distinct advantage of limiting the interaction with the target surface to the topmost atomic layers, and do not produce the substantial radiation damage to the bulk that is associated with swift heavy ions.
Meanwhile a variety of materials has been found, which is susceptible to nano-structuring by the impact of slow HCI. The nature, appearance and stability of the created structures, however, depend heavily on the properties of the target material and the involved interaction processes (determined by the potential and kinetic energy of the projectiles) and can range from hillocks (CaF_2), pits (KBr [2], PMMA), caldera-type structures (TiO_2 [3]) to erasable regions of enhanced friction (HOPG, mica [4]).

2. EXPERIMENT

We have systematically studied HCI induced pit formation on polymethylmetacrylate (PMMA), a polymer commonly used as a photoresist in the semiconductor industry. Samples were irradiated with Xe ions in charge states q = 20 - 50. Final impact energies on the surface ranged from 0.35 - 4.0 keV/amu.
Intermittent contact mode atomic force microscopy (AFM) investigations of the irradiated samples revealed that each individual ion creates a nano-sized pit (fig. 1). While the pit-volume increases with the potential energy of the incoming ions, a variation of the kinetic energy of the HCI seems to solely alter the shape of the pit created. A faster ion leaves behind a deeper and slimmer pit compared to a slower ion, while the total volume removed stays approximately the same in both cases.

On HOPG, we find nanostructures for all combinations of charge states (Ar^{q+}, q = 9 - 16 and Xe^{q+}, q = 13 - 30, 48) and kinetic energies (0.35 - 3.7 keV/amu) via scanning tunneling microscopy. With the AFM, however, these structures only become visible when operated in lateral force mode. The impact sites can therefore be interpreted as regions of enhanced friction while there is no indication for a topographic surface modification in the investigated charge state regime. Employing a wedge calibration method for AFM cantilevers, we have quantitatively determined the microscopic friction force coefficient at the ion impact sites as a function of ion charge state. First results indicate a clear size increase with higher charge states.

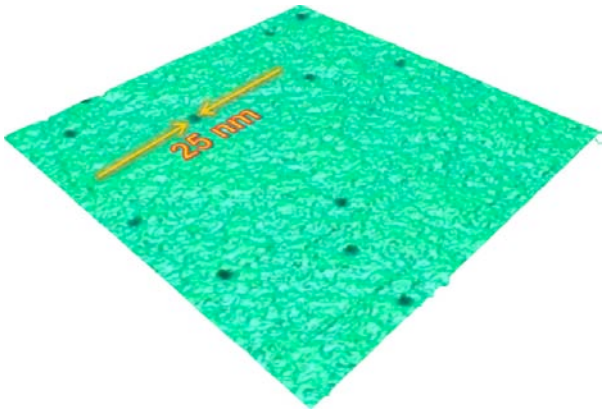

Figure 1: Pits produced on PMMA after bombardment with Xe^{48+} ions (E_{kin} = 3.7 keV/amu), 500nm x 500nm.

3. REFERENCES

[1] A. El-Said, et al., Phys. Rev. Lett. **100** (2008) 237601.
[2] R. Heller, et al., Phys. Rev. Lett. **101** (2008) 096102.
[3] M. Tona, et al. Phys. Rev. B **77** (2008) 155427.
[4] R. Ritter, et al., Vacuum **84** (2010) 1062.

* E-mail: ritter@iap.tuwien.ac.at

ULTRAFAST EXCITATION AND RELAXATION PROCESSES IN SWIFT HEAVY ION IRRADIATED INSULATORS

O. Osmani[1,2,*], *N. Medvedev*[2], *B. Rethfeld*[2], *M. Schleberger*[1]

[1] Faculty of Physics, University of Duisburg-Essen, D-47048 Duisburg, Germany
[2] Technical University of Kaiserslautern, OPTIMAS Research Center, D-67653 Kaiserslautern, Germany

1. ABSTRACT

Swift heavy ion beams penetrating insulators are known to create structural modifications. These modifications may be observed in form of craters or hillock formation. Theoretically these modifications are often treated either within the so called Inelastic thermal spike model or simulated using molecular dynamics. Molecular dynamics simulations can analyze the details of the induced structural changes, such as point defect creation or partial sputtering but neglect the electronic system. Because the ion looses its energy mainly due to electronic stopping the energy transport process within the electronic system is crucial. The inelastic thermal spike (I-TS) model, a set of coupled heat diffusion equations, is often used to calculate the transport of energy and the heating of the target lattice due to electron-phonon coupling. The input parameters needed for the I-ST are material parameters like the specific heat capacity, diffusivity and the electron-phonon coupling parameter. These parameters can be found experimentally while the electron-phonon-coupling parameter is found by fitting to experimental data. However, these parameters do not reflect the strong excitation induced by the ion and are therefore questionable at best. We developed a model that aims to give a detailed understanding of the transient excitation processes happening during the swift heavy ion penetration. Therefore we use Monte Carlo simulations to calculate the excitation and transport of the electrons. Within the MC calculation material parameters like the electron-phonon coupling and the specific heat capacity can be calculated while taking the excitation of the electron into account. These parameters then are used as input for our thermal spike calculation. It will be demonstrated that within our model all necessary parameters are calculated and therefore no fitting is used. Also a strong dependence on the electronic density can be observed which at the moment is taken into account as density dependent parameters for the TS, thus affecting the transport properties. Finally it will be shown that our model indicates that three different zones around the ion impact point can be distinguished by their different transport properties.For our model system we chose Ca ions at 11 MeV/u kinetic energy on SiO2. this corresponds to a recent experiment.

2. REFERENCES

[1] O. Osmani, N. Medvedev, B. Rethfeld, M. Schleberger, e-J. Surf. Sci. Nanotech. Vol. **8** (2010) 31.

[2] N. Medvedev, O. Osmani, B. Rethfeld, M. Schleberger, Nucl. Instrum. Methods B **268** (2010) 3160.

[3] P. Kluth, C. S. Schnohr, O. H. Pakarinen, F. Djurabekova, D. J. Sprouster, R. Giulian, M. C. Ridgway, A. P. Byrne, C. Trautmann, D. J. Cookson, K. Nordlund, and M. Toulemonde, Phys. Rev. Lett. **101**, 175503 (2008)

* E-mail: orkhan.osmani@uni-due.de

SWIFT HEAVY ION IRRADIATION OF EMBEDDED METAL NANOPARTICLES

M.C. Ridgway[1,*], *R. Giulian*[1], *D.J. Sprouster*[1], *P. Kluth*[1], *L.L. Araujo*[1], *D.J. Llewellyn*[1], *A.P. Byrne*[1], *F. Kremer*[2], *P.F.P Fichtner*[2], *G. Rizza*[3], *H. Amekura*[4] *and M. Toulemonde*[5]

[1] Research School of Physics and Engineering, Australian National University, Canberra, Australia
[2] Universidade Federal do Rio Grande do Sul, Porto Alegre, Brazil
[3] Ecole Polytechnique, Palaiseau, France
[4] National Institute for Materials Science, Tsukuba, Japan
[5] Laboratoire CIRIL-GANIL, Caen, France

1. ABSTRACT

Swift heavy ion irradiation of elemental metal nanoparticles embedded in a silica matrix yields a spherical to rod-like shape transformation, with the direction of elongation aligned to that of the incident ion beam. Large and once spherical nanoparticles become progressively more rod-like while subject to dissolution and fragmentation. Small nanoparticles below a critical diameter remain spherical and do not elongate but instead dissolve in the matrix. For this report, we examine the shape transformation for a variety of metals with the aim of achieving mechanistic insight into the transformation process. We demonstrate subtle metal-specific differences in the transformation process and the influence of the thermodynamic properties of both the metal and matrix. For example, the width of elongated nanoparticles saturates at a value comparable to the critical diameter for transformation and is well correlated with the metal melting temperature and energy required for vaporisation. Furthermore, we show the elongation process necessitates the formation of a molten ion track in the silica matrix. This track confines the nanoparticle elongation and as a consequence the saturated nanoparticle width does not exceed the molten ion track diameter.

[*] E-mail: mark.ridgway@anu.edu.au

SECONDARY ION EMISSION FROM KCl(001) SURFACE BY GRAZING-ANGLE INCIDENCE OF SWIFT HEAVY IONS

K. Nakajima[*], *T. Suzuki, M. Suzuki and K. Kimura*

Department of Micro Engineering, Kyoto University, Kyoto 606-8501, Japan

1. INTRODUCTION

When an ion is incident on an atomically flat solid surface at a grazing angle, the ion is mostly reflected at a specular angle without penetrating into the solid. This "specular reflection" of fast ions is very suitable to investigate ion–surface interaction [1,2]. For example, it allowed us to study the generation process of secondary electrons by fast ions separately from other complicated processes, i.e. transportation to and transmission through the surface [2].
In this paper, we report secondary ion (SI) emission from a KCl(001) surface by grazing incidence of 0.05 – 0.21 MeV/u various ions. In particular, the yield (or the production rate) of positive secondary ions is discussed with an emphasis on its correlation with corresponding surface stopping power and secondary electron yield.

2. EXPERIMENTAL

Beams of 0.05 – 0.21 MeV/u various ions (0.8 MeV He^+, 1.37 MeV Li^+, 2.1 MeV B^{2+}, 3 MeV O^{2+}, 1.5 MeV Si^{2+}, and 6.0 MeV Si^{3+}) from accelerators at QSEC in Kyoto University were incident on a clean KCl(001) surface at a grazing angle θ_i of 2 – 6 mrad. The azimuth angle of incident ions was chosen away from any low-index axes on the surface. The target was heated typically up to 180 °C during measurements for the surface to be kept clean and free from the macroscopic charging due to ion beam irradiation (beam current < 0.1 pA). The ions reflected in the specular direction were energy analyzed with a 90° sector magnetic spectrometer in combination with a one-dimensional position sensitive detector (1D-PSD). SIs emitted from the surface were guided into a drift tube equipped in front of the surface and were detected by a microchannel plates (MCP) at the end of the tube. The time of flight (TOF) of each SI with respect to the time at which the corresponding reflected ion was detected by the 1D-PSD was registered in a list form, along with the energy of the corresponding reflected ion.

3. RESULTS

Figure 1 shows an example of the observed TOF spectrum of positive secondary ions from a KCl(001) by incidence of 3 MeV O^{2+} at grazing angle of 4 mrad with respect to the surface. Various singly charged SIs such as Cl^+, K^+, K_2^+, $K(KCl)_n^+$ (n = 1 – 4) were observed distinctly. This considerably high yield of positive SIs shows a sharp contrast with the result for a semiconducting SnTe(001) surface, from which no detectable SI was emitted. Although there was also emission of negative SIs such as Cl^-, $(KCl)_nCl^-$ (n = 1 – 4), their total yield was two orders of magnitude lower than that of positive SIs. In addition, the yield of positive SIs reasonably revealed a direct correlation with the number of secondary electrons. These results suggest that the emission of positive SIs is caused by transient local charging of the surface due to the numerous secondary electrons.

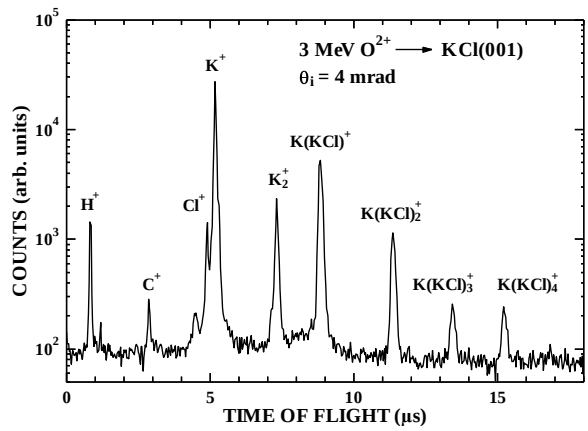

Figure 1: TOF spectrum of positive secondary ions

We have also investigated the yield of SIs at various grazing angles of incidence, which allows us to estimate the production rate $P(x)$ of SIs as a function of the distance x between the projectile ion and the surface. This production rate will be presented in combination with the stopping power of the surface (i.e., linear energy transfer from a projectile to the surface).

4. REFERENCES

[1] M. Mannami, K. Kimura, K. Nakanishi, A. Nishimura, Nucl. Instr. and Meth. B **13**, 587 (1986).
[2] K. Kimura, G. Andou, K. Nakajima, Phys. Rev. Lett. **81**, 5438 (1998).

[*] E-mail: kaoru@kues.kyoto-u.ac.jp

IONIZATION AT INSULATING SURFACES – A REVIEW ABOUT A SUCCESSFUL TECHNIQUE TO MEASURE ENERGETIC NEUTRAL PARTICLES (ENA) IN SPACE

J.A. Scheer [1,*], *and P. Wurz*[1]

[1] Physikalisches Institut, University of Bern, Sidlerstr. 5, 3012 Bern, Switzerland

1. INTRODUCTION

In space science many applications of remote sensing of plasma populations require a high detection efficiency of Energetic Neutral Atoms (ENA) because the sources of these ENAs are very faint [1]. This requires advanced detection techniques, and not before long measurements of ENAs were quite impossible due to the limitations onboard of a spacecraft. The reason is neutral particles have to be ionized before they can be analyzed and ionizing techniques, which work fine in a laboratory on earth can be very difficult, if not impossible, to implement in an instrument, which shall work on a satellite.

In the mid 1990ies reports about unexpected high yields of negative ions upon scattering of positive and neutral particles from various surfaces led to a new type of neutral particle mass spectrometer, which uses the effect of surface ionization and works now successfully on several space missions, such as IMAGE [2] and IBEX [3](NASA) and the CENA instrument (ESA & ISRO) from the Indian mission to moon Chandrayaan-1 [4]. However, it took many years to find good working so-called Conversion Surfaces (CS) [5] and this report will summarize our tests with possible candidates for conversion surfaces, with special emphasis on ionization efficiency and scattering properties. Furthermore, we will report about the actual status and finally explain why the search for the perfect conversion surface did not end yet.

2. REFERENCES

[1] P. Wurz, et al., *Detection of Energetic Neutral Atoms, in The Outer Heliosphere: Beyond the Planets, (eds. K. Scherer, H. Fichtner, and E. Marsch)*, Copernicus Gesellschaft e.V., Katlenburg-Lindau, Germany, 251 (2000).

[2] J.L. Burch, et al., *Views of Earth's Magnetosphere with the IMAGE Satellite*, Science **291** 619 (2001).

[3] S.A. Fuselier, et al., *The IBEX-Lo Sensor*, Space Science Review **146** 117 (2009).

[4] S. Barabash, et al., *Investigation of the solar wind -- Moon interaction onboard Chandrayaan-1 mission with the SARA Experiment*, Current Science **96** 526 (2009).

[5] J.A. Scheer, et al., *Conversion Surfaces for Neutral Particle Imaging Detectors*, Adv. Space Res. **38** 664 (2006).

* E-mail: jscheer@space.unibe.ch

SPIN POLARIZATION OF ORGANIC MOLECULES ON MAGNETIC SURFACES PROBED BY A METASTABLE HELIUM BEAM

Y. Yamauchi[1,*], *X. Sun*[1,2], *S. Entani*[3], *A. Pratt*[1,4], *M. Kurahashi*[1], *and T. Suzuki*[1]

[1] National Institute for Materials Science, 1-2-1 Sengen, Tsukuba 305-0047, Japan
[2] Hefei National Laboratory for Physical Sciences at Microscale and Department of Physics, University of Science and Technology of China, Hefei, Anhui 230026, China
[3] Advanced Science Research Center, JAEA, 2-4 Shirane Shirakata, Tokai, Naka, 319-1195, Japan
[4] York Institute for Materials Research, Department of Physics, University of York, York YO10 5DD, U.K.

1. INTRODUCTION

The broken symmetry at surfaces or the low dimensionality of atomically thin overlayers on magnetic substrates may give rise to spin behaviors distinct from the bulk. Similar differences between interface and bulk also exist in spintronic device structures such as tunneling magnetoresistance devices and should be the key factors in achieving high performance. Thus the surface spins, which are the only directly accessible interface spins between the vacuum and magnetic materials, provide us with fundamental information for developing spintronic devices. As is now well known, recent progress of organic displays and other organic devices has been so remarkable that various attempts have also been initiated to explore organic spin devices. [1] Therefore the question of whether an organic molecule or thin film exhibits spin polarization at the interface of a magnetic substrate, has attracted attention.

2. USE OF A METASTABLE HELIUM BEAM

Spin-polarized metastable deexcitation spectroscopy (SPMDS) is one of the most capable techniques among the various kinds of surface characterization techniques to investigate the spin polarization of the topmost surface of organic thin films. Spin-aligned beams of thermal energy metastable helium atoms have been generated using the nozzle-skimmer discharge method followed by optical pumping or magnetic state selection. [2] As an unprecedented feature of the beam, spin-aligned helium atoms interact with the surface so gently that the spin polarization of only the electrons at the outermost surface can be detected. The secondary electron spectra obtained reflect the local density of states distributed at the vacuum side of the outermost layers. Spin asymmetry, which shows differences in spectral intensity depending on each spin of the helium atoms, indicates the spin polarization of surface electrons.

3. INDUCED SPIN POLARIZATION

Spin asymmetries have been measured for graphene (a single-layer graphite sheet) and other organic layers on ferromagnetic substrates by SPMDS, and spin-resolved electronic structures have also been calculated on the basis of density functional theory. [3] The SPMDS spectra of graphene/Ni(111) show that new electronic states caused by splitting and mixing of the graphene π-orbitals and the substrate states appear around the Fermi level. Spin asymmetry analysis of the SPMDS spectra illustrates that a finite positive spin polarization is induced in the new electronic states. We also clarify the spin polarization of the organic molecules, which are also relevant to organic semiconductor substrates. A detailed analysis of the experimental and theoretical results reveals that spin polarization may not be limited to the neighboring atoms which interact directly with the magnetic substrate, but extends to molecular orbitals distributed in the carbon atom network even several atoms distant from the magnetic substrate. If the spin polarization is commonly induced in molecular orbitals extending over relatively long distances as a consequence of the local interaction with a spin-polarized substrate, graphene or other organic materials with π-orbital networks can be considered, not only as spin transport media, but also as promising monolithic platforms without spin injection through hetero interfaces.

4. REFERENCES

[1] N. Tombros et al., Nature **448** (2007) 57; T. Ikegami, et al., **APL** 92, 153304 (2008).
[2] M. Onellion, M.W. Hart, F.B. Dunning and G.K. Walters: Phys. Rev. Lett. **52**, 380 (1984); G. Baum, W. Raith and H. Steidl: Z. Phys. D **10**, 171 (1988).
[3] X. Sun, et al., Chem. Phys. Lett. **452**, 156 (2008); S. Entani, et al., (to be published).

[*] E-mail: `yamauchi.yasushi@nims.go.jp`

ION-BEAM INDUCED MAGNETIC NANOSTRUCTURES

S. Sha Zaman[1], A.Buchsbaum[1], W.Rupp,[1,2] R.Ritter,[1] Ch.Klein,[2] E.Platzgummer,[2] M.Schmid,[1] P.Varga[1]

[1] Institute for Applied Physics, Vienna University of Technology, Austria,

[2] IMS Nanofabrication AG, 1020 Vienna, Austria

1. Abstract

For epitaxial iron films grown on Cu(100) stabilization of the face-centered cubic (fcc) γ-phase (which is non magnetic,) can be obtained above room temperature. This is in contrast to bulk iron for which the fcc phase is stable only above 1184 K, whereas below this temperature the body-centered cubic (bcc) α-phase (which is ferromagnetic) is thermodynamically stable. The thickness of these nonmagnetic fcc iron films on Cu(100) is for pure iron limited to 5 to 10 monolayers, corresponding to about 0.9–1.8 nm. Films above this thickness range will exhibit a spontaneous structural transition to the body-centered structure which is in plane ferromagnetic whereas below 5 monolayer a strained bcc structure shows an out of plane magnetic moment [1,2,3]

We can show by STM (Scanning tunneling microscopy) with atomic resolution and LEED (Low Energy Electron Diffraction) that this 5-10 ML thick fcc Fe films undergo a transition from fcc to bcc by ion beam irradiation. Since Fe is ferromagnetic only if it is bcc or at least strained bcc but never if it is fcc this gives the possibility to make nonmagnetic Fe film ferromagnetic directly by ion bombardment. The magnetic moment of such an ion induced magnetic transition in dependence of the ion species and ion dose was measured in situ by SMOKE (Surface Magneto-Optical Kerr Effect). We could show that He ions don´t transform the film at all and for Ar ions an energy of 1keV and a dose of $nx10^{12}$ions/cm^2 is necessary to transform the whole film into bcc phase.The the process could be described best by applying the thermal spike model [4].

This ion induced phase transition gives the possibility to form magnetic nanostructures with a resolution determined by the diameter of the used ion beam. Test structures have been produced with nano-sized ion beams by projection mask-less patterning (PMLP) a technique for ion beam lithography developed by IMS Nanofabrication AG, (www.ims.co.at). The resulting magnetic pattern was measured by the help of MFM (Magnetic Force Microscope) and in a first experiment a resolution of 100nm was achieved (see Fig.1) [5].

Since for nanostructures the magnetic behavior is determined by the superparamagnetic limit we also tried to stabilize thicker Fe film in the fcc phase. We could grow such fcc Fe films up to a thickness of 40 ML either by evaporating Fe at increased CO pressure or by co-evaporating Ni and Fe with. We could show that also such thick films can undergo the fcc-bcc transition (i.e.also paramagnetic-ferromagnetic transition) by ion bombardment. The respective magnetic moment was again determined by SMOKE.

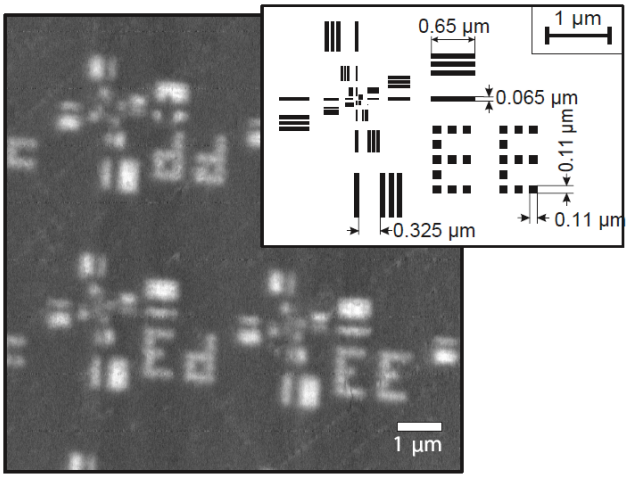

Fig1: Magnetic force image showing a magnetic pattern created by ion lithography (10 keV Ar^+, 2.8 x 10^{14} cm^{-1}) in a 1.6nm Fe film on Cu(100) capped with 2nm Au. The inset shows the mask dimensions multiplied by the demagnification factor of 1/200

2. REFERENCES

[1] A.Biedermann, M.Schmid, P.Varga, Phys.Rev.Lett. 86 (2001) 464-467

[2] A.Biedermann, R.Tscheliessnig, M.Schmid, P.Varga, Phys.Rev.Lett. 87 (2001) 086103

[3] A.Biedermann, R.Tscheliessnig, M.Schmid, P.Varga Appl.Phys. A 78 (2004) 807-816

[4] W.Schillingand H.Ullmaier, Material Science and Technology (Weinheim) Vol 10 (1993) 180-241

[5] W.Rupp, B.Kamenik, R.Ritter, A.Biedermann, Ch.Klein, E.Platzgummer, M.Schmid, and P.Varga, Appl.Phys.Lett. 93 (2008) 063102

* E-mail: rbrown@yahoo.com

ION-INDUCED "INTERNAL" ELECTRON EMISSION STUDIED BY THIN FILM TUNNEL JUNCTIONS

Detlef Diesing

Institut für Physikalische Chemie, Universität Duisburg Essen, Universitaetsstr.5, 45117 Essen, Germany

Since the pioneering works of Hagstrum the process of external electron emission is a well known tool to investigate the interaction of ions with metal surfaces. However, this method is restricted to electrons which have enough energy to overcome the workfunction. This systematic restriction can be released by detecting the excited electrons in a thin film heterosystem with an interstitial insulating layer. The back metal electrode in such a system acts as a counterelectrode similar to that in an electron spectrometer and detects only electrons which overcome the internal barrier or it detects excited holes which are transported beneath the internal barrier. The values for the barrier height in the heterosystems are around 1.5 eV for tantalum oxide and around 3 eV for aluminum oxide layers. By the application of a bias voltage it is possible to distort these internal barriers in situ in the course of an experiment and thereby tune the ratio of excited electron and excited hole induced device currents. In the talk we will show, how the tuning of a barrier can be used to derive the temperature of the excited carriers distribution. Two examples will be given. First, excited carrier distributions released by highly charged argon ions are characterized by tuning aluminum oxide based heterosystems. As a second example the discharge reaction of oxonium (hydronium) ions on platinum surfaces will be presented. The comparably small excitation energy of this reaction can be characterized by the bias induced tuning of tantalum oxide barriers.

* E-mail:.diesing@uni-due.de

HIGHLY CHARGED ION INTERACTIONS WITH THIN INSULATING FILMS

J.M. Pomeroy[1,2,*], *R.E. Lake*[2], *H. Grube*[1], *and C.E. Sosolik*[2]

[1] National Institute of Standards and Technology, 100 Bureau Dr., MS 8423, Gaithersburg, MD 20899-8423
[2] Department of Physics and Astronomy, Clemson University, Clemson, SC 29634

1. INTRODUCTION

In this paper, results from ongoing experiments examining the permanent electronic modification of ultra-thin insulating films due to highly charge ion (HCI) irradiation are presented, see, for example: [1, 2, 3, 4]. The tunnel junctions' (TJ) electrical conductance are seen to increase linearly with the number of ions used to irradiate the device, see Fig. 1. Each HCI modifies the local integrity of the tunnel barrier to enhance the electrical conductance by a discrete value, σ_c - the conductance added per HCI. The value of σ_c depends systematically on the charge state of the HCI, the thickness of the tunnel barrier, and the tunnel barrier stoichiometry. For most combinations of these parameters, the HCI produced features remain TJs that exhibit a low density of electronic hopping states.

2. EXPERIMENTAL DETAILS

Samples are prepared by evaporating metal films through a shadow mask that defines a ≈ 50 μm wire. A thin insulating layer is prepared over the entire sample surface, so that the wires are "coated" on all sides with a thin insulating film. The wire is then irradiated at a well defined location with a predetermined dose of HCIs. Immediately following irradiation, a second wire of similar size is deposited perpendicularly across the HCI irradiated area forming an approximately rectangular TJ. All steps are performed *in situ* within a system of ultra-high vacuum chambers.

This experimental approach utilizes the unique preparation of each sample, enabling studies of the effects of HCI irradiation on a virtually unlimited range of different samples. The encapsulation of the HCI induced features eliminates measurement bias due to the passage of time and preserves samples for different measurements at much later times. Finally, the incorporation of the HCI features into a TJ allows direct electronic interrogation of the features created.

3. CONCLUSIONS

HCI irradiation of thin insulating films on metal surfaces represents an electronic middle ground between the bulk metal and bulk insulating samples studied by others. The underlying metal surface provides a charge reservoir for fast electron transport to the HCI, while the insulating film can trap electronic energy and "record" the effect of the HCI-multilayer interaction. Systematic electronic study of these effects enabled by the TJ geometry compliment and extend the exisiting body of results derived from secondary particle and *post facto* surface studies.

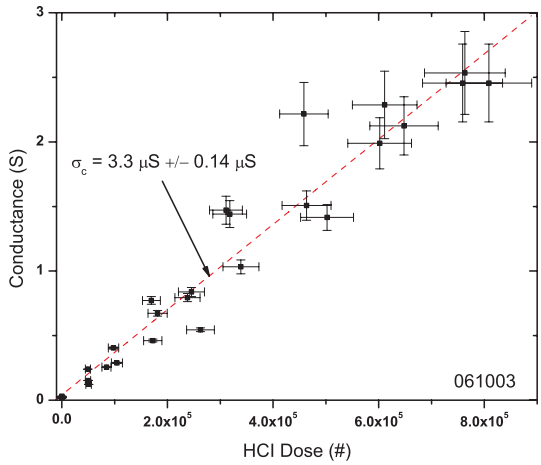

Figure 1: Electrical conductance (G) of a series of TJs as a function of the number (N) of Xe^{44+} ions used to irradiate them, modeled as $G = \sigma_c N + G_0$.

4. REFERENCES

[1] R. E. Lake, J. M. Pomeroy, and C. E. Sosolik, J. Phys. Cond. Mat. **22**, 084008 (2010).

[2] J. M. Pomeroy and H. Grube, Nucl. Instr. and Meth. B **267**, 642 (2009).

[3] J. M. Pomeroy, H. Grube, A. C. Perrella, and J. D. Gillaspy, Appl. Phys. Lett. **91**, 073506 (2007).

[4] J. M. Pomeroy *et al.*, Nucl. Instr. and Meth. B **256**, 319 (2007).

* E-mail: joshua.pomeroy@nist.gov

ELECTRONIC INTERACTIONS OF VERY SLOW IONS AT SOLID SURFACES

P. Bauer, D. Primetzhofer, S.N. Markin, M. Spitz, D. Göbl and S. Rund*

Institut für Experimentalphysik, Johannes Kepler Universität Linz, Linz, Austria

...

1. INTRODUCTION

Electronic interactions of ions, like electron-hole pair excitation or charge exchange can be understood only when the properties of valence/conduction electrons of the target in the presence of the ion are known. In this contribution, selected aspects of electronic interactions are discussed for light ions in the Low Energy Ion Scattering (LEIS) regime, i.e. for ions at a velocity $v \ll v_F$ (where v_F denotes the Fermi velocity of the solid).

2. ELECTRONIC INTERACTIONS

2.1. Electronic stopping

In noble metals (Au, Cu), the contributions of excitations of sp- and d-electrons to the stopping power were investigated. A clear threshold velocity v_{th} for excitation of d-electrons is observed, $v_{th} \approx 0.18$ a.u., as anticipated for a binary collision [1, 2]. In insulators (LiF, AlF3, KCl, SiO_2) velocity-thresholds for the excitation of electron-hole-pairs are found [3, 4], e.g. ~ 0.1 a.u. for LiF – much lower than expected from the unperturbed band-structures of insulators and metals.

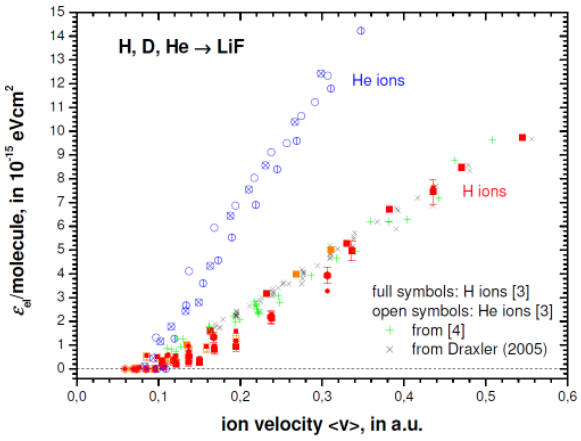

Figure 1: Electronic stopping cross section of LiF per molecule for H- and He-ions.

2.2. Charge exchange of He^+ ions at surfaces

For charge exchange of He^+ ions, two types of processes are relevant: Auger neutralization (AN), and collision induced processes, i.e. reionization (CIR) and neutralization (CIN). Experiments in the AN regime yield a pronounced dependence of the ion fraction P^+ on the crystallographic orientation for noble metal crystals (Cu, Au) [5]. In the CI regime a surprisingly large information depth was observed for single crystals in random scattering geometry. In order to regain surface sensitivity in LEIS, information is needed on the energy dependences of the probabilities for neutralization and reionization, P_{CIN} and P_{CIR}. With these quantities, the information depth can be modelled in a quantitative way.

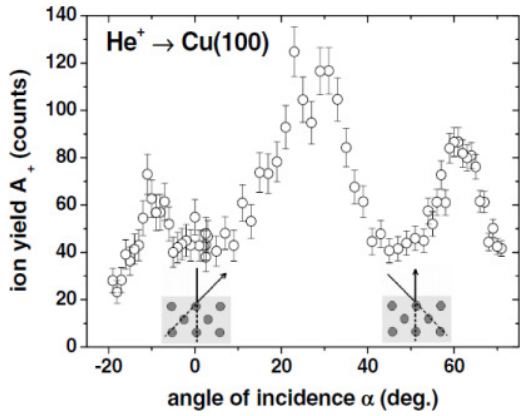

Figure 2: Yield of 6 keV He^+ ions scattered from Cu(110).

3. REFERENCES

[1] J.E. Valdés, J.C. Eckardt, G.H. Lantschner, and N.R. Arista, Phys. Rev. A 49 (1994) 1083.
[2] S.N. Markin, D. Primetzhofer, S. Prusa, and P. Bauer, Phys. Rev. B 78 (2008) 195122.
[3] S.N. Markin, D. Primetzhofer and P. Bauer, Phys. Rev. Lett. 103 (2009) 113201.
[4] L.N. Serkovic Loli, E.A. Sánchez, O. Grizzi, N.R. Arista, Phys. Rev. A 81 (2010) 022902.
[5] D. Primetzhofer, S.N. Markin, J.I. Juaristi, E. Taglauer, P. Bauer, Phys. Rev. Lett. 100 (2008) 213201.

* E-mail: peter.bauer@jku.at

IRRADIATION-INDUCED PHENOMENA IN CARBON AND BORON-NITRIDE NANOSTRUCTURES

A.V. Krasheninnikov[*]

Department of Physics, University of Helsinki, and Department of Applied Physics, Aalto University, Finland

1. INTRODUCTION

Recent experiments (see Refs. [1,2] for an overview) on ion and electron bombardment of nanostructures demonstrate that irradiation can have beneficial effects on such targets and that electron or ion beams can serve as tools to change the morphology and tailor mechanical, electronic and even magnetic properties of various nanostructured materials. It is also evident from the data obtained so far that the conventional theory of defect production in bulk materials not always works at the nanoscale or it requires considerable modifications.

We systematically study irradiation effects in nanomaterilas, including graphene, carbon nanotubes and other forms of nano-structured carbon. By employing various atomistic models ranging from empirical potentials to time-dependent density functional theory we simulate collisions of energetic particles with carbon nanostructures and calculate the properties of the irradiated systems. In this talk, our latest theoretical results on the response of graphene and carbon nanotubes to irradiation will be presented, combined with the experimental results obtained in collaboration with several groups, Fig. 1. The electronic structure of defected graphene sheets with adsorbed transition metal atoms will be discussed, and possible avenues for tailoring the electronic and magnetic structure of graphene by irradiation-induced defects and impurities will be introduced. The effects of ion and electron irradiation on boron-nitride sheets and nanotubes will also be touched upon. Finally, the irradiation response of mechanically strained carbon nanotubes and silicon nanowires will be addressed.

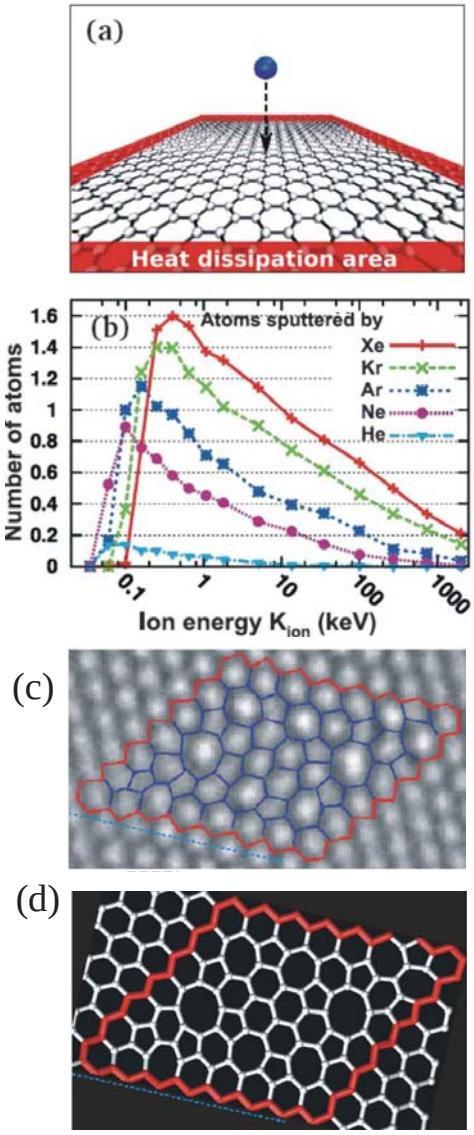

Figure 1: Graphene under ion and electron irradiation. (a) Simulation setup in ion bombardment simultions. (b) Number of sputtered carbon atoms as a function of ion energy. (c) Experimental high-resolution transmission electron microscopy image of irradiated graphene (Courtesy of J. Meyer). (d) Atomistic simulations of the structure shown in panel (c).

2. REFERENCES

[1] Krasheninnikov A. V. and Banhart F., Nature Materials, 6, 723 (2007).
[2] Krasheninnikov A. V. and Nordlund K., J. Appl. Phys. (Appl. Phys. Reviews), 107, 071301 (2010).

[*] E-mail: akrashen@acclab.helsinki.fi

LIGHT EMISSION FROM ION-IRRADIATED SRTIO$_3$

Marika Schleberger[1,*], *Marcel Ruth*[2], *Marko Karlušić*[3] *and Thorsten Peters*[1]

[1] Universität Duisburg-Essen (Germany)
[2] Universität Paderborn (Germany)
[3] Institut *Ruder Bošković*, P.O. Box 180, 10002 Zagreb (Croatia)

Perovskite-type structured compounds with the chemical formula ABO$_3$ (A and B are cations while O is the oxygen anion) are useful in a broad range of electronic applications. Highly charged ions offer a unique possibility for modifications of these materials on a nanometer scale. In recent years many experiments have been performed to investigate such structural surface modifications [1]. As a result one can state that, within certain limits, highly charged ions are a reliable tool for taylored material modifications.

Due to the fast energy dissipation of the incoming ion no direct observation of the involved processes like electron transitions or melting of the crystal lattice is possible (so far). Parameters which cannot be measured directly, like the strength of the electron-phonon-coupling, have to be estimated by the evaluation of AFM measurements [2].

On the other hand photoluminescence (PL) has been proven to be a useful method for investigations of material properties, especially for modified materials and SrTiO$_3$ [3]. The creation of new electronic states after ion irradiation allows the emittance of photons with energies corresponding to the energy level of the states inside the bulk material. A further major advantage of PL is its high sensitivity. Therefore, the material modification due to single ion impact can be investigated.

The SrTiO$_3$ single crystals were irradiated by Xe^{q+} ions extracted directly out of the DRESDEN-EBIT with a kinetic energy of $8\ \mathrm{keV} \cdot q$. For an average charge state of $q = 36$ the potential energy is about 28 keV and the kinetic energy is about 288 keV. For the investigation of single ion impact the fluence was chosen to be roughly about 10^{10} ions/cm^2.

For the PL we used a HeCd-Laser emitting at 325 nm.

PL spectra taken of irradiated and unirradiated samples show a significant change in the emittance behaviour. For the spectra taken at room temperature one can find the dominant light emission at about 530 nm. This value is in good agreement with PL found for amorphous SrTiO$_3$ at room temperature [4]. A less intense but also significant emission can be found at about 425 nm. The origin of these photons can be traced back to electronic excitations caused by oxygen deficiency as reported in recent work [5]. We find that the emission intensity at 425 nm does not increase as expected for low temperatures. This may be an indication for different energy dissipation processes as discussed in [5].

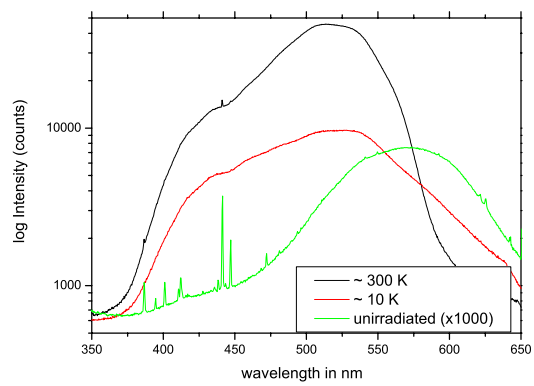

Figure 1: PL spectra of (un-)irradiated SrTiO$_3$, taken at 10 K and 300 K. The spectrum for the unirradiated sample was scaled by a factor of about 1000.

1. REFERENCES

[1] F. Aumayr, A.S. E-Said and W. Meissl, NIM B **266**, 2729 (2008).

[2] M. Karlusic, S. Akcöltekin, O. Osmani, I. Monnet, H. Lebius, M. Jaksic and M. Schleberger, NJP **12** 043009 (2010).

[3] R. Leonelli and J.L. Brebner, Phys. Rev. B **33**, 8649 (1986)

[4] F.M. Pontes, E. Longoa, E.R. Leite, E.J.H. Lee, J.A. Varela, P.S. Pizani, C.E.M. Camposc, F. Lanciotti, V. Mastellaro and C.D. Pinheiro, Materials Chemistry and Physics **77** 598602 (2002)

[5] D. Kan, T. Terashima, R. Kanda, A. Masuno, K. Tanaka, S. Chu, H. Kan, A. Ishizumi, Y. Kanemitsu, Y. Shimakawa and M. Takano, nature materials **4**, 816-819 (2005)

* E-mail: marika.schleberger@uni-due.de

Li^+ ION NEUTRALISATION ON Au(111), Ag(111) AND Ag LAYERS GROWN ON Au(111)

Lin Chen[1], Javier Fhur[2], V.A.Esaulov[1] and M. L. Martiarena[2]

[1]Laboratoire des Collisions Atomiques et Moléculaires, (UMR CNRS - Université Paris-Sud 8625), 91405 Orsay Cedex, FRANCE
[2] CONICET*, and Instituto Balseiro, Centro Atómico Bariloche, Bustillos 9500, 8400 Bariloche, Argentina

Electron transfer processes on surfaces, that play an important role in surface chemistry and influence charge states of ions or atoms scattered on surfaces, have been quite extensively investigated in the past[1]. Recently a renewed activity has developed in relation with some theoretical work, which pointed out that energies and widths of atomic states for fixed atom-surface distance are strongly affected by the existence of band gaps and surface states[2].

Besides, new studies of alkali ion neutralization revealed a very curious feature, which is not understandable in "standard" models. In the limit of complete surface coverage by Au(111) type films it was observed that efficient neutralization of Li occurs. Usual chemisorption calculations [3] corresponding to fairly large (>5au) distances from the surface, show that the alkali metal projected density of states lies above the Fermi level. Similarly, the "upward" image potential induces a shift of the Li(2s) level to lower binding energies, placing it above the Fermi level. Therefore, one can expect that electron capture will be very inefficient for surfaces with work functions of the order of 5 eV and higher. Considering these ideas, the result for the gold film was very surprising. In an endeavour to understand this feature it was performed measurements of Li^+ neutralization on Cu(100), Cu(111), Au(111) and Au(100) surfaces [4]. Such experiments revealed that consistently neutralization is "anomalously" large on these surfaces.

The existence of the L band gap for (111) surfaces was also invoked to allow for larger survival rates for neutralised Li as well as non resonant charge exchange [4] involving surface states. More recent theoretical work of the Li-Cu surface showed that the Li level at distances below 4 au from the first atomic plane shifts again *below* the Fermi level. In this model instead of considering the survival of a Li^+ ion receding from the surface, in scattering one in fact needs to consider neutralization in the ingoing part of the collision and thereafter first reionization and then survival of the Li^+ ions. Thismodel remains incomplete and has been unable to reproduce the features of neutralization changing the metal and the behaviour at low scattering energies. This situation precludes further investigation into nanostuctured systems, since understanding of the simpler case of bulk surfaces is an essential prerequisite.

In view of all these developments we investigate the Li^+ neutralisation on Au(111), Ag(111) and Ag layers grown on Au(111).

We have carried out DFT calculations within the slab-supercell approach by using the ab-initio total energy and molecular dynamics program VASP[6].

To describe the alkali ion neutralization we consider the equation:

$$n(\infty, Eo) = e^{-\int W(z)dz/v_z}\left(Q(z_0) + \int_{z_0}^{\infty} Q_{eq}(z) e^{\int_{z_0}^{z} W(z')dz'/v_z} dz/v_z\right)$$

We use the Bader method [7] to calculate the Li atom charge $Q_{eq}(z)$ (see Fig. 1). Considering the projected density of state, the spatial charge distribution and the L band gap for Li/metal as a function of the Li distance to the surface, we evaluate the transition probability $W(z')$.

The results allow us to explain the main characteristic of the experimental results.

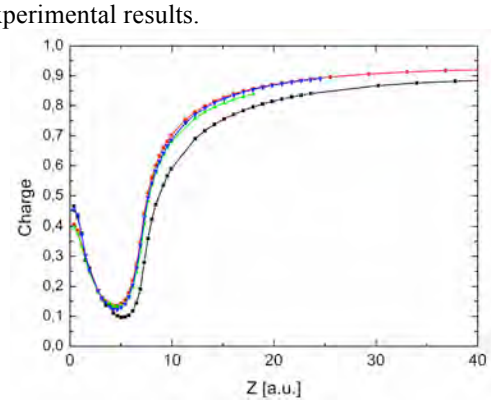

Fig. 1: Li Charge vs distance to the top most metal layer.
■ Au(111); ● Ag(111); ▲ Ag-Au(111); ▼Cu(111).

[1] E. S. Parilis et al, (Elsevier, Amsterdam, (1993)).
[2] A. G. Borisov et al, Phys. Rev. B 65, 235434, (2002); A.R.Canario et al Phys. Rev. B 71, 121401, (2005)
[3] M. Scheffler and C.Stampfl in Handbook of Surface Science, Vol. 2, p.286-356, Elsevier, Amsterdam, 2000
[4] A R Canário et al New J. Phys. 8, 227,(2006)
[5] E. A. García, et al, Surface Science, 603, 597, 2009
[6] G. Kresse and J. Furthmüller, Comput. Mater. Sci. 1996, 6, 15.
[7] E. Sanville, et al *J. Comp. Chem.* **28** 899-908 (2007).

E-mail: mluz@cab.cnea.gov.ar
*Consejo Nacional de Ciencia y Tecnologia

Tuesday, September 28, 2010

Heavy Ion Beam Pelletron Systems

TERMINAL POTENTIALS FROM BELOW 1MV TO ABOVE 25MV

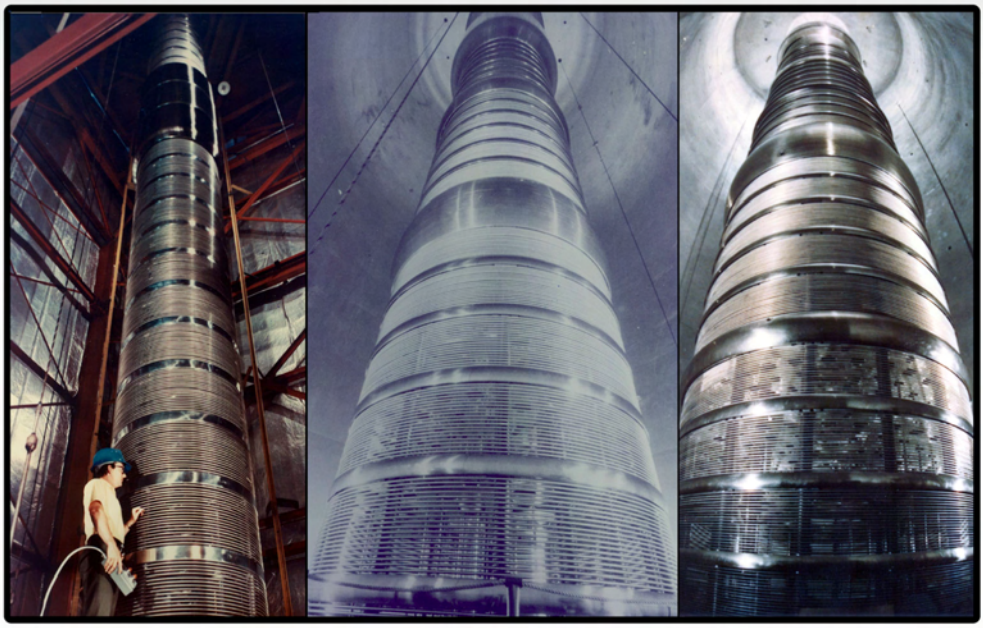

Australian National University
14MV tandem Pelletron
Model 14UD

Japan Atomic Energy Agency
20MV folded tandem Pelletron
Model 20UR

Oak Ridge National Lab
25MV folded tandem Pelletron
Model 25URC

For Applications Involving:
Nuclear Structure and Astrophysics Research
Materials Analysis and Modification
High Energy Proton Microprobes
Accelerator Mass Spectrometry

Complete systems for RBS, Channeling, μRBS, HR-RBS, PIXE, ERDA, NRA, and AMS

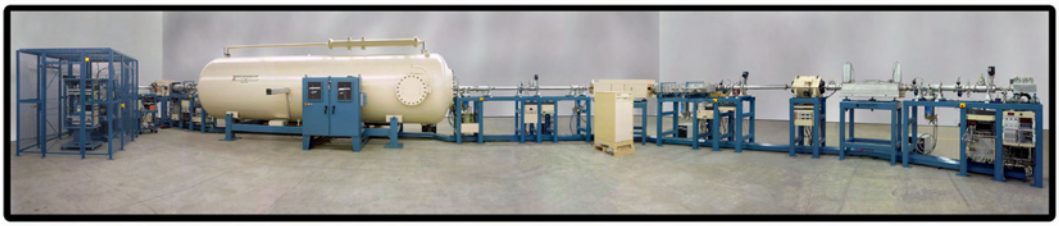

5MV tandem Pelletron for Accelerator Mass Spectrometry

National Electrostatics Corp.
7540 Graber Road, P.O. Box 620310 Middleton, WI 53562-0310 USA
Telephone: (608) 831-7600 | Fax: (608) 831-9591 | Email: nec@pelletron.com | Website: www.pelletron.com

ATOMISTIC SIMULATIONS OF PARTICLE-SURFACE INTERACTIONS

K. Nordlund, C. Björkas, K. Vörtler, A. Meinander, A. Lasa and M. Mehine

Department of Physics, P. O. Box 43, 00014 University of Helsinki, FINLAND

1. ATOMISTIC SIMULATIONS OF PARTICLE-SURFACE INTERACTIONS

Interactions between energetic ions and electrons with a material occur in a multitude of situations, ranging from industrial ion implanters to fusion reactors, arc plasmas and the interaction of the solar wind with moons. Common to all of these situations is that they can – and have been – studied with atom-level molecular dynamics simulations.
In the first part of my talk, I will start by presenting the classical molecular dynamics method and examples of its application to particle-surface interactions. I will also discuss the limitations, especially regarding electronic excitations, and discuss recent efforts to include these on some level in the simulations.

2. PLASMA-SURFACE INTERACTIONS IN FUSION REACTORS

In the second part of my talk I will present recent work on using molecular dynamics simulations to examine plasma-surface interactions in tokamak-like fusion reactors.

2.1. Carbon

Numerous experiments have shown that carbon-based materials can sputter chemically by low-energy H isotope bombardment in fusion reactors, at energies where physical sputtering is impossible [1]. At high temperatures this can be understood to be due to thermally activated desorption. At low temperatures the sputtering can be understood in terms of the swift chemical sputtering mechanism, in which an incoming D penetrates into an energetically unfavourable state between two carbon atoms, leading to bond breaking [2, 3]. The process is endothermal, but can occur athermally enabled by the kinetic energy brought in by the ion. We described this mechanism initially in 1999 [4]. Since then several groups have simulated the same process [3, 5, 6], and it has also received strong support from experiments [3, 7, 8].

2.2. Metals and metal carbides

Metals have in general not been observed to show as pronounced chemical sputtering by low-energy H ions as carbon-based materials, and we argued earlier that the swift chemical sputtering mechanism would not be significant in metals since they have much more neighbours than covalently bonded materials like C and Si [9]. However, we recently proved ourselves wrong by showing that even pure Be can sputter by the swift chemical mechanism [10]. Fortunately, from a fusion reactor point of view, the yields are much lower than in carbon.
We are now extending these studies to encompass the full range of elements relevant in ITER; namely Be, C and W as well as all their mixtures, to get a comprehensive view of the chemical sputtering in tokamaks. The initial results indicate that in addition to pure C and Be, any carbide sputters chemically. The most recent results will be discussed at the meeting.

3. REFERENCES

[1] J. Roth, in *Sputtering by Particle bombardment*, edited by R. Behrisch (Springer, Berlin, 1981), Vol. I, pp. 91–146.

[2] E. Salonen, K. Nordlund, J. Keinonen, and C. H. Wu, Phys. Rev. B **63**, 195415 (2001).

[3] P. S. Krstic, C. O. Reinhold, and S. Stuart, New J. Phys. **9**, 209 (2007).

[4] E. Salonen *et al.*, Phys. Rev. B (Rapid Comm.) **60**, 14005 (1999).

[5] J. Marian *et al.*, J. Appl. Phys. **101**, 044506 (2007).

[6] P. N. Maya, U. von Toussaint, and C. Hopf, New J. Phys. **10**, 023002 (2008).

[7] F. W. Meyer *et al.*, Physica Scripta **T128**, 50 (2007).

[8] E. de Juan Pardo *et al.*, Physica Scripta **T111**, 62 (2004).

[9] K. Nordlund, E. Salonen, A. V. Krasheninnikov, and J. Keinonen, Pure and Applied Chemistry **78**, 1203 (2006).

[10] C. Björkas *et al.*, New J. Phys. **11**, 123017 (2009).

* E-mail: kai.nordlund@helsinki.fi

INTERACTIONS OF FULLERENES DURING GRAZING SCATTERING FROM SURFACES

S. Wethekam[1,*], *H. Zettergren*[2], *H. Cederquist*[2], *M. Busch*[1], *U. Specht*[1], *J. Merck*[1], *Ch. Linsmeier*[3], *and H. Winter*[1]

[1] Institut für Physik, Humboldt-Universität zu Berlin, Newtonstr. 15, D-12489 Berlin, Germany
[2] Department of Physics, Stockholm University, SE-106 91 Stockholm, Sweden
[3] Max-Planck-Institut für Plasmaphysik, EURATOM Association, Boltzmannstr. 2, D-85748 Garching, Germany

1. INTRODUCTION

Recent work on the interaction of keV fullerene ions during grazing scattering from surfaces [1, 2] is reviewed. With experiments and theoretical models for charge transfer and excitation of internal degrees of freedom, we have studied the scattering of C_{60} and C_{70} ions from metal and insulator surfaces. The role of elastic properties and internal excitations of the fullerenes as well as the electronic structure of the surface is discussed.

2. EXPERIMENTS AND RESULTS

Charge transfer and excitation of internal degrees of freedom for keV C_{60}^{+} and C_{60}^{2+} as well as C_{70}^{+} ions scattered from atomically clean and flat metal and insulator surfaces under grazing angles is studied via angular, fragment, and charge state distributions. At low energies for the motion along the surface normal, fullerene ions are scattered nearly elastically, whereas for larger normal energies, energy dissipation is substantial with pronounced differences for metal and insulator surfaces.

We compare our results to classical trajectory calculations based on analytical bond-order potentials [1] and deduce the internal energy of scattered clusters from the analysis of fragments [3]. For metal surfaces, the loss of kinetic energy for the motion along the surface normal is completely transferred to internal excitations of the cluster, whereas for alkali halide surfaces, the interaction is more complex due to the ionic character of the surface [4]. Our data demonstrate that internal elastic properties of fullerenes can be strongly affected by a nearby surface. For scattering from a KCl(001) surface at larger energies, we find evidence for negative ion formation and post-collision multifragmentation [5].

From shifts of angular distributions for incident C_{60}^{2+} and C_{60}^{+} ions due to image charge interactions prior to neutralization, distances for charge transfer for C_{60}^{2+} ions in front of Al(001) and Be(0001) surfaces are deduced [6, 7]. These distances are consistent with a classical over-the-barrier model [8] indicating that the suppression of charge transfer, observed for atomic projectiles in front of metal surfaces with a projected band gap [9], is absent for fullerenes. This effect is attributed to the shape of the tunneling barrier and the spatial extension of the molecule.

* E-mail: stephan.wethekam@physik.hu-berlin.de

3. ACKNOWLEDGEMENTS

Financial support by the Deutsche Forschungsgemeinschaft (DFG) (Project No. Wi 1336) and the Swedish Research Council is gratefully acknowledged. We thank K. Maass and A. Schüller for their assistance in the preparation of the experiments.

4. REFERENCES

[1] E.E.B. Campbell and F. Rohmund, Rep. Prog. Phys. **63**, 1061 (2000).

[2] H. Winter, Phys. Rep. **367**, 387 (2002).

[3] S. Wethekam and H. Winter, Phys. Rev. A **76**, 032901 (2007).

[4] T. Matsushita, K. Nakajima, M. Suzuki, and K. Kimura, Phys. Rev. A **76**, 032903 (2007).

[5] A. Kaplan, A. Bekkerman, B. Tsipinyuk, and E. Kolodney, Phys. Rev. B **79**, 233405 (2009).

[6] S. Wethekam, H. Winter, H. Cederquist, and H. Zettergren, Phys. Rev. Lett. **99**, 037601 (2007).

[7] S. Wethekam, H. Zettergren, Ch. Linsmeier, H. Cederquist, and H. Winter, Phys. Rev. B **81**, 121416(R) (2010).

[8] H. Zettergren *et al.*, Phys. Rev. A **66**, 032710 (2002).

[9] J.P. Gauyacq, A.G. Borisov, and M. Bauer M, Prog. Surf. Sci. **82**, 244 (2007).

SPUTTERED NEUTRAL Si_xC_y CLUSTERS AS A MONITOR FOR CARBON IMPLANTATION DURING C_{60}^+ BOMBARDMENT OF SILICON

A. Wucher[*], *A. Kucher*[§], *N. Winograd*[§], *C.A. Briner*[#] *and K. D. Krantzman*[#]

*Fakultät für Physik, Universität Duisburg-Essen, 47048 Duisburg, Germany
[§]Department of Chemistry, The Pennsylvania State University, University Park, PA 16802, USA
[#]Department of Chemistry and Biochemistry, College of Charleston, Charleston, SC 29424, USA

1. INTRODUCTION

The bombardment of silicon with energetic C_{60}^+ cluster ions leads to the incorporation of carbon into the Si target [1]. Many Si clusters of varying sizes are sputtered from the surface. However the carbon atoms are only sputtered within Si_xC_y clusters with various Si to C ratios. In principle, one would expect the distribution of x and y among these clusters to be related to the chemical composition of the surface, which evolves with accumulating projectile ion fluence until eventually a steady state is reached. In a recently published study, Henkel and coworkers therefore investigated the yield distribution of Si_xC_y+ secondary cluster ions as a function of C_{60}^+ fluence [2]. The results were interpreted in terms of recent molecular dynamics (MD) simulations of C_{60} bombardment of silicon [3].

An important question that remained unanswered in ref. [2] is to which extent the measured secondary ion yields reflect the true composition of the sputtered material. It is well known that the majority of the sputtered particles are emitted as neutrals. Moreover, it has been established many times that ionization probabilities of sputtered clusters may well depend on the cluster size. Since the MD simulations cannot predict the ionization state of the emitted particles, the results of such calculations should in principle be compared to the yield distribution of sputtered *neutral* clusters rather than secondary ions.

In the present work, we therefore used a high-intensity infrared laser photoionization scheme in order to detect the sputtered neutral Si_xC_y clusters and compare the resulting yields to those measured for the corresponding secondary ions. The neutral yield distributions are compared to the outcome of recent MD simulations modeling the effects of accumulating C_{60} fluence onto a silicon surface [4].

2. EXPERIMENT AND SIMULATIONS

The experiments were performed using a high intensity femtosecond laser system [5] delivering approximately 0.4 mJ of energy into a pulse of 120 fs duration at a wavelength of 1450 and 1785 nm. The idea is to operate in the field ionization regime in order to minimize photofragmentation during the post-ionization process.

The MD simulations were performed with successive impacts of 20-keV C_{60} impinging at normal incidence onto a reconstructed Si(100) surface. In order to model the effects of accumulating fluence, the surface was equilibrated after each impact, and the next impact was aimed at an arbitrary point on the modified surface [4].

3. RESULTS

The experimental results reveal that the neutral cluster distribution is quite different from that of the corresponding secondary ions. Therefore, these experiments show that the ionization probability of the sputtered clusters depends strongly on their composition and the distribution of the sputtered ions cannot be evaluated relative to results from the MD simulations. In this paper, measured neutral yield distributions of sputtered Si_xC_y clusters are compared with data predicted by the MD simulations. The implications to the changing composition of the Si target as a function of projectile fluence is discussed.

4. REFERENCES

[1] G. Gillen et al, Appl. Surf. Sci **252** , 6521 (2006).
[2] I. Lyon, T. Henkel, D. Rost, to appear in Appl. Surf. Sci. (2010)
[3] K.D. Krantzman, B.J. Garrison, J. Phys. Chem. C **113**, 3239 (2009).
[4] K.D. Krantzman, A. Wucher, J. Phys. Chem. C **114**, 5480 (2010).
[5] D. Willingham, D.A. Brenes, A. Wucher, N. Winograd, J. Phys. Chem. C **114**, 5391 (2010).

[*] E-mail: Andreas.Wucher@uni-due.de

ION INTERACTIONS WITH CARBON NANO-STRUCTURES

Z. L. Miskovic*

Department of Applied Mathematics, University of Waterloo, Waterloo, Ontario, Canada N2L 3G1

1. INTRODUCTION

Investigation into the properties of carbon nano-structures, involving fullerene molecules, carbon nanotubes (CNTs), and the recently contrived graphene has been growing at a relentless rate for several years owing to the many exciting prospects of their applications in nanotechnology. Interaction with particle beams has been an important part of this research endeavor, e.g., in the context of probing plasmon excitations in those structures by using electron energy loss spectroscopy (EELS) [1]. In addition, the use of energetic electron and ion beams has recently emerged as novel engineering tool for modification of the atomic structure with the goal of changing and controlling the electronic properties of carbon nano-materials (as reviewed in [2]). However, ion interaction with CNTs and graphene under conditions where no atomic-scale defects are produced is still relatively unexplored area that can benefit from using the accumulated knowledge in the field of inelastic ion-surface collisions.

2. CARBON NANOTUBES

Large hollow regions in individual CNTs, as well as high degree of their atomic ordering and alignment within nanotube ropes or bundles, provide unique possibility for achieving the effect of particle channeling. Having in mind the broad range of possible applications, a number of theoretical studies appeared recently dealing with ion channeling through CNTs at energies from keV to TeV (as reviewed in [3]). Because of high ion energies and the extended range of ion interaction with CNTs (on the order of nanotube length), it was necessary to implement tractable models for their electronic response, such as a two-dimensional, two-fluid hydrodynamic model that takes into account the different nature of the σ and π electrons in CNTs [4]. While using this model in the context of ion channeling revealed a prominent role played by the dynamic image interaction with CNTs, which was not noticed in ordinary crystals [5], the two-fluid model also showed its merits in studying the plasmon excitation in single-walled CNTs due to aloof interaction with charged particles under oblique angles of incidence [1], as well as in studying the propagation of electromagnetic radiation through CNTs [6].

* E-mail: zmiskovi@uwaterloo.ca

3. GRAPHENE

Ion irradiation effects at high impact energies are much less studied in graphene than in CNTs, mostly due to complications arising from supporting substrate on which graphene layers are usually deposited by using mechanical exfoliation or epitaxial growth. On the other hand, prospects of sensor applications of graphene-based field-effect transistors have prompted recent interest in interactions with ions moving at low energies, where the electronic response of graphene is dominated by the peculiar structure of its π electron bands. By using Mermin's modification of graphene's dielectric function in random phase approximation, one reveals strong effects in ion stopping due to the inter-band electron excitations at low doping levels of graphene, as well as due to the coupling of graphene's π plasmon mode with optical phonons in the substrate at high doping levels [7, 8]. Furthermore, one finds surprisingly strong non-linear effects in both screening and image interaction of charged impurities near graphene [9] that may affect graphene's conductivity and the image potential states on its surface [10].

4. REFERENCES

[1] C. Kramberger *et al.*, Phys. Rev. Lett. **100**, 196803 (2008).

[2] A.V. Krasheninnikov and F. Banhart, Nature Materials **6**, 723 (2007).

[3] Z.L. Miskovic, Radiat. Eff. Def. Solids **162**, 185 (2007).

[4] D.J. Mowbray, Z.L. Miskovic, and F.O. Goodman, Phys. Rev. B **74**, 195435 (2006).

[5] D. Borka *et al.*, Phys. Rev. A **77**, 032903 (2008).

[6] A. Moradi, Optics Commun. **283**, 160 (2010).

[7] K. F. Allison and Z. L. Miskovic, Nanotechnology **21**, 134017 (2010).

[8] Y. Liu and R.F. Willis, Phys. Rev. B **81**, 081406(R) (2010).

[9] M. Ghaznavi, Z.L. Miskovic, and F.O. Goodman, Phys. Rev. B **81**, 085416 (2010).

[10] S. Bose *et al.*, New J. Phys. **12**, 023028 (2010).

HCI induced secondary electron yields from thin films of C60

E. Bodewits, H. Bekker, A.J. de Nijs, and R. Hoekstra
KVI – Atomic and Molecular Physics, University of Groningen,
Zernikelaan 25, 9747 AA Groningen, the Netherlands

D. Winklehner, B. Daniel, G. Kowarik, K. Dobes and F. Aumayr
Institut für Allgemeine Physik, Technische Universität Wien,
A - 1040 Vienna, Austria

1. INTRODUCTION

The multi-electron dynamics of slow highly charged ions on surfaces depends strongly on the electronic structure of the surface as is known from comparing metallic and insulating surfaces. Using thin films of metals on insulators or the other way around one may be able to study in a controlled manner the transition from insulator to conductor behavior by means of electron emission yields. In order to investigate these processes for the highest possible charged ions, which will become available at the HITRAP facility at GSI, the so called IISIS (Inelastic Ion Surface Interactions Set-up) has been build and is now being tested at KVI. The whole experiment can be floated on high voltage allowing for the deceleration of the incoming highly charged ions. This would allow the ions delivered by HITRAP to be decelerated down to basically 0 eV, giving access to extremely slow, fully stripped ions.

In order to measure the secondary electron yield IISIS is equipped with an electron statistics detector supplied by the TU Wien group and a quartz microbalance and an e-beam evaporator to produce controllably thin films.

To test the experimental procedures and evaporator and detector systems we have started measurements on C60 films on a Au substrate. For this combination well established recipes for producing a single monolayer exist.

The preliminary results of secondary electron yields for impact of multiply charged xenon ions on Au show that the yield is increasing with increasing layer thickness of the C60. The question of why this is so remains to be answered; is it the particular density of states of the C60 or is it the enlarged escape depth of the electrons from an insulator material?

* E-mail: ebodewits@kvi.nl

Molecular Dynamics Simulations of Multi-Impact Bombardment of Si with 20 keV C_{60} with Applications to Depth Profiling Experiments

K. D. Krantzman, C. A Briner*, E. L. Cook*, B. J. Garrison[§] and A. Wucher[#]*

*Department of Chemistry and Biochemistry, College of Charleston, Charleston, SC 29424, USA
[§]Department of Chemistry, The Pennsylvania State University, University Park, PA 16802, USA
[#] Fakultät für Physik, Universität Duisburg-Essen, 47048 Duisburg, Germany

1. INTRODUCTION

C_{60} ion beams have been successful for high resolution sputter depth profiling of metallic multilayer structures. However, when applied to Si, sputter depth profiling experiments by Gillen, et al. [1] have shown unique results. Previous molecular dynamics (MD) simulations of single impacts of C_{60} on a Si surface have been able to explain some of the unusual observations [2]. Strong bonds can be formed between projectile C atoms and substrate Si atoms, which lead to nearly all of the atoms from the projectile being incorporated into the surface.

The insights gained from these single-impact MD simulations are limited because they cannot model the cumulative result of successive bombardments on the surface. In this presentation, the results of multiple-impacts of 20-keV C_{60} at normal incidence on a single Si microcrystallite are presented. In order to isolate the effect of Si-C bond formation, these results are compared to those obtained from simulations calculated without any Si-C attractive potential energy terms [3].

2. MD SIMULATIONS

The simulations use a "divide and conquer" scheme developed by Russo, et. al. [4] developed to treat multiple projectile impacts on the same surface area. The Si sample is successively bombarded by 20-keV C_{60} projectiles at normal incidence using a set of impact points chosen randomly over the entire surface of a large master Si crystal. The trajectory for each impact point is run using a smaller cylindrical sample extracted from the master crystal and then reinserted after the trajectory is complete. An empirical many body potential developed by Tersoff is used to model the Si-Si, C-C and Si-C interactions.

3. RESULTS

Successive bombardment of C_{60} on the Si substrate results in a significant change in the surface topography. When the C_{60} projectile bombards the fresh undisturbed surface, the impact produces a crater centered at the impact, which is surrounded with a rim of Si atoms. The static limit occurs at ~ 10 impacts, where there is still little overlap between the disturbed regions. Once C_{60} bombards regions already disturbed by former impacts, a complex and ever changing topography evolves. In addition, nearly all of the C atoms from the projectile form bonds with Si substrate atoms and are incorporated into the Si lattice, which results in a change in chemical composition of the surface as a function of projectile fluence.

A statistical sputtering model developed from fundamental principles is coupled with data calculated from the MD simulations to extrapolate the results from the simulations to higher fluences [5]. A major finding from these studies is that the statistical nature of the sputtering process has a significant effect on the achievable depth resolution. The optimum delta layer response width for Si is estimated to be about 3 nm, while corresponding values of the order of 10 nm are predicted for molecular systems.

4. REFERENCES

[1] G. Gillen et al, Appl. Surf. Sci. 252, 6521 (2006).
[2] K. D. Krantzman, D. B. Kingsbury, B. J. Garrison, Appl. Surf. Sci. 252, 6463 (2009).
[3] K. D. Krantzman, B. J. Garrison, Surf. Interface Anal., DOI 10.1002/sia.3438 (2010).
[4] M. F. Russo, Jr., Z. Postawa, Z.; B. J. Garrison, J. Phys. Chem. C 114, 3270 (2009)
[5] K.D. Krantzman, A. Wucher, J. Phys. Chem. C 114, 5480 (2010).

* E-mail: krantzmank@cofc.edu

LARGE THIRD-ORDER OPTICAL NONLINEARITY OF METAL-COLLOIDS IN SILICA GLASSES SYNTHESIZED BY ION IMPLANTATION

Binita Ghosh and Purushottam Chakraborty*

Saha Institute of Nuclear physics
1/AF Bidhannagar, Kolkata 700 064
INDIA

Ion implantation has become a versatile and powerful technique for synthesizing high-density nanometer-sized metal colloids in fused silica glasses and the high precipitate volume fraction and small size of these nanoclusters in glasses lead to the generation of third-order susceptibility (Kerr susceptibilities) much greater than those formed by melt-glass fabrication. Future opportunities in optical switching and information processing depend critically on the development of improved photonic materials with enhanced Kerr susceptibilities, as these materials are still in a relatively early stage of development.

These metal nanoclusters are zero-dimensional particles (known as quantum dots) with diameters much smaller than the wavelength of light. Electrons in QDs are confined between infinite potential barriers and leads to the decomposition of bulk conduction and valence bands into a set of discrete levels. Thus, the oscillator strengths of many continuous states are concentrated in a few discrete states. The non-linear response of QD materials arises from saturable absorption at the excitonic levels. This effect drastically modifes the quantum states of the electrons and their interaction with applied optical fields; it is referred to as quantum confinement. Second, when the size of the nanoclusters is much smaller than the wavelength (λ) of the applied optical field (i.e. for clusters with diameters less than $\lambda/20$), the electric field that acts on and polarizes the free charges of these clusters can be vastly different from the macroscopic field outside the metal clusters in the surrounding medium. This polarization, in turn, modifies the dielectric constant of the composite medium. This effect is called dielectric or classical confinement. Owing to the difference in dielectric constants between the QDs and the surrounding host material, local field effects arising from dielectric confinement strongly influence the optical properties and can produce major changes in optical response.

We have synthesized metal (Ni, Ag, Au, Cu, etc) nanoclusters in fused silica glasses by high current ion implantation and the formation of colloidal particles is evidenced by an absorption band, revealed in the linear optical absorption measurements in the UV-visible range, at the characteristic surface plasmon resonance (SPR) frequency of the metal. Heat treatments on the metal-implanted silica glasses give pronounced effects on the formation of the metal colloids of larger sizes through aggregation of the implanted metal atoms, arising out of greater mobility of the metal atoms under heating or due to the formation of metal oxide clusters under beam induced mixing. Either of the two effects can be manifested by a shift of the SPR band towards higher wavelength. It has been demonstrated that metal nanoclusters of various sizes can be safely created in 'as implanted' as well as in annealed glass samples, as evidenced by the pronounced optical absorption bands in both the cases. Rutherford Backscattering spectrometry (RBS) has been used to measure the concentrations of these nanoclusters as a function of depth of the materials.
Nonlinear optical techniques like Z-scan and ARINS (Anti-resonant Interferometric Nonlinear Spectroscopy) have been used for accurate measurements of nonlinear optical responses. The sign of the nonlinear refraction is readily obtained from Z-scan signature. The nonlinear refractive index, nonlinear absorption coefficient, and the real and imaginary parts of the third-order nonlinear susceptibility were extracted. The innovative ARINS technique utilizes the dressing of two unequal intensity counter-propagating pulsed laser beams with differential nonlinear phases that occur upon traversing the sample. The difference in phase manifests itself in the intensity-dependent transmission. The photo-detection of the transmission of the ARINS signal yields spatially and temporally integrated response.

* E-mail: purushottam.chakraborty@saha.ac.in

MULTI-ELECTRON EFFECTS IN LOW ENERGY Sr^+ ION SCATTERING

*X. He and J.A. Yarmoff**

Department of Physics and Astronomy, University of California, Riverside, CA 92521 USA

1. INTRODUCTION

A system of many electrons can display emergent phenomena that cannot be extrapolated from the behavior of independent electrons. A method for triggering this behavior is to introduce a spin impurity into a metal, which then causes the free electrons to respond collectively. This arrangement can be modeled by low energy ion scattering (LEIS) experiments that employ a projectile with an unpaired valence electron [1,2], such as a singly charged alkaline earth metal ion. Here, we report measurements of the neutralization of scattered Strontium ions (Sr^+) from polycrystalline gold (Au) as a function of surface temperature, which shows clear evidence of electron correlations.

2. RESULTS

The spin of the single valence electron of a singly charged alkaline earth ion behaves as a magnetic impurity that interacts with the continuum of many-body excitations in the metal, resulting in Kondo and mixed valence resonances near the Fermi energy, as illustrated in Fig. 1 [1,2].

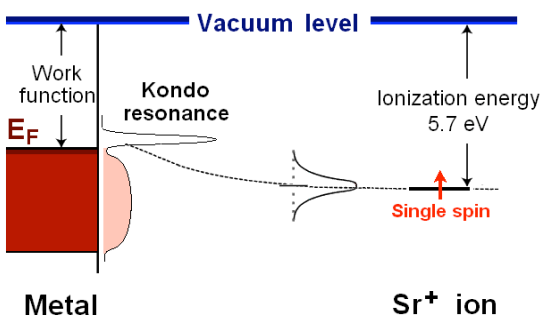

Figure 1. Schematic diagram showing the formation of a resonance at the Fermi energy when an isolated spin is in the vicinity of the surface.

The occupation of these resonances is acutely sensitive to the surface temperature, which leads to an anomalous temperature dependence of the ion neutralization probability.

Time-of-flight spectroscopy was used to obtain charge-resolved spectra of the 2-4 keV Sr^+ projectiles scattered from polycrystalline gold. Figure 2 shows the measured neutralization probability of the singly scattered projectiles as a function of surface temperature.

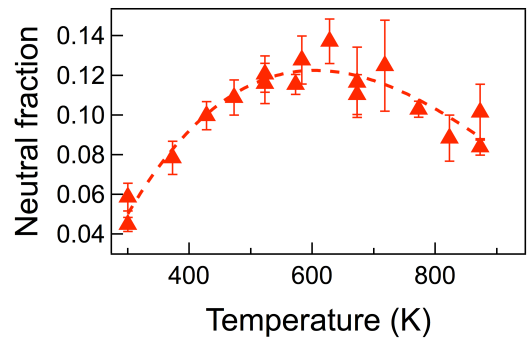

Figure 2. Neutralization probability of 2 keV Sr^+ scattered from clean Au as a function of surface temperature.

A maximum in the neutralization probability is observed near 600 K. The rise in neutralization with temperature below 600 K can be explained as the normal expectation as states above E_F are populated. The decrease above 600 K, however, can only be explained via correlated electron physics.

3. CONCLUSIONS

The role of correlated-electron effects has been established for the scattering of low energy alkaline earth ions from a solid surface. Correlated electron effects, which have traditionally been manifest at low temperature, are observable well above room temperature because the projectile's ionization level shifts and crosses the target's Fermi energy as it approaches the surface where the interaction between the localized and extended electrons is very strong. This is a new approach for investigating the electronic structure of complex materials, which could lead to a better understanding of collective phenomena in general.

4. REFERENCES

[1] H. X. Shao, P. Nordlander, and D. C. Langreth, Phys. Rev. Lett. **77**, 948 (1996).
[2] J. Merino and J. B. Marston, Phys. Rev. B **58**, 6982 (1998).

* E-mail: yarmoff@ucr.edu

POSTER PRESENTATIONS

SURFACE NANOSTRUCTURING OF $SrTiO_3$ SINGLE CRYSTALS BY SLOW HIGHLY CHARGED IONS AND SWIFT HEAVY IONS

A.S. El-Said[1,2], R. Heller[1], S. Fascko[1], C. Trautmann[3] and F. Aumayr[4*]*

[1] *Institute of Ion Beam Physics and Materials Research, Forschungszentrum Dresden-Rossendorf (FZD), 01328 Dresden, Germany*
[2] *Nuclear and Radiation Physics Lab, Physics Department, Faculty of Science, Mansoura University, 35516 Mansoura, Egypt*
[3] *GSI Helmholtzzentrum, 64291 Darmstadt, Germany*
[4] *Institute of Applied Physics, TU Wien - Vienna University of Technology, 1040 Vienna, Austria*

In many solids, the irradiation with swift heavy ions (SHI) of MeV – GeV energy leads to track formation along each ion trajectory and to nanometric surface hillocks on the impact sites. Both phenomena require that the electronic energy loss *dE/dx* of the projectile surpasses a certain material dependent threshold [1]. Recently, similar surface modifications have been demonstrated for the impact of individual slow highly charged ions (HCI), if their potential energy exceeds a critical value [2-4].

The striking similarity between the two cases is probably a result of the fact that both SHI and slow HCI initially transfer their energy to the electronic system of the target, leading to a region of high electronic excitation. In materials with strong electron-phonon coupling, this electronic excitation energy is effectively transferred to the target atoms, leading to pronounced lattice heating. Within this description, the formation of surface hillocks is ascribed to a melting process [2, 3].

In this contribution we irradiated single crystals of strontium titanate ($SrTiO_3$) with both slow highly charged Xe ions (1.29 keV/amu) extracted from an Electron Beam Ion Trap at FZD and swift Xe ions (11.2 MeV/amu) provided by the UNILAC (Universal Linear Accelerator) at GSI. The use of $SrTiO_3$ is motivated by its promising material properties such as high dielectric constant and easy growth of ultrathin layers on silicon, making $SrTiO_3$ interesting as an insulation material in microelectronics. It is also of special interest because multiple, equally spaced nanodots can be created by grazing incidence SHI irradiation [5, 6].

The irradiated surfaces were inspected by scanning force microscopy (SFM) revealing nanometric hillocks for SHI as well as HCI irradiated crystals (see e.g. fig. 1). The ones found for HCI irradiation are, however, somewhat smaller than the hillocks reported in [7]. Our results will be discussed in terms of the underlying creation mechanism driven by the different energy dissipation mechanisms.

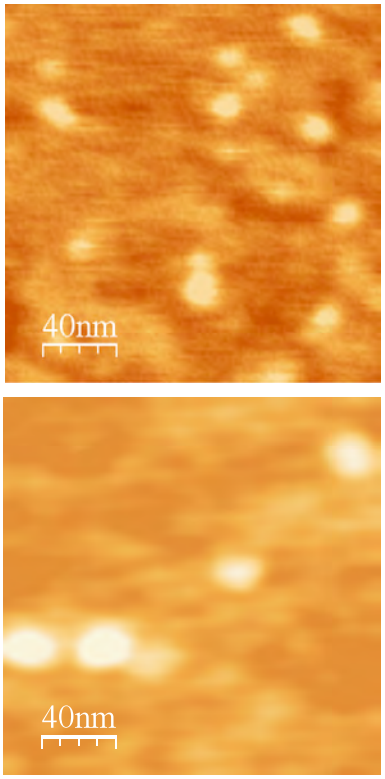

Figure 1: SFM topographic images of $SrTiO_3$ surfaces irradiated with 1.29 keV/amu Xe^{37+} ions (top), and 11.2 MeV/amu Xe ions (bottom).

[1] R. Neumann, NIMB **151**, 42 (1999).
[2] A. S. El-Said, et al., Phys. Rev. Lett. **100**, 237601 (2008).
[3] F. Aumayr, et al. NIMB **266**, 2729 (2008).
[4] R. Heller, et al., Phys. Rev. Lett. **101**, 096102 (2008).
[5] E. Akcöltekin, et al. Nature Nanotechn. **2**, 290 (2007).
[6] E. Akcöltekin, et al. New J. Phys. **10**. 053007 (2008).
[7] T. Peters, et al., NIMB **267**, 687 (2009).

* E-mail: aumayr@iap.tuwien.ac.at; a.s.el-said@fzd.de

Molecular Dynamics Simulations to Explore the Effects of Si-C Chemistry in 20-keV C_{60} Bombardment of Si

*C. A Briner**, *K. D. Krantzman* and B. J. Garrison*[§]

*Department of Chemistry and Biochemistry, College of Charleston, Charleston, SC 29424, USA
[§]Department of Chemistry, The Pennsylvania State University, University Park, PA 16802, USA

1. INTRODUCTION

C_{60} ion beams have been successful for high resolution sputter depth profiling of metallic multilayer structures. However, in experiments of C_{60}^+ bombardment of Si, unusual effects are observed [1], which are thought to be due to the strong covalent bonds that can be formed between C atoms from the projectile and Si atoms from the substrate [2]. Similar effects have been observed in experiments on organic materials with C_{60}^+ projectile.

We have adopted a recently developed scheme [3] to model multi-impact bombardment of C_{60} on a single Si surface [4, 5]. Recent experiments have shown that C atoms are primarily ejected in the form Si_3C^+[4], a result which has led the authors to conclude that C atoms from the projectile are incorporated into the substrate by bonding to three neighboring Si atoms. In this poster, we present the results of molecular dynamics (MD) simulations to model cumulative effects of successive C_{60} bombardment.

2. MD SIMULATIONS

In order to model depth profiling, the "divide and conquer" scheme developed by Russo, et. al. [3] to treat multiple impacts on a single surface has been adopted. A detailed description of the simulations as applied to C_{60} bombardment of Si is described elsewhere [4, 5]. The Si sample is successively bombarded by 20-keV C_{60} projectiles at normal incidence using a set of impact points chosen randomly over the entire surface of a large master Si crystal. The trajectory for each impact point is run using a smaller cylindrical sample extracted from the master crystal and then reinserted after the trajectory is complete. An empirical many body potential developed by Tersoff is used to model the Si-Si, C-C and Si-C interactions [7]. The trajectories are calculated for a total of 200 cumulative impacts, which corresponds to a fluence of 3.5×10^{13} cm^{-2}.

3. RESULTS

The bonds that form between Si and C are stronger than the bonds between the Si atoms in the substrate. Consequently, an average of fifty out of sixty carbon atoms from each projectile (about 83%) form bonds with Si substrate atoms and are incorporated into the Si lattice, The carbon atoms are deposited an average of 20 Å below the original surface and the majority form three bonds with neighboring Si atoms in the substrate.

The sputtering yields of both silicon and carbon atoms, as well as cluster species containing silicon and carbon, Si_xC_y, are determined as a function of the number of impacts. In order to test the hypothesis by Lyon, et. al., we have investigated the correspondence between atoms in sputtered clusters and the local geometry in the substrate. It is found that 20.8% of Si-C and 12.6% of Si-Si bonds in ejected clusters were present in the substrate prior to ejection. Therefore, most of the clusters are produced by a recombination of atoms originally in the substrate and only a few of the bonds are reflective of the original bonds located in the substrate.

4. REFERENCES

[1] G. Gillen et al, Appl. Surf. Sci. 252, 6521 (2006).
[2] K. D. Krantzman, D. B. Kingsbury, B. J. Garrison, Appl. Surf. Sci. 252, 6463 (2009).
[3] M. F. Russo, Jr., Z. Postawa, Z.; B. J. Garrison, J. Phys. Chem. C 114, 3270 (2009)
[4] K. D. Krantzman and A. Wucher, J. Phys Chem. C 114, 5480 (2010).
[5] K. D. Krantzman and B. J. Garrison, Surf. Interface Anal., in press (2010), DOI 10.1002/sia.3438.
[6] I. Lyon, T. Henkel and D. Rost, Appl. Surf. Sci. 256, 6480 (2010).
[7] J. Tersoff, Phys. Rev. B, 39, 5566 (1989).

* E-mail: cabriner@edisto.cofc.edu

LOW-ENERGY Ne^+ SCATTERING BY III-V COMPOUND SEMICONDUCTORS

N. Bundaleski[1,*], N. Ivanović[2], C. Pagura[3], I. Radisavljević[2], and A. Tolstogouzov[1]

[1] Centre for Physics and Technological Research (CeFITec), Dep. de Física da Faculdade de Ciências e Tecnologia, Universidade Nova de Lisboa, 2829-516 Caparica, Portugal
[2] Institute of Nuclear Sciences "Vinča", P.O. Box 522, 11001 Belgrade, Serbia
[3] Istituto per l'Energetica e le Interfasi (IENI-CNR), Corso Stati Uniti 4, 35127 Padova, Italy

1. INTRODUCTION

For several years now, low-energy ion scattering (LEIS) has been successfully applied to surface analysis and quantification of metals, alloys and oxides [1]. At the same time, few LEIS studies concern III-V compound semiconductors (see, e.g., [2] and references cited therein). The goal of the present work was to investigate the characteristic features of mass-separated energy spectra of Ne^+ scattered from GaP, GaAs, InP and InAs, and from metal components (Ga, In) of these compounds.

2. EXPERIMENTAL AND RESULTS

The samples were single-crystalline (100) semiconductor wafers and 6N purity gallium and indium. We used mass-resolved ion scattering spectrometry (MARISS) [3, 4] allowing eliminating the overall background signal related to sputtering of the target materials. The incident angle was 60° with respect to the sample surface, and the ions backscattered at 120° were mass and energy analyzed by the Hiden EQS 1000. All measurements were fulfilled using "in-plane" geometry under the steady-state bombarding conditions, when the scattered ion yields are stabilized.

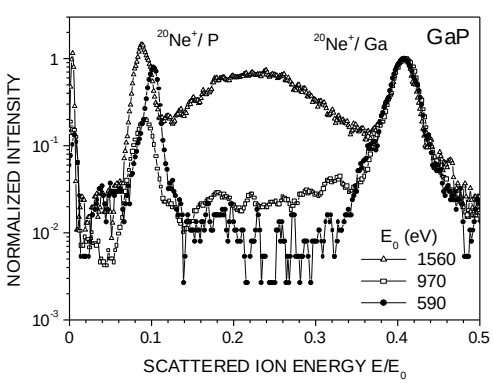

Figure: MARISS spectra of $^{20}Ne^+$ scattering by GaP.

Figure shows the MARISS spectra of $^{20}Ne^+$ scattering by GaP at different incident energies E_0. The ion intensities are scaled to the intensity of the single binary collision peak $^{20}Ne^+$/Ga. No corrections such as background subtraction, smoothing, etc. have been applied to the spectra. The spectrum recorded at E_0=1560 eV contains the broad hump with maximum located near 0.2 E/E_0. Similar hump was registered for Ne^+ scattering by InP surface. For pure Ga and In samples, as well as for GaAs and InAs compounds, the background signals were less intense and without the broad maximum.

3. DISCUSSION

Generally, the tail in LEIS spectra is attributed to reionized primary ions scattered from the atoms in deeper layers after generally multiple collision events [1]. In the case of P-based compounds, which demonstrate non monotonic decrease of the background signals towards low-energy threshold, we assume that projectile suffers at least two collisions, and the second one takes place with P atom. In that collision Ne can be reionized. Using ZBL potential, the distance of closest approach needed to achieve reionization is estimated to be about 0.4 Å. This is further supported by the ab initio analysis of the binary collision events using the LCAO method in the unrestricted Hartree–Fock approximation.

4. REFERENCES

[1] H. H. Brongersma, M. Draxler, M. de Ridder, P. Bauer, Surf. Sci. Rep. **62,** 63 (2007).
[2] A. Tolstogouzov, S. Daolio, C. Pagura, Nucl. Instr. Meth. **B217**, 246 (2004).
[3] K. Wittmaack, Surf. Sci. **345**, 110 (1996).
[4] A. Tolstogouzov, S. Daolio, C. Pagura, C.L. Greenwood, Surf. Sci. **531**, 95 (2003).

* E-mail: n.bundaleski@fct.unl.pt

A statistical analysis of the lateral displacement of Si atoms in molecular dynamics simulations of successive bombardment with 20-keV C_{60} projectiles

*E. L. Cook**, *K. D .Krantzman, B. J. Garrison*[§] *and A. Wucher*[#]

*Department of Chemistry and Biochemistry, College of Charleston, Charleston, SC 29424, USA
[§]Department of Chemistry, The Pennsylvania State University, University Park, PA 16802, USA
[#] Fakultät für Physik, Universität Duisburg-Essen, 47048 Duisburg, Germany

1. INTRODUCTION

An important observation in all experiments involving sputter erosion of surfaces is that surface material is being relocated laterally, i.e., parallel to the original surface due to the cumulative ion bombardment. This effect is well known in Focused Ion Beam (FIB) nanostructuring, where it leads to discrepancies between the applied ion fluence profile and the actually eroded structure. It is also important in sputter depth profiling experiments, because material being relocated from the edge of the eroded crater onto other positions at the crater bottom may falsify the analysis. Ultimately, one would want to determine how far a surface atom can on average travel away from its original position before it finally gets removed from the surface by sputtering. This "relocation length" is of great interest, since it represents, for instance, the ultimate limit of the lateral resolution that can be achieved in a mass spectrometric 3D imaging technique.

In order to investigate the microscopic mechanisms behind this finding, molecular dynamics (MD) simulations have been performed to model the successive bombardment of Si with 20 keV C_{60} at normal incidence. In this poster, we present a statistical analysis of the lateral movement of Si atoms that originate from the topmost layer of the virgin, unbombarded surface. The results of the analysis show that this movement can be described by the same formalism as would be employed for a simple two-dimensional diffusion process.

2. METHOD

The simulations use a “divide and conquer” scheme developed by Russo, et. al.[1],which outlines a protocol to treat multiple projectile impacts on the same surface area. A detailed description of the simulations as applied to C_{60} bombardment of Si is described elsewhere [2,3].

If the lateral motion is statistical in nature, the displacement can be described by a Gaussian distribution. There is a linear relationship between the average value of the square lateral displacement and *t*, $\left\langle \Delta r^2 \right\rangle = 4Dt$. In the statistical analysis used here, time is described by the number of impacts, N_{imp}. The value of *D* is then given in Å^2/impact and can then be obtained from the slope of a plot of $\left\langle \Delta r^2 \right\rangle$ as a function of N_{imp}.

2. RESULTS

From the MD simulation data, the square of the lateral distance moved by each substrate atom from the original topmost layer is calculated and the average value is determined after each successive impact. A least square fit to the data, which has been restricted by the requirement to include the origin, yields a slope of $4D = 13.54 \pm 0.09$ Å$^{2/}$impact, thus yielding a *D* value of 3.4 Å^2/impact.

From the statistical sputtering model [2], it can be estimated that about 20 ML of material must be removed in order to remove 99 % of all atoms originally from the topmost layer. Under the conditions implied here, this would require approximately 800 successive impacts. Using the *D*-value the value of $\left\langle \Delta r^2 \right\rangle \sim 10^2$ nm^2, which corresponds to a maximum root mean square displacement of the order of 10 nm. Therefore, the extrapolated simulations predict that atoms from the topmost layer will move an average of 100 Å before being sputtered from the surface.

Although the lateral motion of atoms can be described by the diffusion equation, the actual motion of the atoms described by the molecular dynamics simulations does not exactly behave in the way diffusion is normally characterized. The total distance travelled by an atom is not a result of an accumulation of even, small hops over each impact. Rather, the relocation distance is small during most of the impacts. During a few impacts, the atoms move a large distance, and these large hops are what contribute the greatest to the total distance moved.

REFERENCES

[1] M. F. Russo, Jr., Z. Postawa and B. J. Garrison, J. Phys. Chem. C, **113**, 3270 (2009).
[2] K.D. Krantzman, A. Wucher, J. Phys. Chem. C **114**, 5480 (2010).
[3] K. D. Krantzman and B. J. Garrison, Surf. and Inter. Anal. in press (2010).

* E-mail: `elcook@edisto.cofc.edu`.

CHEMICAL SPUTTERING OF DEUTERATED AMORPHOUS CARBON AT VARIOUS SURFACE TEMPERATURES

J. Dadras[1,2,*] *and P. S. Krstic*[1,2]

[1] Department of Physics and Astronomy, University of Tennessee, Knoxville, TN 37996
[2] Physics Division, Oak Ridge National Laboratory, Oak Ridge, TN 37831

1. INTRODUCTION

Many current and future fusion reactors (e.g. ITER, DEMO) rely on carbon based plasma-facing materials, either for divertor plates or as a substrate for the deposited metal walls. Sputtering of hydrocarbons, besides eroding the walls, pollutes the plasma, degrading reactor performance, while tritium retention in the walls of a D-T reactor creates an issue of radioactive waste.

The surface temperature of the plasma-exposed walls in an energy conversion reactor (e.g. DEMO) is expected to be elevated to about 1,000 K. Thus, characterization of the chemical sputtering yields as function of surface temperature, for surfaces bombarded by hydrogen particles in the least studied energy range of a typical divertor environment (up to a few tens of eV, not counting ELMs and disruptions), is of great importance. This is the subject of the present study.

2. RESULTS

We study by classical molecular dynamics (MD) the chemical sputtering yield of deuterated amorphous carbon (a-C:D) surfaces irradiated by 1 – 50 eV deuterium atoms, at surface temperatures between 300 – 1200 K. A quasi-stationary state of the surface, established by the same number of impacting and ejected deuterium atoms, is reached through cumulative bombardment, for each ion energy and surface temperature. The stationary sputtering yields are calculated. Dependences of the mass, translational and rotational energy, ejection angle of sputtered hydrocarbons, as well as of hybridized moiety densities, on surface temperature and impact energy are also studied. Results are compared with available experimental data from beam-surface experiments on sputtered acetylene, methane, and total carbon. Further details on the surface creation and preparation can be found in [1]. The Brenner-Tersoff type reactive bond-order (REBO) potential, 2002 parameterization [2], is employed. Figure 1 shows our results on the "reduced" total carbon yield (C_xH_y, x=1-4) for 15 eV deuterium bombardment, as function of the surface temperature, in remarkable agreement with the experimental data of Balden et al [3].

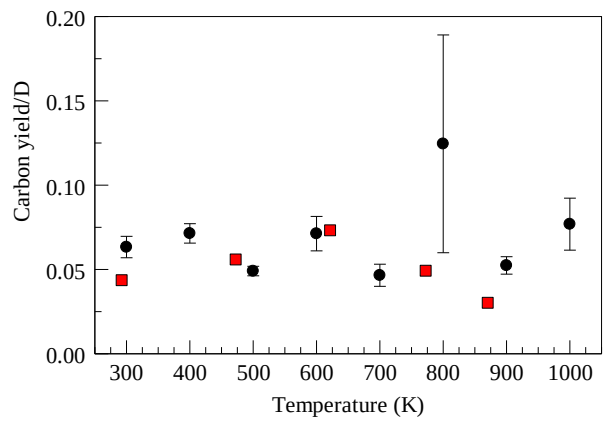

Figure 1: Carbon sputtering yields vs. temperature. Black dots with error bars are simulation results, red squares are experimental results from [3].

We acknowledge support of OFES of the U.S. DoE and Laboratory Directed Research and Development Program of ORNL, under contract No. DE-AC05 00OR22725 with UT-Battelle, LLC, and partial support through SciDAC. This research used resources of the ORNL Leadership Computational Facility, which is supported by the Office of Science of the U.S. DoE.

3. REFERENCES

[1] P. S. Krstic, C. O. Reinhold, and S. J. Stuart, New Journal of Physics 9 (2007)
[2] D. W. Brenner, et. al., Journal of Physics: Condensed Matter 14(4) (2002).
[3] M. Balden and J. Roth, Journal of Nuclear Materials 280 (2000).

* E-mail: jonny@utk.edu

ELECTRON TRANSMISSION THROUGH A MICROSIZE TAPERED GLASS CAPILLARY

G. G. De Silva, B. S. Dassanayake, D. Keerthisinghe and J. A. Tanis

Department of Physics, Western Michigan University, Kalamazoo, MI 49008 USA

Transmission of highly charged ions (HCI) through different kinds of nanocapillary foils [1, 2] has been reported since it was first discovered in 2002 [3]. Recently, attention has focused on tapered glass capillaries, especially because of their vast potential applications [4]. Although there have been reports for transmission of electrons through nano- and micro- scale single and multiple capillaries [5,6], electron transmission through tapered glass capillaries has not been reported so far.

In the present work we report fast electron transmission through a tapered Borosilicate (80.9% SiO_2, 12.7% B_2O_3 2.3% Al_2O_3, Na_2O/K_2O) glass capillary with an inlet inner diameter of 720 □m and an outlet diameter of 22 □m. The length of the tapered capillary was 25 mm. The samples were prepared by the RIKEN laboratory in Japan and the measurements were conducted at the Van de Graaff accelerator laboratory at Western Michigan University.

Transmission of 500, 800, and 1000 eV energy electrons through the capillary sample was studied. Results revealed the existence of a "threshold energy" for the onset of electron transmission through the tapered capillary since no considerable transmission at 500 eV was observed, but was observed at the higher energies. Angular distributions for electron transmission through the tapered glass capillary were obtained for 800 and 1000 eV by tilting the capillary axis with respect to the incident beam direction. The distribution of normalized intensities of transmitted electrons at 1000 eV is shown in Fig. 1. As seen, the transmitted electron intensity shows a decrease with capillary tilt angle ψ, agreeing with what has been observed for slow ions and electron transmission through straight and tapered glass capillaries, respectively [4,5].

Transmitted electrons through the tapered glass capillary were found to lose energy with increasing sample tilt angle, in agreement with what has been reported for electron transmission through foils and single glass capillaries [5,6]. The characteristic guiding angles ψ_c (angle at which the transmitted intensity drops to 1/e of its $\psi = 0^0$ value) for 1000 and 800 eV were calculated and found to be $0.33^0 \pm 0.05^0$ and $0.67^0 \pm 0.40^0$, respectively. The increase in guiding ability with decreasing energy is a notable deviation from the recently reported electron transmission through a straight macroscopic glass capillary [5].

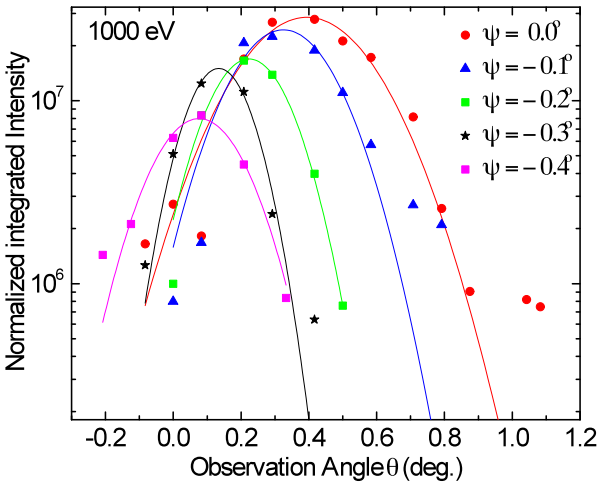

Figure 1. Angular distributions of integrated normalized transmitted electron intensities for 1000 eV as a function of observation angle θ for different tilt angles ψ. Data points were fit with Gaussian functions as indicated by the solid lines. The transmitted intensities were normalized with respective to the incident beam current.

Furthermore, the time (charge) dependence of the transmitted intensity at 1000 eV was examined at $\psi = 0.0^0$, 0.2^0, 0.6^0 and 1.0^0 and evidence of charge accumulation and discharge was observed. Transmission never reached a stable equilibrium and sudden bursts of elastic transmission at lower tilt angles were seen. The results reveal unique features of electron transmission through tapered glass capillaries compared to what has been observed for HCIs so far [7]. Further investigations are planned for the future.

References:

[1]N. Stolterfoht *et al*, Phys. Rev. A **79**, 042902 (2009).
[2]M. B. Sahana *et al.*, Phys. Rev. A **73**, 040901(R) (2006).
[3]N. Stolterfoht *et al.*, Phys. Rev. Lett. **88**, 133201 (2002).
[4]T. Ikeda *et al.*, Phys. Lett. **89**, 163502 (2006).
[5]B. S. Dassanayake *et al*, Phys. Rev. A **81**, 020701(R) (2010).
[6]S. Das *et al.*, Phys. Rev. A **76**, 042716 (2007).
[7]A. Cassimi *et al.*, Nucl. Instrum. Meth. Phys. Res. B **267**, 674 (2009).

E-mail: galappaththi.g.desilva@wmich.edu

BOMBARDING OF GRAPHENE BY LIGHT ATOMS: CHANGE OF CHEMISTRY, INDUCED DEFECTS, AND QUANTUM ELECTRON TRANSPORT THROUGH DAMAGED GRAPHENE

R. C. Ehemann[1,*], *J. Dadras*[2,3] *and P. S. Krstic*[2,3]

[1] Department of Physics and Astronomy, Middle Tennessee State University, Murfreesboro, TN 37130
[2] Department of Physics and Astronomy, University of Tennessee, Knoxville, TN 37996
[3] Physics Division, Oak Ridge National Laboratory, Oak Ridge, TN 37831

1. INTRODUCTION

With one of the highest known conductivities, graphene is used in a variety of electronic applications. Research has shown that its gas-holding capabilities also make it a useful material when exposing delicate systems like living cells to ion beam analysis [1]. Sensitivity of graphene conductivity to even minimal changes in its structure suggests that it could be used as a hypersensitive sensor of particles and their properties. Application of graphene as an electronic element in spacecraft requires study of its sensitivity to cosmic radiation. We theoretically study these effects in two parts: 1) Bombarding graphene with hydrogen and carbon particles in a wide range of energies; 2) Performing calculations of changes in graphene's quantum conductance due to the bombardment. Simulations in 1) are done applying classical molecular dynamics (MD), while 2) is obtained applying the Landauer approach to quantum transport of electrons through graphene with attached gold electrodes [3].

MD simulations, used to bombard graphene sheets and graphite samples (collated graphene sheets) with deuterium atoms employ a modification to the reactive empirical bond-order (REBO) potential to consider long-range van der Waals interactions and torsions. This modification is known as the adaptive intermolecular REBO (AIREBO) potential [2], and has a range of approximately eleven Angstroms (more than five times that of the traditional REBO potential). A mapping of this long-range potential is depicted in Figure 1, showing the strong multi-body character of the graphene potential energy, interacting with hydrogen, which is very distinct from the binary H-C potential. Bonding and reflective properties of graphene to the slow irradiation are also obvious from Figure 1.

In the MD simulations, energies ranging from 0.1 eV to 1 keV are considered. In addition, the angle of incidence varies from small angles of 5° to 90°. These ranges allow us to determine the most efficient way of producing damaged graphite samples for study; and provide insight into the applicability of graphene-based electronics in presence of natural sources of radiation, like the solar wind.

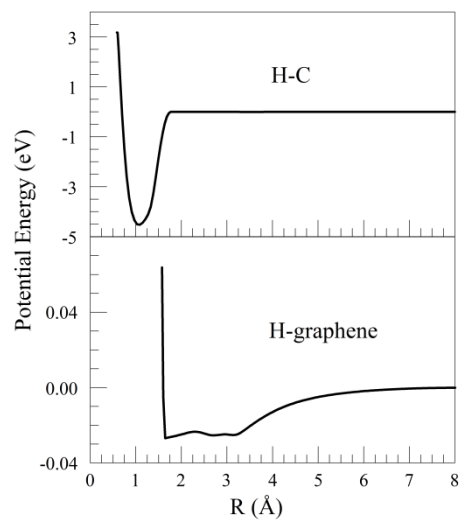

Figure 1: Comparison of the hydrogen interaction potential with graphene and a single carbon atom, based on AIREBO.

We acknowledge support of DoE and Laboratory Directed Research and Development Program of ORNL, under contract No. DE-AC05 00OR 22725 with UT-Battelle, LLC. RCE acknowledges the ORISE/ORAU program SULI and DoE for supporting his research at ORNL.

2. REFERENCES

[1] O. Lehtinen, J. Kotakoski, A. V. Krasheninnikov, A Tolvanen, K. Nordlund, and J. Keinonen, Phys. Rev. B **81**, 153401 (2010).

[2] Stuart, Steven J.; Tutein, A. B.; Harrison, Judith A. J. Chem. Phys. **112**, 6472 (2000).

[2] P. S. Krstić, X.-G. Zhang, and W. H. Butler, Phys. Rev. B **66**, 205319 (2002).

E-mail: rcehemann@gmail.com

CALCULATION OF AUGER-NEUTRALIZATION PROBABILITIES FOR HE$^+$-IONS IN LEIS

D. Goebl[1*], R. C. Monreal[2], D. Valdés[2], D. Primetzhofer[1] and P. Bauer[1]

[1] Institut für Experimentalphysik, Johannes Kepler Universität, Altenbergerstr. 69, A-4040 Linz (Austria)
[2] Departamento de Física Teórica de la Materia Condensada C05, Universidad Autónoma de Madrid, Francisco Tomás y Valiente 7, E-28049 Madrid (Spain)

1. INTRODUCTION

In low energy ion scattering (LEIS), charge exchange is exclusively due to Auger-neutralization when the particles impinge with an energy below a certain threshold E_{th}. By using a linear combination of atomic orbitals (LCAO) based model of Auger-neutralization, neutralization probabilities are calculated. The results are compared to recent experiments and show excellent agreement.

2. RESULTS AND DISCUSSION

According to [1] the ion survival probability or ion fraction P^+ can be expressed by the following equation:

$$P^+ = e^{-\int \Gamma(\vec{r}(t))\,dt} = e^{-\int \Gamma(\vec{r})\,\frac{dt}{dz}dz} \approx e^{-\frac{v_c}{v_\perp}} \qquad (1)$$

where Γ denotes the Auger-neutralization rate and the characteristic velocity $v_c = \int\langle\Gamma(z)\rangle dz$ is an indicator of the neutralization ability of a given surface.

For the Ag(110) surface, recent experiments have shown a noteworthy dependence of v_c on the scattering direction caused by the shadowing of deeper layers by first layer atoms in $[1\bar{1}2]$ direction [2]. To investigate this behaviour, ion trajectories were obtained from molecular dynamics simulations using KALYPSO [3] for [001], $[1\bar{1}0]$ and $[1\bar{1}2]$ direction with the premise of exclusive single scattering. Using the LCAO-based model described in [4], $\Gamma(\vec{r})$ was calculated for specific positions in front of a Ag(110) surface. According to eq. (1) P$^+$ was evaluated by integration of the Auger-neutralization rate Γ along the trajectory.

Comparison with experiment shows excellent agreement as depicted in Fig. 1 which gives confidence in the validity of this model in the LEIS regime. From these calculations, detailed information on the neutralization process like the contribution of certain orbitals can be extracted.

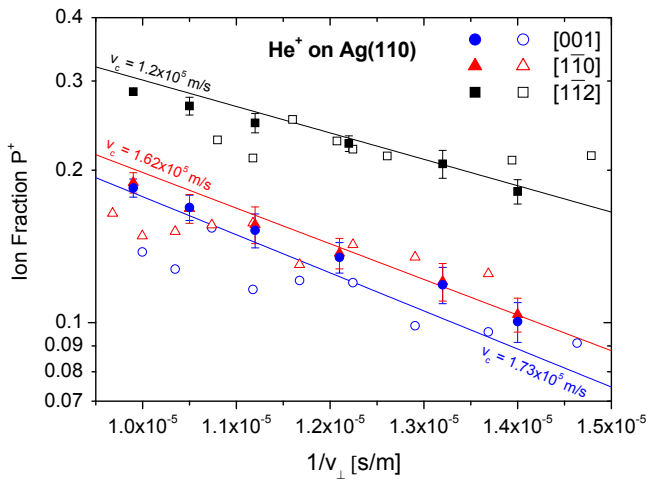

Figure 1: Ion fraction of He$^+$ particles scattered from a Ag(110) surface in different azimuth directions. Open symbols are experimental values, lines represent fits of v_c according to (1), full symbols are calculated values.

3. REFERENCES

[1] HH. Brongersma, M. Draxler, M. De Ridder and P. Bauer, Surf. Sci. Rep. **62**, 3, 63-109 (2007)

[2] D. Primetzhofer, M. Spitz, S. N. Markin, E.Taglauer and P. Bauer , Phys. Rev. B **80**, 125425 (2009).

[3] MA. Karolewski, Nucl. Instr. Meth. B **230**, 1-4, 402-405 (2005).

[4] D. Valdés, J. M. Blanco, V.A. Esaulov and R. C. Monreal, Phys. Rev. Lett. **97**, 047601 (2006).

* E-mail: dominik.goebl@jku.at

DIFFRACTION OF SWIFT N ATOMS FROM Ag(111) SURFACES

M.S. Gravielle[1,*], G. Bocán[2], and R. Díez Muiño[3]

[1]Instituto de Astronomía y Física del Espacio, CONICET, Buenos Aires, Argentina, and Depto de Física, FCEN, UBA.
[2]Centro Atómico Bariloche, CNEA and CONICET, S.C. de Bariloche, Río Negro, Argentina.
[3]Donostia International Physics Center (DIPC) and Centro de Física de Materiales CSIC-UPV/EHU, San Sebastián, Spain.

1. INTRODUCTION

Diffraction from crystal surfaces produced by grazing scattering of atoms in the keV energy range is nowadays attracting considerable attention. The first experimental evidences of this effect were reported for insulator surfaces [1] for which the presence of a band gap strongly suppresses inelastic electronic processes, favoring the conservation of quantum coherence. However, this diffraction effect has recently been observed at metallic materials [2,3] as well, although electron excitations were supposed to smudge interference signatures for these surfaces. The aim of this work is to study the atomic diffraction from metal surfaces by considering keV nitrogen atoms impinging grazingly on Ag(111) .

2. THEORETICAL MODEL

To describe the scattering process we employ a distorted-wave model - the surface-eikonal approximation [4] - that makes use of the eikonal wave function to represent the elastic collision with the surface, while the movement of the fast projectile is described classically by considering axially channeled trajectories for different initial conditions. The surface-eikonal T-matrix element reads:

$$T_{if}^{(eik)} = \int d\vec{R}_{os}\; a_{if}(\vec{R}_{os}), \quad (1)$$

where $\vec{R}_{os}$ determines the initial position of the projectile on the surface plane and

$$a_{if}(\vec{R}_{os}) = (2\pi)^{-3} \int dt\, |v_z(\vec{R}_P)| \times \exp[-i\vec{Q}.\vec{R}_P - i\,\eta(\vec{R}_P)]\; V_{SP}(\vec{R}_P) \quad (2)$$

is the transition amplitude associated with the classical path $\vec{R}_P(\vec{R}_{os},t)$, with $\vec{Q}$ the projectile momentum transfer and $v_z(\vec{R}_P)$ the component of the projectile velocity perpendicular to the surface plane. In Eq. (2), $\eta(\vec{R}_P)$ is the eikonal-Maslov phase that takes into account the action of the projectile-surface potential $V_{SP}(\vec{R}_P)$ along the classical path.

An accurate potential energy surface for the N/Ag(111) system was derived from density functional theory (DFT) calculations as implemented in the "Vienna Ab-initio Simulation Program" (VASP) code [5], combined with an elaborate interpolation method [6].

3. RESULTS

We apply the theoretical model to evaluate angular projectile distributions for impact along different low-index crystallographic directions. The influence of the incidence energy and the symmetry of the considered channel are both analyzed.

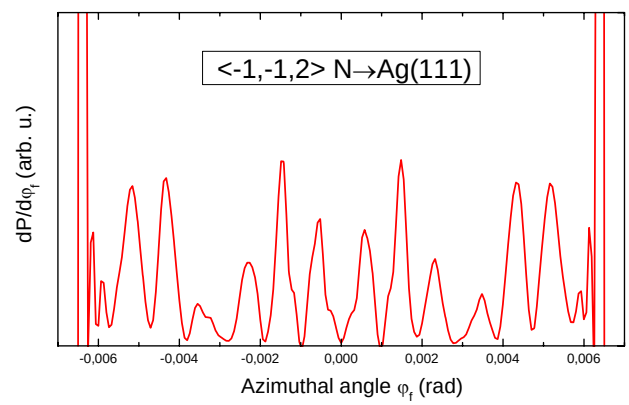

Figure 1: Azimuthal angular distribution of elastically scattered projectiles for 3 keV N atoms impinging on Ag(111) along the direction ⟨-1,-1,2⟩, with a glancing angle (θ_i =0.4678 deg.)

[1] A. Schüller *et al.*, Phys. Rev. Lett. **98**, 016103 (2007); P. Rousseau *et al.*, Phys. Rev. Lett. **98**, 016104 (2007).
[2] N. Bundaleski *et al.*, Phys. Rev. Lett. **101**, 177601 (2008).
[3] M. Busch *et al.*, Surf. Sci. **603**, L23 (2009).
[4] M.S. Gravielle *et al.*, Phys. Rev. A. **78**, 022901 (2008).
[5] G. Kreese and J. Hafner, Phys. Rev B **47**, 558 (1993).
[6] H.F. Busnengo *et al.*, J. Chem. Phys. **112**, 7641 (2000)

* E-mail: msilvia@iafe.uba.ar

PHOTOELECTRON EMISSION FROM LIF SURFACES BY ULTRASHORT PULSES

Mario. A. Acuña[1] *and* *M.S. Gravielle*[1,2,*]

[1] Instituto de Astronomía y Física del Espacio (IAFE) C.C. 67, Suc. 28 (1428) Buenos Aires, Argentina
[2] Departamento de Física, FCEN, Universidad de Buenos Aires, Argentina

The present work is focused on electron emission produced by incidence of ultra-short laser pulses on LiF(001) surfaces. To describe this process we employ a time-dependent distorted-wave method, here named Surface-Volkov (SV) approximation, which is based on the use of Volkov phase [1] to represent the interaction of the active electron with the external field. This kind of one-active electron theories has been recently applied to study different laser-induced electron emission processes from metal surfaces, providing reasonable predictions [2, 3, 4].

Due to the localized character of the electrons in insulator surfaces, the initial unperturbed state $\phi_i(\vec{r},t) = \phi_i(\vec{r})e^{(-i\varepsilon_i t)}$ is represented by means of the tight-binding method [5] as

$$\phi_i(\vec{r}) = \sum_{\vec{R}} e^{i\vec{K}\cdot\vec{R}}\ \varphi_i(\vec{r}-\vec{R}), \qquad (1)$$

where the wave vector $\vec{K}$ identifies a given crystal state within the surface band. The function $\varphi_i(\vec{r}-\vec{R})$ represents the Wannier function centered on the lattice site $\vec{R}$ and the sum involves all $\vec{R}$ positions of target ions. Since the overlap between wave functions corresponding to nearest-neighbor atoms is small, we approximate the Wannier function to the atomic wave function.

The final distorted state is described with the SV wave function:

$$\chi_f^{(SV)-}(\vec{r},t) = \phi_f(\vec{r}) \exp\left[iD_V^-(\vec{k}_f,\vec{r},t) - i\varepsilon_f\ t\right], \quad (2)$$

where $\phi_f(\vec{r})$ represents the final unperturbed state, including the distortion introduced by the surface in the exit channel, and $D_V^-(\vec{k}_f,\vec{r},t)$ is the Volkov phase[1].

By using Eqs (1) and (2) within the distorted-wave formalism, the SV transition matrix reads:

$$\begin{aligned} T_{if}^{(SV)} &= S_f(0)\ \left\langle \chi_f^{(at)-}(0)|\varphi_i(0)\right\rangle \\ -i\int_0^\tau & S_f(t)\ \left\langle \chi_f^{(at)-}(t)\left|\mathcal{W}_f^\dagger(t)\right|\varphi_i(t)\right\rangle dt, \quad (3) \end{aligned}$$

where $\chi_f^{(at)-}$ is the Coulomb-Volkov wave function associated with the atomic continuum state of the target ion. In Eq.(3), the function $S_f(t)$ takes into account the crystallographic structure of the surface and $\mathcal{W}_f(t)$ is the final distortion potential.

In order to study the interference effects produced by the crystal lattice, we oriented the linear polarized external field $\vec{F}(t)$ parallel to the surface plane, along the $\langle 100\rangle$ crystallographic direction (i.e. $\phi = 0$). Angular and energy spectra for electrons emitted from the surface with a glancing angle are analyzed, comparing them with those of the atomic case.

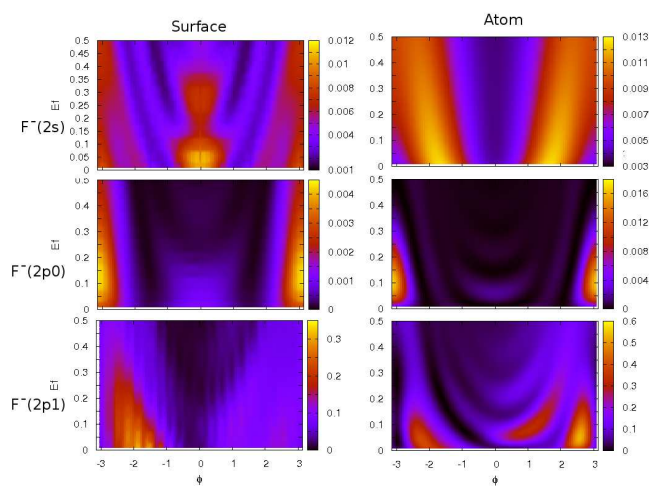

Figure 1: Differential probability of electron emission from different initial states, for a one cycle laser pulse $F(t) = F_0 \sin(\omega t + \varphi)\sin^2(\pi t/\tau)$, for $0 < t < \tau$, with F_0=0.05 a.u., w=0.171 a.u. and τ=36.74 a.u..

1. REFERENCES

[1] D. M. Volkov, Z. Phys. **94**, 250 (1935).

[2] M. N. Faraggi *et al*, Phys. Rev. A **76**, 012903 (2007).

[3] J.C. Baggesen and L.B. Madsen, Phys. Rev. A **78**, 032903 (2008).

[4] C.-H. Zhang *et al*, Phys. Rev. Lett. **102**, 123601 (2009).

[5] N. W. Ashcroft, N. D. Mermin (1976). Solid State Physics. Brooks/Cole, Cengage Learning.

* E-mail: msilvia@iafe.uba.ar

SURFACE STATE EFFECTS IN ELECTRON EMISSION FROM BERYLLIUM SURFACES

C. Archubi[1,*] **M. S. Gravielle**[1,2] **and V. M. Silkin**[3,4]
[1] Instituto de Astronomía y Física del Espacio, CONICET-UBA, Buenos Aires, Argentina
[2] Dep. de Física, Fac. de C. Exactas y Naturales, Universidad de Buenos Aires, Buenos Aires, Argentina
[3]Donostia International Physics Center (DIPC), 20018 San Sebastián, Spain
[4]IKERBASQUE, Basque Foundation for Science, 48011 Bilbao, Spain

1. INTRODUCTION

Recently it has been demonstrated that occupied surface states can modify the dielectric properties of metal surfaces [1]. Thus, with the aim of investigating the influence of surface states on electron emission, we study electron distributions originated by fast protons colliding grazing with a Be(0001) surface. Beryllium presents a technological interest in modern fusion reactors and it is expected that its surface states play an important role in inelastic electronic processes.

To describe the electron emission process we employ the Band-structure-based (BSB) model [2], which includes an accurate description of the electron-surface potential, incorporating information about the band structure of the solid. Within the BSB approach the surface interaction is described by a realistic one-dimensional model potential [3], while the dynamic response of the medium is derived in consistent way from the unperturbed electronic states by using a linear response theory. This method has been succesfully employed to study energy loss and electron emission from Al surfaces, where the effects of the surface states were found negligible [4].

2. THEORY AND RESULTS

Within the binary collisional formalism, the differential probability per unit path for the electronic transition $i \to f$ reads

$$P_{if}(z) = \frac{2\pi}{v_s}\delta(\Delta)\left|T_{if}\right|^2 , \qquad (1)$$

where z is the projectile distance to the surface, v_s is the projectile velocity parallel to the surface plane, and the Dirac delta expresses the energy conservation. In Eq (1) T_{if} represents the T-matrix element, which is evaluated within a first-order-perturbation theory.

In this work we employ the BSB model to derive both the unperturbed electronic wave functions and the surface induced potential. The differential probability of electron transition to a given final state with momentum $\vec{k}$, is $\frac{dP}{dk}$, obtained from Eq (1) by integrating along the classical projectile trajectory, after adding the contributions coming from the different initial states.

In Fig. 1 we display the differential electron emission probability for 100 keV protons impinging grazing on a Be (0001) surface considering three different ejection angles in the scattering plane. Due to the contribution of surface occupied states, electron spectra display pronounced shoulders at intermediate energies, which are not present when simpler surface descriptions are considered. These shoulders are also observed for emission out of the scattering plane and their positions are gradually shifted to lower electron energies as the emission angle increases.

Remarkably, surface state effects completely dissapear when we calculate the total emission probability as a function of the electron energy.

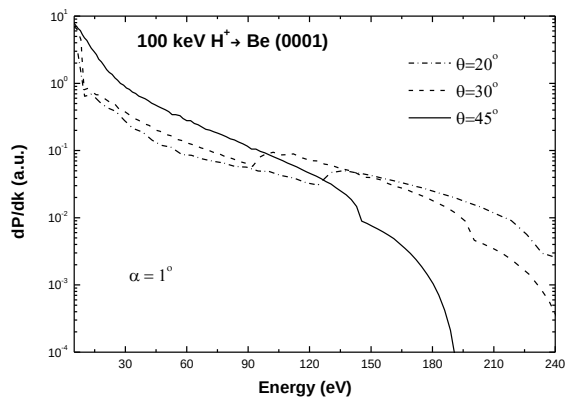

Figure 1: Differential probability of electron emission from the valence band, as a function of the electron energy, for 100 keV protons impinging on a Be(0001) surface with the angle $\alpha=1^o$. Three different electron emission angles, meassured with respect to the surface plane, are considered: $\theta = 20, 30$ and 45 ^{o}.

REFERENCES

[1] V.M. Silkin *et al*, J. Phys.: Condens. Matter **20**, 304209 (2008)
[2] M. N. Faraggi *et al*, Phys. Rev. A **69,** 042901 (2004)
[3] E. V. Chulkov, V. M. Silkin and P. M. Echenique, Surf. Sci**. 391**, L1217 (1997); **437**, 330 (1999)
[4] M. N. Faraggi *et al*, Phys. Rev. A 72, 012901 (2005).

* E-mail: archubi@iafe.uba.ar

Deuterium ion-surface interactions of lithium thin films on micro-porous molybdenum substrates.

B.Heim[12*], C. Taylor[1], S. Ortoleva[1], D. Zigon[1], J.P Allain[1,2]

[1] Purdue University, West Lafayette, 400 Central Drive, IN 47907, USA
[2] Birck Nanotechnology Center, Discovery Park, Purdue University, West Lafayette, IN 47907, USA

1. Abstract

Lithium has been utilized to enhance the plasma performance for a variety of fusion devices such as TFTR, CDX-U and NSTX. Lithium in both solid and liquid state has been studied extensively in its role of hydrogen retention and reduction in sputtering yield [1]. Advancing lithium applications for plasma facing surfaces, a liquid lithium diverter (LLD) has recently been installed in the National Spherical Torus Experiment (NSTX) that is partially constructed from porous molybdenum (0.152mm) on a stainless steel substrate. Despite well documented deuterium retention studies and chemical analyses on other substrates and other machines [2,3], such studies have not been conducted for a moly-mesh matrix. Understanding of chemical behavior holds insight into the performance of the LLD in NSTX.

2. Experimental Setup

Two lithium evaporators (LITERS) in NSTX currently supply the diverter region with grams of lithium coverage [4], such LITERS fill the LLD with desired lithium amounts. Heating of the LLD to 220° C phase changes the evaporated lithium into a liquid. Plasma experiments are then conducted to measure the impact of the liquid lithium Plasma Facing Surface (PFS) interface. Reduction of edge-localized mode (ELM), decrease in plasma density, and increases in electron temperature illustrate some of the improvements lithium PFS has on NSTX plasma performance, however improvements with a liquid lithium interactions is unknown. [5]

Obtaining samples of LLD micro-porous molybdenum material and a surface characterization laboratory capable of in-vacuo lithium evaporation and deuterium bombardment, Purdue's Radiation Surface Science and Engineering Laboratory (RSSEL) can not only simulate the NSTX plasma environment, but characterize the sample's chemical functionalities with surface sensitive techniques.

X-ray photoelectron spectroscopy (XPS) and thermal desorption spectroscopy (TDS) is conducted to construct a chemical binding layout of linking elements of Mo, C, O, Li and D. Electron microscopy is used to investigate the liquid lithium distribution manifested in the moly-mesh matrix. The data is then compared to the known deuterium interactions that occur for lithiated graphite based on past studies [1].

3. Background and Results

Fig.1 shows the O1s XPS chemical functionality of a lithiated graphite sample related to the fluency of deuterium ions on the surface. The resulting data show the bonding functionalities between Li-O-D (manifest at 533.0ev) and Li-O (manifest at 530ev) [1]. Correlation to the effect of deuterium interactions can been seen as the 533 eV peak gains relative intensity over the 530eV peak with increasing deuterium fluency. Similarly measurements are conducted on RT and 200 C Moly mesh surfaces and their impact on ion-surface collisions and interactions. In particular we study the impact of lithium-deposited coatings on secondary ion sputtered fraction and overall sputtering as well as correlate the emission with in-situ surface characterization as a function of D+ fluence.

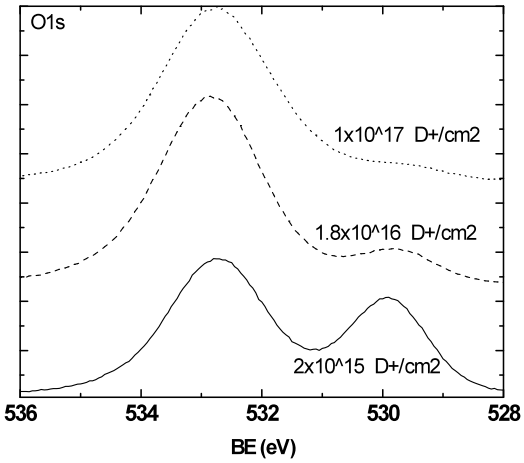

Figure 1: O1s spectrum for 2-µm lithium evaporated polycrystalline graphite with corresponding deuterium fluency.

4. REFERENCES

[1] J.P. Allain et al., J. Nucl. Mater. (2009), doi:10.1016/j.jnucmat.2009.01.242
[2] R. Majeski et al., Nucl. Fusion 45 (2005) 519-523
[3] M.J Baldwin et al., Nucl Fusion 42 (2002) 1318-1323
[4] H.W. Jugel et al., J. Nucl Mater. (2009), doi:10.1016/j.jnucmat.2009.01.262
[5] H.W Kugel et al., Physics of Plasmas 15, 056118 (2008)

* E-mail: bheim@purdue.edu

KINETIC EXCITATION OF SOLIDS INDUCED BY ENERGETIC PARTICLE BOMBARDMENT: LATEST RESULTS AND NEW APPROACHES

C. Heuser[1*], *M. Marpe*[1], *A. Bernard*[1], *C. Bobisch*[1], *D. Diesing*[2], *R. Möller*[1] *and A. Wucher*[1]

[1]Fakultät für Physik, Universität Duisburg-Essen, D-47048 Duisburg, Germany
[2] Fakultät für Chemie, Universität Duisburg-Essen, D-45117 Essen, Germany

1. INTRODUCTION

When a particle impinges onto a solid surface, it's energy is transferred to the target atoms as well as to the electronic subsystem. While the former leads to the development of collisional cascades accompanied by the emission of particles (*sputtering*), the latter manifests itself in a local and temporal heating of the electron gas, which causes the emission of electrons into vacuum [1] and may influence the ionization probability of sputtered particles [2].

Due to the surface barrier only electrons can be detected, which have sufficient energy to overcome the work function. Since most of the "hot" electrons created by moving atoms have lower energies [3], many of the excited electrons remain undetectable in the solid.

In an attempt to gain information about these electrons we use MIM (metal-isolator-metal) junctions. Bombarding the top metal surface of such a device it is possible to measure an internal emission current generated by hot electrons overcoming the oxide barrier [4].

In the past we have studied the dependence of these internal emission currents on different target parameters and on the kinetic energy and the charge state of the projectile. The experimental results regarding, for instance, the impact angle dependence of the measured internal emission yields, were interpreted in terms of a simple two temperatures model containing the oxide barrier height and width as essential parameters [5-7].

In this work we present first results where the spectroscopic transmission of the oxide barrier was determined experimentally using a Ballistic Electron Emission Microscope (BEEM).

2. EXPERIMENT

The MIM junctions used in our experiments are Ag-AlO_x-Al junctions consisting of two metal electrodes of polycrystalline Ag and Al of variable thickness separated by an insulating AlO_x layer with a thickness of about 3nm.

The top metal film of the MIM structure represents the actual target which is bombarded by a 5…15keV noble gas (Ar, Kr, Xe) ion beam. In order to minimize the ion beam induced damage of the sample the ion source is operated in a pulsed mode. The internal electron emission yield is determined by dividing the measured internal current by the primary ion current.

The BEEM measurements were performed using a four-probe scanning tunneling microscope. A MIM structure with a nominal Ag layer thickness of 10nm was contacted by two gold tip electrodes to establish a preselected potential difference between the two metal layers, while a third sharp tip was used to locally inject electrons with a preselected energy. Relating the measured BEEM current into the surface electrode to inject electron current then yields the transmission of the MIM as a function of energy.

3. RESULTS

We present the influence of the projectile impact angle on the internal emission yield under conditions with varying top metal layer thickness, bias voltage between the two metal electrodes and the projectile type and energy.

The results are compared to similar experiments detecting the external electron emission yield into vacuum and both analogies and differences are discussed. The measured internal emission yields are compared with two temperature simulations based on realistic microscopic barrier properties.

4. REFERENCES

[1] R. A. Baragiola, Nucl. Instrum. Methods B **78**, 223 (1993).
[2] A. Wucher, Appl. Surf. Sci. **255**, 1194 (2008)
[3] Z. Sroubek, Appl. Phys. Lett. **45**, 849 (1984).
[4] D. Diesing, G. Kritzler, M. Stermann, D. Nolting, and A. Otto, J. Sol. State Electrochem. **7**, 389 (2003).
[5] S. Meyer, D. Diesing, and A. Wucher, Phys. Rev. Lett. **93**, 137601-1 (2004).
[6] S. Meyer, Ch. Heuser, D. Diesing, and A. Wucher, Phys. Rev. B **78**, 035428 (2008).
[7] C. Heuser, M. Marpe, D. Diesing, and A. Wucher, Nucl. Instrum. Methods B **267**, 601 (2009)

* E-mail: `Christian.Heuser@uni-due.de`

TIME-DEPENDENT QUANTUM MECHANICAL SIMULATIONS OF ELECTRONS IN CARBON NANOMATERIALS RESEARCH

J. Jakowski[1,*], *S. Irle*[2], *and K. Morokuma*[3]

[1] National Institute for Computational Sciences, JICS-ORNL, Oak Ridge, TN 37831
[2] Institute for Advanced Research and Department of Chemistry, Nagoya University, Nagoya 464-8602, Japan
[3] Fukui Institute for Fundamental Chemistry, Kyoto University, Sakyo, Kyoto 6006-8103, Japan

1. INTRODUCTION

A common factor of methods for fabrication of carbon nanomaterials is that the new materials are synthesized in extreme condition environments including very high temperature, plasma, high pressure, electric field. The reaction selectivity for carbon nano-material fabrication is difficult to control and typically several structures beside the target structure are also produced. The controlled growth of single-walled carbon nanotubes and furthermore the ability to control of assembling of smaller carbon nano-blocks into larger units with a specific physico-chemical properties is a major challenge in nanotechnology for material science and carbon nano-tube research.
Our theoretical efforts have been concerned on improving understanding of processes related to the fabrication of carbon nano-materials. We present our progress on the development and application of first principles molecular dynamics called Liouville-von Neumann Molecular Dynamics [2].

2. THEORY

The proposed Liouville-von Neumann molecular dynamics (LvNMD), is based on classical Liouville propagation of nuclei and on von Neumann equation of motion for $P(t)$ electronic densities

$$\imath\hbar\frac{dP(t)}{dt} = [F(t), P(t)], \tag{1}$$

where $F(t)$ is the Fock operator at time t. Quantity $P(t)$ is a density matrix that be written as

$$P = CfC^T, \tag{2}$$

where C is the molecular orbitals matrix and f the is diagonal matrix of orbital occupancies. For thermally excited electrons at electronic temperature T_{el} occupancies are related to the Fermi-Dirac distribution and Fermi level (or chemical potential) μ as follows

$$f(\varepsilon) = \left(1 + \exp[(\varepsilon - \mu)/(k_B T_{el})]\right)^{-1}. \tag{3}$$

The final expression for the $P(t)$ is

$$P(t) = P - \imath t[\mathcal{F}, P] - \frac{t^2}{2!}[\mathcal{F}, [\mathcal{F}, P]] + \imath\frac{t^3}{3!}[\mathcal{F}, [\mathcal{F}, [\mathcal{F}, P]]] + \ldots \tag{4}$$

where P stands for $P(0)$ and $\mathcal{F}$ is obtained by truncation of Magnus expansion. Due to the special, recursive character of the algorithm (commutator expansion) the method seems to be well suited for the GPU.

3. SUMMARY

The LvNMD method is appropriate for Hartree-Fock, density functional and tight-binding calculations, and employs atom centered basis functions. Current implementation is based on semi-empirical self-consistent tight binding model [1]. The model is adequate compromise between computational cost and accuracy/reliability, as is shown by the good agreement obtained with experimental studies. The LvNMD method (a) is very stable and has very good conservation of energy, (b) is free of constraint and fictitious parameters, (c) avoids diagonalization of Fock operator, and (d) can be used in the case of fractional occupation as in metallic systems. Explicitly time-dependent quantum mechanical treatment for electrons makes LvNMD applicable in studies of charge transfer and non-adiabatic processes in which coupling between electronic and nuclear degrees of freedom is essential. Furthermore, LvNMD can be extended to describe interaction with strong perturbations (for example laser field), and to molecular electronics applications. Outlook on GPU implementation, further development and perspective applications is presented.

4. REFERENCES

[1] M. Elstner, D. Porezag, G. Jungnickel, J. Elsner, M. Haugk, Th. Frauenheim, S. Suhai, and G. Seifert. *Phys. Rev. B*, 58, 7260, (1998).

[2] J. Jakowski, K. Morokuma, S. Irle, *J. Chem. Phys.*, 130, 229 (2007).

* E-mail: `jjakowsk@utk.edu`

SCATTERING OF LOW ENERGY N_2 MOLECULES FROM THE W(110) SURFACE USING DIFFERENT EXCHANGE CORRELATION FUNCTIONALS

K. R. Geethalakshmi[1,2], *J. I. Juaristi*[1,2,3*], *R. Díez Muiño*[1,2], *and M. Alducin*[1,2]

[1] Centro de Física de Materiales (CSIC-UPV/EHU) - Materials Physics Center MPC,
P. Manuel de Lardizabal 5, 20018 San Sebastián, Spain
[2] Donostia International Physics Center DIPC, P. Manuel de Lardizabal 4, 20018 San Sebastián, Spain
[3] Departamento de Física de Materiales, Facultad de Químicas, Apartado 1072, 20080 San Sebastián, Spain

In the numerical simulations of the interaction of diatomic molecules, with energies in the eV range, impinging on metal surfaces the problem is usually split in two parts. First, the six-dimensional potential energy surface (PES) for the molecule-surface interaction is obtained. Second, on top of this PES classical or quantum mechanical dynamics are performed.

As a consequence, the accuracy of this approach to simulate the molecule-surface interaction relies on the quality of the PES. The PES is calculated from the interpolation of ab-initio density functional (DFT) energies calculated for a set of different molecule-surface configurations. DFT is, in principle, an exact theory, that loses its accuracy in practice due to the unknown form of the exchange-correlation (XC) functional to be used in the Kohn-Sham scheme. In this respect, the generalized gradient approximation (GGA) in which the XC energies are a functional of both the electronic density and its gradient, is the standard accurate gas/surface description employed in this kind of calculations. Since there are different GGAs available, an analysis of how the theoretical predictions are affected by the choice of the XC functional provides information on the level of accuracy that can be achieved. In a recent work [1] it has been presented a comparison between the theoretical predictions for the dissociative adsorption of N_2 on different tungsten surfaces, when using the potential energy surfaces calculated with the PW91 [2] and RPBE [3] XC-functionals. It was shown, that the results obtained for the dissociative adsorption probability with the two functionals differ significantly. Comparison with the results from molecular beam experiments for different incident energies and different angles of incidence of the impinging molecules, did not lead to a definite conclusion as to which functional provides the better PES. The reason is that each functional performed better for different initial conditions. Briefly, it was concluded that the RPBE functional appeared to produce a too repulsive PES far from the surface, thought it seemed to describe better than the PW91 the regions close to the chemisorption well. A limitation in extracting information uniquely from the obtained results for the dissociative adsorption probability is that the final state of the dissociation process is not directly accessible. For this reason, it is interesting to analyze the dynamics of the scattered molecules for which their final state can also be analyzed.

In this work, we use both the PW91 and RPBE PES to study the scattering of N_2 molecules in the W(110) surface. Results for the angular distribution of the reflected molecules and their rotational state population distributions are presented. Comparison between the results obtained with the two different PESs and with available experimental data [4] allows us to gain a more detailed insight on the virtues and shortcomings of the different functionals to study the dynamics of molecule-surface scattering. In general, the PW91 PES is more corrugated tan the RPBE one in all the configuration space, meaning that there is a stronger dependence of the potential energy on the molecular orientation and position. Furthermore, we find that the larger corrugation and the less repulsive character exhibited by the PW91 PES seems to be realistic at distances above the chemisorptions well. In contrast, the less corrugated RPBE PES performs better in the region below the chemisorption well.

REFERENCES

[1] G. A. Bocan, R. Díez Muiño, M. Alducin, H. F. Busnengo, and A. Salin, J. Chem. Phys. **128**, 154704 (2008).
[2] J. P. Perdew, J. A. Chevary, S. H. Vosko, K. A. Jackson, M. R. Pederson, D. J. Singh, and C. Fiolhais, Phys. Rev. B. **46**, 6671 (1992).
[3] B. Hammer, L. B. Hansen, and J. K. Nörskov, Phys. Rev. B **59**, 7413 (1999).
[4] T. F. Hanisco and A. C. Kummel, J. Vac. Sci. Technol.A **11**, 1907 (1993).

* E-mail: josebainaki.juaristi@ehu.es

AUGER NEUTRALIZATION IN THE SCATTERING OF HE$^+$ IONS FROM A POLYCRYSTALLINE Cu SURFACE

K. Khalal-Kouache[1,*], *D. Primetzhofer*[2] *and P. Bauer*[2]

[1] Faculté de Physique, USTHB, BP 32 El Alia, Bab Ezzouar, Algiers, Algeria
[2] Institut für Experimentalphysik, Johannes Kepler Universität, Altenbergstr. 69, A-4040 Linz, Austria

1. ABSTRACT

We consider charge exchange in the scattering of He$^+$ $(2\ \mathrm{keV})$ ions from a polycrystalline copper surface. At this energy, neutralization of the incident ions is due to Auger transition. The scattering angle measured from the incident beam is $\theta = 129°$. A modified [1] TRIM [2] version is used to calculate TOF spectra at this energy regime where multiple scattering become important. The used Monte Carlo method is based on the binary collision approximation and takes into account charge exchange processes. The Auger transition rate is considered as a free parameter in the simulation. We compare the TOF-spectra obtained from the simulations to experimental spectra and discuss the results.

2. REFERENCES

[1] K.Khalal-Kouache, A.C.Chami, M.Boudjema, C.Benazeth, Nucl. Instr. and Meth. **B258**, 40 (2007).
[2] J.F.Ziegler, J.P.Biersack, U.Littmark, *The Stopping and Ranges of Ions in Solids*, (Pergamon Press, New York, 1985).

[*] E-mail: kkouache@yahoo.fr

INTERNAL EXCITATION OF SLOW C_{60}^+ IONS DURING GRAZING ANGLE SCATTERING AT A KCl(001) SURFACE

S. Takagi, S. Maekawa, K. Nakajima, M. Suzuki, and K. Kimura

Department of Micro Engineering, Kyoto University, Kyoto 606-8501, Japan

1. INTRODUCTION

When C_{60}^+ ions are incident on single crystal surfaces at a grazing angle, most C_{60}^+ ions are reflected from the surface without fragmentation. Rest of the incident C_{60}^+ ions, however, emit one or several C_2 molecules and the resultant C_{60-2n}^+ ions are reflected from the surface [1, 2]. The mechanism of the C_2 loss is well understood for metal surfaces [1]. A large part of the normal energy of C_{60}^+ (energy for the motion along the surface normal) is lost during the grazing scattering. This energy loss is transferred to internal excitations of C_{60}^+, which results in C_2 emission. In the case of a KCl(001) surface, however, the situation is different [2]. While a substantial fraction of C_{60-2n}^+ ions are also reflected from KCl(001), these ions are reflected at a specular angle, *i.e.* there is no energy loss in the normal motion, showing that the C_2 loss mechanism is different from the metal surface.

A possible mechanism of the internal excitation of the C_{60}^+ ions is related to a strong corrugation of the surface potential for ionic crystals. The C_{60}^+ ions feel a strong alternate electric field (pseudophoton field) in front of the KCl(001) surface. The amplitude of the electric field can be as high as ~0.1 a.u., which may cause a strong internal excitation of C_{60}^+ when the frequency of the pseudophoton field mach one of the internal excitation energies (resonant coherent excitation: RCE). In order to examine this possibility, we have measured azimuth angle dependence of the C_2 emission probability.

2. RESULTS AND DISCUSSION

A beam of 3 keV C_{60}^+ ions was produced by a 10-GHz ECR ion source. The beam was incident on a (001) surface of a KCl single crystal at a grazing angle θ_i. A narrow slit (width 0.1 mm) was placed at 365 mm behind the KCl crystal. The ions passing through the slit were dispersed in an electric field and detected by a two-dimensional position-sensitive detector. This allows us to measure the fragment-size distribution of the scattered C_{60-2n}^+ ions. It is noteworthy that the neutral fraction of the reflected ions was small. This is because the ionization energies of C_{60-2n} (*e.g.* 7.6 eV for C_{60}) are located in the band gap of KCl, which prohibits both resonant and Auger neutralization processes. Thus, the present measurement does not suffer from the neutralization process and this simple setup allows us to measure the C_2 loss probability rather accurately.

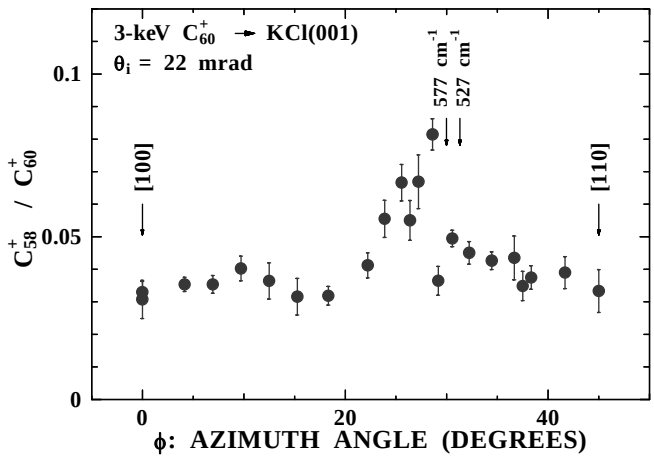

Figure 1: Observed yield ratio of C_{58}^+/C_{60}^+ as a function of the azimuth angle.

Figure 1 shows the observed yield ratio of C_{58}^+/C_{60}^+ as a function of the azimuth angle φ with respect to the [100] direction when 3 keV C_{60}^+ ions are incident on KCl(001) at a grazing angle of 22 mrad. The data points are rather scattered but there is a broad peak at φ ~ 27º. The RCE energy corresponding to this peak is ~ 640 cm^{-1} (~ 80 meV), which roughly agrees with the excitation energies of the C_{60} vibrational modes 527 and 577 cm^{-1} (65 and 72 meV) observed by FTIR.

3. REFERENCES

[1] S. Wethekam and H. Winter, Phys. Rev. A **76**, 032901 (2007).

[2] T. Matsushita, K. Nakajima, M. Suzuki and K. Kimura, Phys. Rev. A **76**, 032903 (2007) 032903.

* E-mail: kimura@kues.kyoto-u.ac.jp

ION-INDUCED BERYLLIUM NITRIDE FORMATION AND ITS INFLUENCE ON DEUTERIUM RETENTION

*M. Köppen, T.-V. Phan, M. Oberkofler, Ch. Linsmeier**

Max-Planck-Institut für Plasmaphysik, EURATOM Association, Boltzmannstr. 2, 85748 Garching b. München, Germany

1. BACKGROUND

The exposure of clean beryllium metal to air leads to the formation of BeO only, the formation of beryllium nitrides is not observed. This is surprising, since the free energies of formation for BeO and beryllium nitride, Be_3N_2, are with values of 5.54 eV for Be_3N_2 and 6.02 eV for BeO similar and both strongly exothermic [1]. The oxide is readily formed both by exposure of Be metal to molecular and atomic oxygen [2]. The nitride, however, can be formed by laser ablating beryllium in a molecular nitrogen atmosphere [3]. This suggests that a high activation barrier exists for the formation of the nitride from the elements, possibly related to the dissociation of the N_2 molecule. In this study the formation of beryllium nitride is demonstrated from nitrogen ions implanted into clean beryllium surfaces at room temperature.

The beryllium–nitrogen interaction is in particular of importance for fusion experiments which operate with Be at the first wall, like JET and ITER. Nitrogen gas has been used successfully as seeding gas for the edge and divertor plasmas, e.g. in ASDEX Upgrade. Seeding of impurities to the edge plasma reduces the edge plasma temperature significantly and opens a way to limit the power flux to the first wall and divertor structures. Besides the edge cooling, the nitrogen seeding also increased the overall plasma performance [4]. If beryllium nitride is formed at the first wall, this nitride can alter the retention behavior for hydrogen isotopes or, due to its large band gap of more than 4 eV, can induce arcing. Both phenomena depend on the thickness of the formed nitride layer and are important issues for the prediction of plasma-wall interaction processes with a beryllium first wall.

2. NITRIDE FORMATION

The interaction between nitrogen and beryllium is investigated by implanting nitrogen ions in the keV energy range into polycrystalline beryllium. X-ray photoelectron spectroscopy (XPS) is used for qualitative and quantitative analysis, determining the formed compounds and the amount of retained nitrogen. The total amounts of nitrogen are additionally quantified ex situ by Rutherford backscattering spectrometry (RBS). Thermal desorption spectroscopy (TDS) is applied to investigate the stability of the nitride. The formed chemical phases are determined as a function of the nitrogen fluence and of the substrate temperature during nitrogen ion implantation. Different nitrogen implantation energies in the range between several 100 eV to keV are applied, varying the depth distribution of nitrogen in beryllium. The experimental implantation profiles are compared to simulations with the Monte Carlo code SDTrim.SP.

First investigations implanting nitrogen at 3 keV into cleaned polycrystalline beryllium samples at room temperature lead to the formation of a surface compound with a Be/N ratio of approximately 1. Both the Be $1s$ and N $1s$ core level signals show a strong chemical shift compared to the elemental signals, indicating compound formation. The measured binding energy for Be $1s$ after annealing of the nitride layer corresponds to the value reported in [3], for the nitride layers produced by laser ablation. After deuterium implantation into the formed nitride layer, however, an additional Be $1s$ shift to higher binding energies is observed. This indicates different chemical phases produced by the implantation of nitrogen only and nitrogen together with deuterium species into beryllium.

3. REFERENCES

[1] I. Barin, *Thermochemical Data of Pure Substances*, volume 1 & 2 (VCH, Weinheim, 1995), 3rd edition.

[2] Ch. Linsmeier and J. Wanner, Surf. Sci. 454-456 (2000) 305.

[3] G. Soto, J. A. Díaz, R. Machorro, A. Reyes-Serrato, and W. de la Cruz, Mater. Lett. 52 (2002) 29.

[4] A. Kallenbach, R. Dux, M. Mayer, R. Neu, T. Pütterich, V. Bobkov, J.C. Fuchs, T. Eich, L. Giannone, O. Gruber, A. Herrmann, L.D. Horton, C.F. Maggi, H. Meister, H.W. Müller, V. Rohde, A. Sips, A. Stäbler, J. Stober, and ASDEX Upgrade Team, Nucl. Fusion 49 (2009) 045007.

* E-mail: linsmeier@ipp.mpg.de

SULPHUR INDUCED RECONSTRUCTION OF Ag(111) SURFACES

H. L. Álvarez Soria and M. L. Martiarena

Consejo Nacional de Ciencia y Tecnología (CONICET), and Instituto Balseiro,
Centro Atómico Bariloche Av. Bustillos 9500, 8400 Bariloche, Argentina

The sulphur-induced metal surface reconstruction is a hot topic in the field of thiols self-assembly, where many recent works report contradictory experimental and theoretical results[1]. The elucidation of the S/metal interface is important since sulphur constitutes the head and anchorage group and its adsorption could modify the characteristic of the metallic subtract.

Sulphur monolayers can be easily formed on Au and also on Ag by simple immersion in sulfide-containing solutions (S^{-2}, SH^{-} or SH_2 species) or by sample exposure to gaseous S_2 or SO_2 [2]. Though, it seems to be generally accepted that this phase is associated with the formation of a sulphide structure similar to that of a bulk Ag_2S crystalline phase[2-3], there has been no explicit conclusive description of the selvedge structure in terms of the positions of the S and Ag atoms. Some authors explain that, in some situations, the ordering corresponds to a multilayer "bulk" sulphide film on the surface [2] but there is also evidence of a single layer phase having the same periodicity [3]. In general, however, these methods do not provide any direct, and certainly quantitative, information on the S-headgroup/metal interface structure.

We have carried out DFT calculations within the slab-supercell approach using the ab-initio total energy and molecular dynamics program VASP (Vienna ab-initio simulation program) [4], rely on the generalized gradient approximation to electronic exchange and correlation proposed by Perdew and Wang. We use the Projector Augmented Wave method, a plane wave basis set with energy cut-off of 350 eV and a 9x9x1 Monkhorst-Pack k-point mesh.

The Ag(111) surface was represented for a six-layer slab in a $\sqrt{(7)} * \sqrt{(7)}$R 19.1° unit cell, using a 7x7x1 k-point mesh and during full geometry optimizations we allowed relaxation of the four top-most layer metal atoms and all the S atoms until reaching forces smaller than 0.02 eV/ Å.

We study the energetic, the charge displacements generated by sulphur atoms, the projected density of states, and simulate in the Tersoff- Hamann approach the STM images. All those studies were done as a function of the sulphur coverage (Θ= 1/7, 2/7 and 3/7) and at different two temperatures (T=0 and 293 K).

We show that when the coverage is high enough, (Θ= 3/7) the adsorption of sulphur atoms is produced on in-equivalent sites (FCC, HCP and TOP). Due to the charge displacements generated by previously adsorbed S atoms, the addition of a third atom at the minimum energy TOP site, produces the motion of the atoms of the two topmost layers of silver and the immersion of the HCP-S atom through a sub-superficial site.

The simulated STM images for this system, considering different V_{bias} (-0.77 eV, and -1.08 eV), gives a very good agreement with the experiment. We can explain, studying the intrinsic contribution that introduces the sulphur electrons to the projected density of states around E_{Fermi} + V_{bias}, the changes observed in the STM images.

The molecular dynamic study at T=293K allows us to indentify the coexistence of two phases not yet recognized, but that it can be observed, in the STM images.

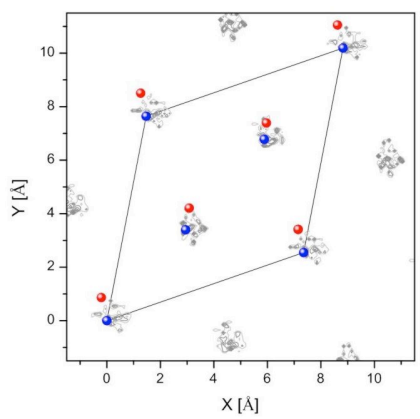

Fig1: Contour plot of frequency count in plane XY. Blue balls: equilibrium S atoms positions at T = 0K; Red balls: local minima obtained by molecular dynamics at T = 293K. Both positions characterize two phases in the experimental STM images [4].

[1] P. Maksymovych et al, Phys. Rev. Lett. 2006, 97, 146103; R. Mazzarello et al, Phys. Rev. Lett. 2007, 98, 016102; V. Srinivasan et al, Phys. Rev. Lett. 2008, 101, 185504; A. Chaudhuri et al, Phys. Rev B 2009, 79, 195439; A. Chaudhuri et al, Phys. Rev. Lett 2009, 102, 126101.

[2] F. Schreiber, Prog. Surf. Sci. 2000, 65, 151; J. Love et al, Chem.Rev 2005105, 1103; D. .P. Woodruff, Phys. Chem. Chem. Phys. 10, 7211 (2008); C. Vericat et al , Chem. Soc. Rev. 39, 1805 (2010);

[3] M. Yu et al, Phys. Chem. C 2007, 111, 3152

[4] G. Kresse and J. Furthmüller, Comput. Mater. Sci. 1996, 6, 15.

E-mail: mluz@cab.cnea.gov.ar

THE ROLE OF SUBSTRATE VACANCIES IN THE STRUCTURING OF METHYLTHIOLATE MONOLAYERS ON Ag(111)

P.N.Abufager[1], L. Alvarez Soria[2], K.Reuter[3], M.L.Martiarena[2] and H.F.Busnengo[1]

[1] Instituto de Física Rosario, CONICET and Universidad Nacional de Rosario, Pellegrini 250 (2000) Rosario, Argentina

[2] CONICET, Centro Atómico Bariloche and Instituto Balseiro, Av. Bustillos 9500, 8400 Bariloche, Argentina

[3] Department Chemie, Technische Universit at München, Lichtenbergstr. 4, D-85747 Garching, Germany.

The intensely studied [1-3] adsorption of methylthiolates (SCH_3) on surfaces of coinage metals Cu, Ag, and Au represents an ideal benchmark system to understand self-assembled monolayers (SAMs) of alkylthiolates. These systems have a great number of technological applications, in e.g. molecular electronics or molecular recognition due to their ability of nanostructuring surfaces [3]. In recent years there is increasing experimental evidence for a strong SCH_3-induced reconstruction of even the close-packed Cu(111), Ag(111) and Au(111) surfaces [3]. Nevertheless, the actual structure of the SCH_3/substrate selvedge remains in general controversial [2,3].

As a representative example we focus here on the SAM of methylthiolates on Ag(111). It is widely accepted that it is characterized by a $(\sqrt{(7)}*\sqrt{(7)})$R19° periodicity with three molecules per surface unit cell[3]. The simplest conceivable model considers a hexagonal arrangement of SCH_3 on the unreconstructed substrate, chemisorbed at inequivalent sites (fcc, hcp and top site). With an anticipated much higher height of the anchoring S atom in the latter site, this model predicts a significant rumpling of molecular heights within the unit cell. However, this is not consistent with scanning tunneling microscopy (STM) [4], normal incidence X-ray standing wave (NIXSW)[5] and medium energy ion scattering (MEIS)[6] results. In light of this data, a model involving four Ag vacancies in the topmost metal layer was proposed, which allows all three SCH_3 molecules to adsorb on enlarged threefold hollow sites[4-6]. The stability of this and other structures involving four vacancies was subsequently investigated by Density-Functional Theory (DFT) calculations [2,6]. Obtaining essentially identical stabilities compared to the unreconstructed surface a coexistence of all phases was suggested [6]. This was inconsistent with the experimental observations [3].

In this work we revisit the problem with a systematic DFT study of the stability of an extended range of possible adsorption models consistent with a $(\sqrt{(7)}*\sqrt{(7)})$R19° periodicity, a coverage Θ=3/7, and involving from zero (unreconstructed surface) to X =1-4 topmost layer Ag atom vacancies.

Our DFT and *ab initio* thermodynamics results (see Fig:1) results unambiguously show that the SAM of methylthiolates on Ag(111) is stabilized by a strong adsorption induced substrate reconstruction, which entails a reduced density of Ag atoms in the outer-most substrate layer in line with the interpretation of STM, NIXSW and MEIS experiments [4,5].

In particular, the most stable structure we have found R7.R7-2v involves a 5/7 density of top-most layer Ag atoms. The R7.R7-2v phase properly accounts for the small corrugation amplitude of the anchoring S atoms and the height of the S layer above the substrate predicted from experiments, as well as experimental STM images.

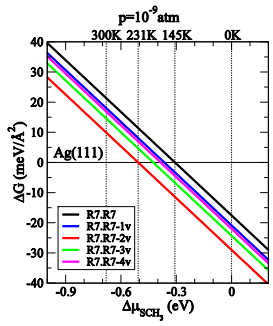

Fig1: Gibbs free energy of adsorption per unit area ΔG vs $\Delta\mu(SCH_3)$, for the various structural models studied. Upper x-axis: dependence on the gas-phase chemical potential (μ) cast into a temperature scale for $p=10^{-9}$atm.

[1] J.C. Love et al Chem. Rev. 105,1103(2005).
[2] C. Vericat et al , Chem. Soc. Rev. 39, 1805 (2010).
[3] D. .P. Woodruff, Phys. Chem. Chem. Phys. 10, 7211 (2008).
[4] M.Yu et al, Langmuir 21,7285(2005); M.Yu et al, J.Phys.Chem. B110, 2164 (2006).
[5] G.S.Parkinson et al, Surf.Sci. 601, 50 (2007).
[6] D.Torres et al, Phys.Rev.Lett. 97, 226103 (2006).

* E-mail: mluz@cab.cnea.gov.ar

SPUTTERING OF LUNAR REGOLITH SIMULANT BY PROTONS AND MULTICHARGED HEAVY IONS AT SOLAR WIND ENERGIES[&]

F.W. Meyer[1*], *P.R. Harris*[1], *C.N. Taylor*[1#], *H.M. Meyer III*[2]

[1] Physics Division, Oak Ridge National Laboratory, P.O. Box 2008, Oak Ridge, TN 37831
[2]Material Sciences and Technology Division, Oak Ridge National Laboratory, P.O. Box 2008, Oak Ridge, TN 37831

1. INTRODUCTION

We report preliminary results on sputtering of a lunar regolith simulant sample by singly and multiply charged solar wind ions using a line-of-sight time-of-flight (TOF) mass spectrometry approach. Sputtering of the lunar regolith by solar wind heavy ions is an important particle source that contributes to the composition of the lunar exosphere, and is a possible mechanism for lunar surface ageing and compositional modification [1]. The measurements were performed in order to assess the relative sputtering efficiency of protons, which are the dominant constituent of the solar wind, and heavier, but lower abundance, solar wind constituents, which have higher physical sputtering yields than isovelocity protons, and whose sputtering yields may be further enhanced due to potential sputtering, since the heavier ion solar wind constituents are all highly charged.

2. EXPERIMENT

The ions were generated using an electron cyclotron resonance (ECR) ion source operated at source potentials between 10-15kV. After being extracted, transported, and decelerated, the ions are normally incident on a JSC-1A AGGL lunar regolith simulant sample that is situated within a floating UHV scattering chamber. The relative bias between the ECR ion source and the surface end station was adjusted to produce a constant impact energy of 0.375keV/amu for each of the ion beams investigated. To reduce sample charging and to improve sample uniformity, the simulant sample was first sifted to select particles smaller than 180 microns. The sifted sample was then sprinkled onto carbon tape, and gently finger pressed to improve adhesion with the tape. XPS and SEM were used to confirm the sample chemical composition and morphology. An electron flood gun was installed in the surface chamber to permit sample charge neutralization as required, and to permit surface analysis by ESD. Deposition of the simulant on carbon tape was investigated since a previous attempt [2], employing a pressed sample, was hampered by sample charging effects which made spectrum normalization problematic. Also, the target press method was found to destroy the amorphous rim structure around the individual dust grains where most of the sputtering interactions at solar wind relevant energies occur.

3. RESULTS

Figure 1 shows an SEM image of the sample prepared in the manner described above. Preliminary sputtering yields for solar wind singly and multiply charged ions incident on this target will be presented at the conference.

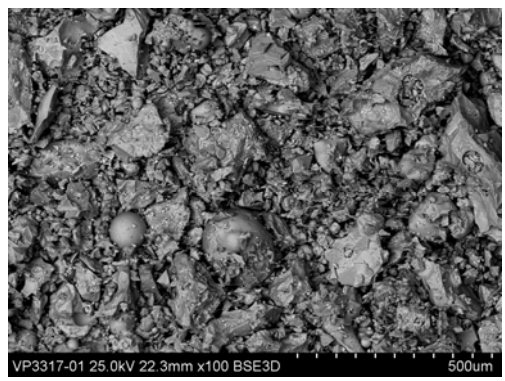

Figure 1: SEM of sifted JSC-1A-AGGL lunar simulant target on carbon tape.

[&]This research is supported by the ORNL LDRD program, and the U.S. Department of Energy, Office of Basic Energy Sciences under contract number DE-AC05-00OR22725 with UT-Battelle, LLC.
[#]HERE participant from the Purdue University School of Nuclear Engineering.

4. REFERENCES

[1] A.F. Barghouty, J.H. Adams, F.W. Meyer, L. Mansur, and C. Reinhold, Poster P-31B-1402, AUG Conference, San Francisco, CA Dec. 15-19, 2008.
[2] P.R. Harris, F.W. Meyer, H. Meyer III, A. Barghouty, and J. Adams, SELAC workshop, Athens, GA, 3/30/10; www.physast.uga.edu/workshops/dustandice/abstracts.

[*] E-mail: meyerfw@ornl.gov

INFLUENCE OF SCREENING LENGTH MODIFICATION ON THE SCATTERING CROSS SECTION IN LEIS

D. Primetzhofer[*,1], *S.N. Markin*[1], *D.V. Efrosinin*[2], *E. Steinbauer*[1], *R. Andrzejewski*[1] *and P.Bauer*

[1] Institut fuer Experimentalphysik, Johannes Kepler Universitaet Linz, Altenbergerstr. 69, A-4040 Linz, Austria
2 Institut fuer Stochastik, Johannes Kepler Universitaet, Altenbergerstr. 69, A-4040 Linz, Austria

1. INTRODUCTION

Low-Energy Ion Scattering (LEIS) is a commonly used tool for the analysis of composition and structure of the outermost atomic layers [1]. Furthermore, it permits to probe the electronic structure of a solid by investigation of ion neutralization and electronic energy loss. In all these applications precise knowledge of the scattering cross section is required for quantification of experimental data. The interaction is described by a screened Coulomb potential, e.g. within the Thomas-Fermi-Molière (TFM) model. The absolute potential strength can be modified by a multiplicative correction c_a to the screening length a [2].

2. RESULTS

Scattering cross sections $d\sigma/d\Omega$ calculated for He^+ ions and different target atoms in the TFM model for different values of c_a are presented. Results are compared to the Rutherford cross section and to a correction for $d\sigma/d\Omega$ typically used for MEIS energies (30-200 keV) [3].
Furthermore, it is shown that different screening length modifications as an input parameter for Monte-Carlo simulations lead to a systematic change in physical quantities deduced from experimental spectra, e.g. the electronic energy loss of backscattered projectiles.

2.1. Scattering cross sections

Scattering cross sections were calculated for H and He ions scattered from Al, Cu and Au atoms at primary energies E in the range 100 eV to 200 keV. The ratio $d\sigma(c_a\neq1)/d\sigma(c_a=1)$ shows universal scaling with the atomic numbers Z of target and projectile atoms and E, the effects being largest for low E and high Z. The accuracy of the approximations employed in the MEIS regime is found to be most accurate for target atoms with low Z.

2.2. Implications

Very good agreement can be achieved between experimental and simulated energy spectra, even if quite different c_a values are used as an input, when the electronic energy loss ε in the solid is accordingly tuned. Fig. 1 shows an experimental spectrum obtained for 5 keV D_2^+ ions scattered from Cu and three simulations; note the perfect agreement even if the input parameters for c_a and ε differ by up to ~ 60% from one simulation to another.

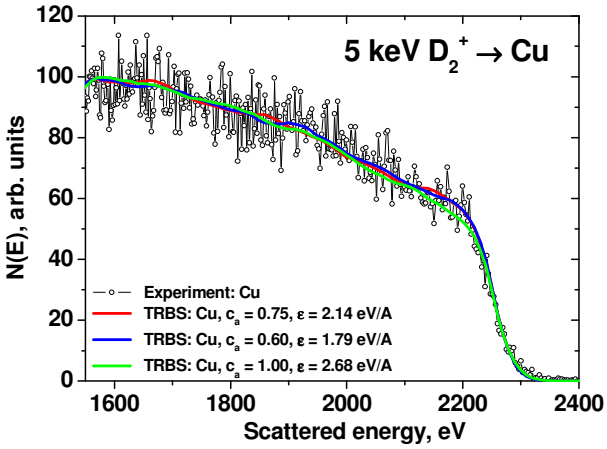

Fig.1: Experimental and simulated spectra for 5 keV D_2^+ scattered from polycrystalline Cu.

These results indicate that wrong physical properties might be deduced from experimental spectra when an improper choice is made for the screening length correction c_a. This indicates the enormous importance of precise knowledge of the interaction potential strength or the use of reference samples.

3. REFERENCES

[1] H.H. Brongersma, M. Draxler, M. de Ridder, P. Bauer, Surf. Sci. Rep. **62** (2007) 63.
[2] H. Winter, Phys. Rep. **367** (2002) 388.
[3] H.H. Andersen, F. Besenbacher, P. Loftager, and W. Möller, Phys. Rev. A **21** (1980) 1891

[*] E-mail:. daniel.primetzhofer@jku.at

A MULTI-ELEMENT ORGANIC COMPOUND STUDIED BY HIGH-RESOLUTION RUTHERFORD BACKSCATTERING SPECTROMETRY

D. Primetzhofer[*], *and P.Bauer*

Institut für Experimentalphysik, Johannes Kepler Universitaet Linz, A-4040 Linz, Austria

1. INTRODUCTION

Rutherford backscattering spectrometry (RBS) is a versatile tool for analysis of composition and thickness of nm-films. Other ion beam based techniques (e.g. SIMS, PIXE) have been successfully applied also for investigations of organic materials [1,2]. In the present work the potential of high-resolution RBS for detection of trace elements in an organic compound, i.e. human blood, was tested.

2. EXPERIMENT AND RESULTS

2.1. Set-up and sample preparation

The experiments were performed employing the AN-700 accelerator at the Johannes Kepler University of Linz, which can provide monoenergetic beams of H,D and He ions with up to 700 keV primary energy. A high resolution LN_2 cooled surface barrier detector was used to record the spectra of backscattered projectiles [3]. The blood sample was prepared in the following way: a droplet of human blood was deposited on a graphite sample, dried in air and subsequently transferred to the target chamber together with a second graphite reference target.

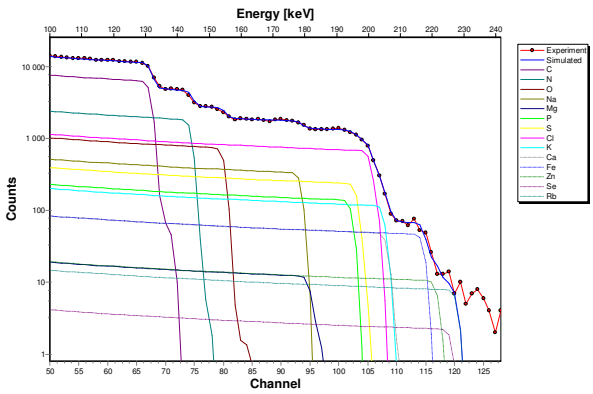

Figure 1: RBS spectrum for 250 keV D^+ scattered from a film of human blood deposited on graphite. Shown are the experiment and a fit obtained by SIMNRA [4].

2.2. Experimental results

RBS spectra were recorded for 250 keV D^+ ions scattered from the blood film and the reference sample. Simulations of the RBS spectra were performed using the program SIMNRA [4]. For the graphite reference target elements other than C were below a concentration of 1.5 at%. From the shape of the RBS spectrum of the organic sample it can be ascertained that the substrate signal is not visible. It was possible to identify at least 10 chemical elements with high accuracy, as can be seen in Fig.1. For instance, the concentration of Fe was determined to 350 +/- 10 ppm equivalent to 400 mg/L in perfect agreement with standard blood test values. The detection limit for elements with atomic number higher than Fe is found to be below 20 ppm. Note that it would be possible to resolve a concentration gradient within the film by high-resolution RBS.

2.3. Conclusion

The results presented clearly indicate the potential of high-resolution RBS for identification of trace elements in organic samples. The main advantage of using RBS is that relative and absolute concentrations of present elements can be determined with very high accuracy and no matrix effects have to be expected.

3. REFERENCES

[1] A. Benninghoven, and W.K. Sichtermann, Analytical Chemistry **50** (1978) 1180

[2] R. Lobinski, C. Moulin, and R. Ortega, Biochimie **88** (2006) 1591

[3] M. Geretschläger, Nucl. Instr. and Meth. B **204** (1983) 479

[4] M. Mayer, Application of accelerators in research and industry **475** (1999) 541

[*] E-mail:. daniel.primetzhofer@jku.at

Directed irradiation synthesis and in-situ characterization of self-assembled nanostructures in the Particle and Radiation Interaction with Hard and Soft Matter (PRIHSM) facility

D.L. Rokusek[1,*], O. El-Atwani[2], S. Ortoleva[1], B. Heim[1], and J.P. Allain[1,3]

[1] School of Nuclear Engineering, Purdue University, West Lafayette, IN 47907, USA
[2] School of Materials Engineering, Purdue University, West Lafayette, IN 47907, USA
[3] Birck Nanotechnology Center, Discovery Park, Purdue University, West Lafayette, IN 47907, USA

1. DIRECTED IRRADIATION SYNTHESIS

Radiation in the form of energetic charged particles can induce patterned nanostructures by sputtering and other surface-related processes. Thorough reviews of nanostructure synthesis by ion beam techniques are given by Krasheninnikov and Banhart [1] as well as Dhara [2]. A thorough understanding of the self-organization process from in-situ characterization during irradiation is needed in order to tailor function to such systems.

This work will investigate the relationship between surface composition, incident species, dose, and structure formation. Motivated by the ordered nanodots on Ar-sputtered GaSb seen by Facsko *et al.* [3], this work will extend recent work performed near and below sputter-threshold [4]. A broad beam ion source will be used to deliver a varied dose (10^{17} to $5x10^{18}$ cm^{-2}) of low energy (10 – 200 eV) ions at normal incidence to GaSb and InP (100) surfaces. Irradiation with Ar and Xe ions is investigated.

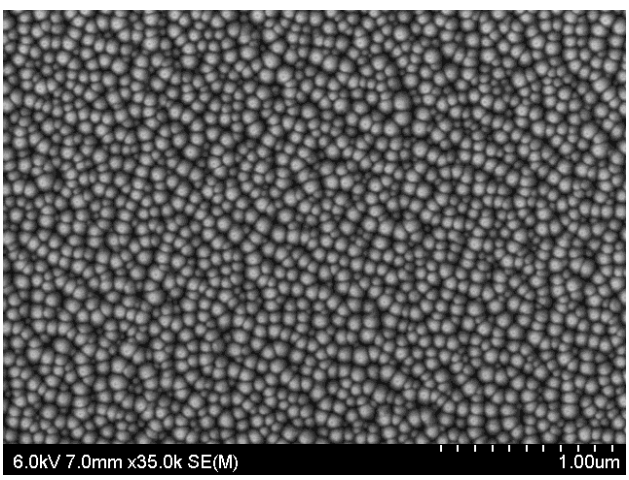

Figure 1. 1000 eV Ar^+ on GaSb(100) at normal incidence. Ion fluence > 10^{17} cm^{-2}.

Irradiation-induced changes in surface composition as well as size and density of the synthesized nanostructures will be compared using ion scattering spectroscopy (ISS) in forward and backward modes, x-ray and ultraviolet photoelectron spectroscopy (XPS, UPS), and sputter measurements with a quartz crystal microbalance (QCM). Secondary ion emission and its dependence on nano topography will also be examined. Ex-situ surface analysis consists of atomic force microscopy and scanning electron microscopy. Results will show structure formation at low energy as well as a relationship between structure formation and incident species.

2. THE PRIHSM FACILITY

A new multi-probing diagnostic surface characterization experiment has been designed and built at Purdue University. The Particle and Radiation Interaction with Hard and Soft Matter (PRIHSM) experimental facility combines a collection of modifiers and probes to provide in-situ surface characterization for a variety of surfaces. Designed to examine irradiation-induced modification of surfaces and interfaces, the PRIHSM facility studies in-situ how energetic radiation affects the mechanical, chemical, and electronic properties of low-dimensional state materials.

The effects of energetic particle bombardment are analyzed in-situ with a two-dimensional hemispherical electron analyzer used in conjunction with excitation sources to conduct UPS, XPS, low-energy ion scattering spectroscopy (LEISS), and angle resolved photoemission spectroscopy (ARPES). During directed irradiation synthesis of self-organized nanostructures, erosion rates can be monitored in real time with a QCM. Sputter measurements from initial QCM commissioning as well as ISS, UPS, XPS calibration data are presented, demonstrating the ability to give elemental and chemical state information at the first 2-3 monolayers.

3. REFERENCES

[1] A. V. Krasheninnikov and F. Banhart, Nat. Mater. **6**, 723 (2007).
[2] S. Dhara, Crit. Rev. Solid State **32**, 1 (2007).
[3] S. Facsko, *et al.*, Science **285**, 1551 (1999).
[4] J. P. Allain, *et al.*, Nucl. Instr. and Meth. B (to be published, IBMM 2010).

* E-mail: drokusek@purdue.edu

CHARGE EXCHANGE OF He^+ IONS ON ALUMINIUM SURFACES

S. Rund[*], *D. Primetzhofer, S.N. Markin and P. Bauer*

[1] Institut fuer Experimentalphysik, Johannes Kepler Universitaet Linz, A-4040 Linz, Austria.

1. INTRODUCTION

The efficient neutralization of low energy ions scattered from surface atoms is the basis of the superior surface sensitivity in Low-Energy Ion Scattering (LEIS) [1]. Below a reionization threshold E_{th} non-local Auger neutralization (AN) is the only relevant charge exchange process and permits to describe the ion fraction P^+ by

$$P^+ = \exp(-\int_0^\infty \Gamma_A(z(t))dt) \equiv \exp(-\frac{v_c}{v_\perp}) \qquad (1)$$

with the Auger transition rate Γ_A, the characteristic velocity v_c and the velocity of the projectile perpendicular to the surface $v_\perp$.

At primary energies $E > E_{th}$ local charge exchange processes, i.e. collision induced reionization (CIR) and collision induced neutralization (CIN) start to contribute.

2. EXPERIMENTAL RESULTS

An Al(111) single crystalline surface and polycrystalline aluminium have been investigated by electrostatic analyzer low-energy ion scattering (ESA-LEIS) using $^3He^+$ and $^4He^+$ ions. Experiments were performed with the set up MiniMobis which permits precise analysis of the energy of ions backscattered in single collision from surface atoms at very low primary energies (down to 280 eV).

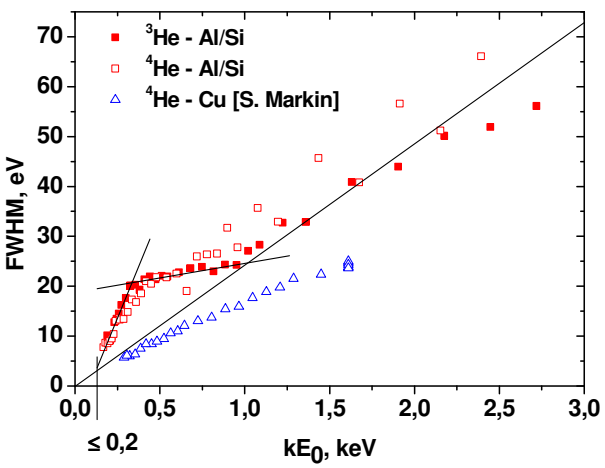

Figure 1: FWHM of the detected ion intensity backscattered from Al (squares) and Cu (triangles).

The reionization threshold E_{th} was deduced from the energy dependence of the FWHM of the ion peak. For Cu where AN dominates up to 2 keV ΔE~E is observed [2], as expected for an ESA. In contrast, the FWHM of the ion peak in spectra recorded for He^+ and Al exhibits a significant broadening at 0.2– 1 keV (see Fig. 1). Since reionization leads to an energy loss (~ 15 – 20 eV) the increasing contribution of CIR will also increase the FWHM and additionally shift the ion peak to smaller energies. Extrapolating data points of ^4He and ^3He scattered from Al/Si at higher energies one obtains E_{th} = 200 eV.

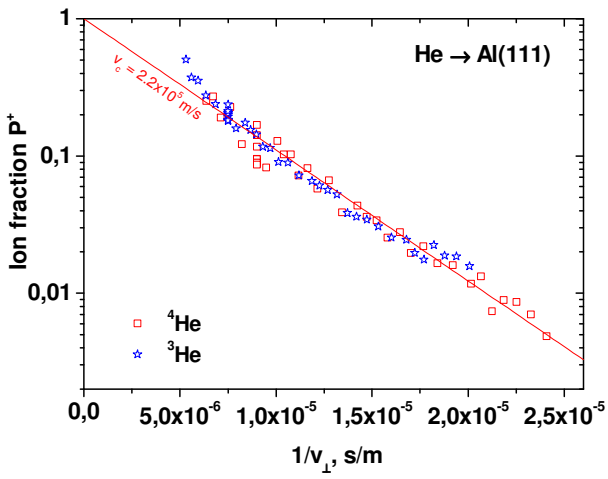

Figure 2: Experimentally deduced ion fraction P^+ of He^+ scattered from Al(111)

The experimentally deduced P^+ is depicted in Fig. 2. Although all data presented are recorded at $E > E_{th}$, very good agreement with a fit according to Eq. 1 is found. No significant deviation is observed even for the highest energies, pointing to a qualitatively different neutralisation behaviour than for Cu were a strong deviation was observed for $E > E_{th}$ [2].

3. REFERENCES

[1] H.H. Brongersma, M. Draxler, M. de Ridder, P. Bauer, Surf. Sci. Rep. 62 (2007) 63.

[2] M. Draxler, R. Gruber, H.H. Brongersma, P. Bauer, Phys. Rev. Lett. 89 (2002) 263201

[*] E-mail: stefanie.rund@jku.at

MECHANISMS FOR ELECTRON EMISSION IN COLLISIONS OF SLOW IONS WITH INSULATORS

R. A. Baragiola[1,*], *C. A. Dukes*[1], *G. Ruano*[2], *R. A. Vidal*[2], *and J. Ferrón*[2]

[1] University of Virginia, Laboratory for Atomic and Surface Physics, Charlottesville, VA, USA
[2] INTEC, CONICET and Universidad Nacional del Litoral, Santa Fe, Argentina

1. INTRODUCTION

We will report on measurements of energy spectra of electrons emitted from the surfaces of aluminum fluoride, lithium fluoride and water ice by low-energy noble gas ions. The spectra show interesting structure that can be isolated by factor analysis [1] of the projectile energy dependence. We will discuss different excitation mechanisms and the role of excitons [2,3] and autoionizing states [4].

The research seeks the understanding of basic physics of inelastic ion-surface collisions and will be presented in the context of applications to plasma devices and electrostatic charging of astronomical surfaces such as lunar and asteroidal dust, planetary rings particles and interstellar grains.

2. REFERENCES

[1] N. Bajales, S. Montoro, E. C. Goldberg, R. A. Baragiola, and J. Ferrón, Surface Sci. Lett. **579**, L97 (2005).
[2] P. Riccardi, M. Ishimoto and R.A. Baragiola, Surface Sci. Lett. **571**, L305 (2004).
[3] N. Bajales, L. Cristina, S. Mendoza, R.A. Baragiola, E.C. Goldberg and J. Ferrón Phys. Rev. Lett. **100** 227604 (2008).
[4] C. D. Wilson, C. A. Dukes, and R. A. Baragiola, Phys. Rev. B **63**, 1101 (2001)

* E-mail: raul@virginia.edu

H(1s) angular distributions calculations for H^+ impinging on Al(111) at grazing incidences

H. Jouin[1,*] *and F.A. Gutierrez*[2]

[1] CELIA (UMR 5107 Université Bordeaux 1 – CNRS – CEA), Université Bordeaux 1, 351 Cours de la Libération, 33405 Talence Cedex, France
[2] Departamento de Física, Universidad de Concepción, Casilla 160-C, Concepción, Chile

1. INTRODUCTION

In a recent work [1], we have computed outgoing H(1s) fractions in the energy range 1 keV – 100 keV for protons impinging on Al(111) with a grazing incidence of 0.5°. The role of capture and loss for both resonant (R) and Auger (A) processes was investigated together with the relevance of the surface-plasmon-assisted electron capture channel (P). Consideration of all these mechanisms (RAP) together yield a good agreement between experimental neutral fractions [2] and a set of calculations performed by using various theoretical results [3-5] for the resonant process. Since angular distributions are much more sensitive than neutral fractions to the details of the simulations, here we have computed angular distributions which are compared to available experimental results [6] in order to obtain a deeper understanding of the interaction at various impact energies.

2. CALCULATIONS and RESULTS

2.1. Description of simulations

The ETISC1D code [7] has been used to perform dynamical calculations. Since resonant [3-5] and Auger rates [8] have been so far obtained only in the static case, we use the approximate "kinematic factor" approach proposed in [9] to compute velocity-dependent capture and loss resonant and Auger transition rates. Velocity-dependent rates for surface-plasmon assisted electron capture process have been obtained as detailed in [10].
Furthermore, we use a fitted representation [1] of the dynamical image potential reported in [11] while the purely repulsive potential is described by means of the ZBL screening function [12].

2.2. Results

In Fig. 1, we report a comparison between H(1s) experimental angular distribution for 25 keV impinging protons and three calculations in which all the processes have been considered together. Calculations I, II and III correspond to the use of the H(1s) energy and width (supplemented with the kinematic factors) of [3], [4] and [5], respectively. There is a pretty good agreement between calculations I (and III) and experiment [6]. We have also performed calculations for other impact energies (1, 6.25, 49 keV) and in those cases, we observe more differences between our three calculations than in Fig. 1.These predictive results have to be verified experimentally: such comparisons should allow to discriminate between the various theoretical reports for the resonant mechanism.

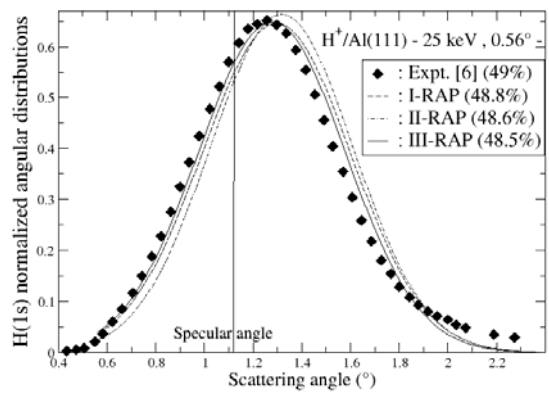

Figure 1: Angular distributions of scattered H(1s) after grazing (0.56°) collisions of 25 keV protons with Al(111) as functions of the scattering angle.

3. REFERENCES

[1] H. Jouin and F.A. Gutierrez, Phys. Rev. A **80**, 042901 (2009).
[2] H. Winter, Phys. Rep. **367**, 38 (2002).
[3] P. Nordlander and J.C. Tully, Phys. Rev. B **42**, 5564 (1990).
[4] A.G. Borisov, D. Teillet-Billy and J.P. Gauyacq, Nucl. Instrum. Methods Phys. Research B **78**, 49 (1993).
[5] S.A. Deutscher, X. Yang and J. Burgdörfer, Phys. Rev. A **55**, 466 (1997).
[6] H. Winter and M. Sommer, Physics Letters A **168**, 409 (1992).
[7] S. Jequier, H. Jouin, C. Harel and F.A. Gutierrez, Surface Science **570**, 189 (2004).
[8] R. Hentschke, K.J. Snowdon, P. Hertel and W. Heiland, Surface Science **173**, 565 (1986).
[9] Z.L. Mišković and R.K. Janev, Surface Science **221**, 317 (1989).
[10] F.A. Gutierrez and H. Jouin, Phys. Rev. A **68**, 012903 (2003).
[11] F. J. Garcia de Abajo and P. M. Echenique, Phys. Rev. B **48**, 13399 (1993).
[12] J. P. Ziegler, J. P. Biersack and U. Littmark, *The stopping and range of ions in solids* (Pergamon, New-York, 1985).

* E-mail: jouin@celia.u-bordeaux1.fr

CORRELATED DOUBLE ELECTRON CAPTURE BY SLOW HELIUM IONS ABOVE TRANSITION METAL SURFACES

C. Tusche[1,*], and J. Kirschner[1]

[1] Max-Planck-Institut für Mikrostrukturphysik, Weinberg 2, 06120 Halle, Germany

1. INTRODUCTION

We studied the electron-capture by slow Helium ions (kinetic energy ≤ 30 eV) scattered at epitaxial films of the transition metals Fe and Ni, grown on W(110) and W(100) substrates. At a distance of 2-5Å above the surface, metastable He^{**} is formed by resonant transfer of electrons from the metal to the 2s or 2p shells of the projectile. The decay of He^{**} proceeds via the emission of a He-KLL Auger electron with an energy of ≈ 34.5 eV or 36.0 eV for triplet (^{3}P+^{1}S) or singlet (^{1}P+^{1}D) terms, respectively. In the experiment, either a beam of metastable He^{*+} (2s), or doubly charged He^{++} is used. In the former case, only one electron is transferred to the He ion, while He^{++} captures two electrons.
Based on the assumption of two subsequent, but independent one-electron transitions Unipan et al. [1] related the population of singlet and triplet terms simply to the spin-polarization of the surface.

2. RESULTS

Figure 1 shows two He KLL Auger electron spectra obtained for single electron capture (He^{*+} (2s)) and double electron capture (He^{++}) form the same target surface, a clean 4ML Iron film grown on W(110). In contrast to Ref. [1], we observe an almost completely suppressed triplet contribution on the clean metal surface, i.e., the probability to capture two parallel spins, using He^{++}, as compared to He^{*+} (2s). However, the triplet population is not suppressed on surfaces covered by adsorbates, like 0.1ML Carbon. These results can not be explained by a two-step capture process, where the second electron transfer would be the same as for He^{*+} (2s).
Instead, we propose a simultaneous capture of two correlated electrons that avoids an occupation of the ^{3}P term. Such correlation effects, acting in the metal target, were first described by Slater as the exchange-correlation (xc) hole [2], where the repulsive coulomb interaction leads to a reduced charge density around each electron. Additionally, two electrons with the same spin (up or down), avoid to share the same volume in phase space, due to the Pauli principle.

A simultaneous electron-capture is further confirmed by the work function ,Φ_S, dependence of triplet (T) and singlet (S) intensities. For He^{*+} (2s), resonant capture into the ^{1}P+^{1}D terms (binding energy ≈ -5.4 eV) is not possible at high work function surfaces, i.e., when the ^{1}P and ^{1}D energy levels are shifted above the Fermi Energy. This leads to an increased T/S intensity ratio when $\Phi_S > 4.7$ eV.
For double-electron-capture we take into account the two-electron binding energies for ^{1}P+^{1}D ($E_{bind} = 2 \cdot -9.5$ eV) and ^{3}P+^{1}S ($E_{bind} = 2 \cdot -10.5$ eV). In good agreement with a model where both electrons share their energy in the simultaneous capture, an increased T/S ratio for the He^{++} neutralization is found only when $\Phi_S > 6$ eV, i.e., about 1.5 eV higher as compared to the single-electron-capture. We hope that our work will stimulate theoretical studies that take into account correlation effects in the resonant electron transfer between metal surfaces and ions.

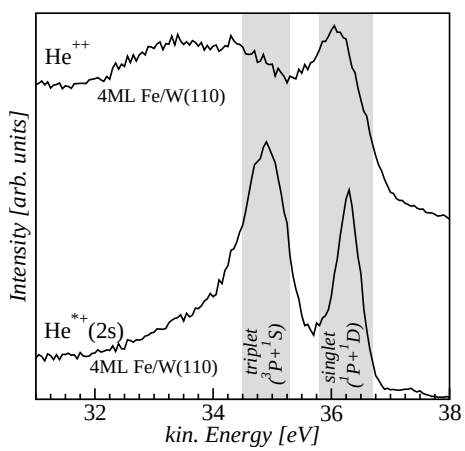

Figure 1: He KLL Auger electron spectra of 30eV He^{*+}(2s) and He^{++} ions scattered at a 4ML Fe/W(110) film.

3. REFERENCES

[1] M. Unipan, A. Robin, R. Morgenstern and R. Hoekstra, Phys. Rev. Lett. **96**, 177601 (2006)

[2] J. C. Slater, Rev. Mod. Phys. **6**, p. 209-280 (1934)

* E-mail: tusche@mpi-halle.mpg.de

INFLUENCE OF PROJECTILE CHARGE STATE ON THE IONIZATION PROBABILITY OF SPUTTERED PARTICLE

*B. Weidtmann**, *S. Hanke, A. Duvenbeck and A. Wucher*

Faculty of Physics, University Duisburg-Essen, 47048 Duisburg

1. INTRODUCTION

We present a computer simulation study of the ionization probability of sputtered particles and the external electron emission following the impact of highly charged atoms onto an amorphous silver target. Both, the kinetic excitation induced by particle kinetics and the potential energy of the projectile are taken into account to calculate a time- and space-dependent excitation energy profile within the cascade volume. This is parametrized by an electron temperature T_e which is then the essential parameter for the calculation of electron emission and the ionization probability of sputtered particles.

2. MODEL

Our model is based on several parts. We employ a molecular dynamics simulation to obtain the time- and space- resolved particle dynamics $\vec{r}_i(t)$. Two kinetic excitation mechanisms - electronic friction and electron promotion - are taken into account to calculate the amount of excitation energy introduced into the electronic system. For electronic friction, a velocity proportional friction force is implemented according to the Lindhard model of electronic stopping [3]. The resulting frictional kinetic energy loss of moving cascade atoms is then taken as a source of excitation energy. Electron promotion considers auto-ionization processes above the Fermi level during the transient formation of diabatic virtual bound states in close collision [2]. In addition, the potential energy carried by the highly charged projectile is considered as an additional channel for energy conversion. If a highly charged atom approaches the surface, it is neutralized by electrons from the conduction band of the target. These electron primarily occupy highly excited Rydberg states. This way a so-called "hollow atom" is formed [1], which still contains most of its original potential energy. Following the completion of the empty states, hot electrons may be created in Auger de-excitations of the hollow atom. These hot electrons constitute a further source of excitation in addition to electronic friction and electron promotion. Due to the uncertainty concerning the dynamics of the Auger processes, we assume a continuous time structure of the generation of potential excitation energy in the cascade according to an inverse exponential law. The latter is governed by a characteristic life time τ of the Rydberg states of the hollow atom.

The transport of the excitation energy away from the spot of generation is calculated in terms of a diffusion equation. This yields a four-dimensional excitation energy profile $E(\vec{r}, t)$ which is then parametrized by a electron temperature $T_e(\vec{r}, t)$. For different choices of the parameter τ we evaluate the electron temperature distribution $T_e(\vec{r}, t)$ in view of kinetic electron emission yields and ionization probabilities of sputtered atoms.

3. REFERENCES

[1] J.P. Briand, L. de Billy, P. Charles, S. Essabaa, P. Briand, R. Geller, J.P. Desclaux, S. Bliman, and C. Ristori. Production of hollow atoms by the excitation of highly charged ions in interaction with a metallic surface. *Phys. Rev. Lett.*, 65:159, 1990.

[2] A. Duvenbeck, B. Weidtmann, O. Weingart, and A. Wucher. Modeling hot-electron generation induced by electron promotion in atomic collision cascades in metals. *Phys. Rev. B*, 77:245444, 2008.

[3] J. Lindhard and M. Scharff. Energy dissipation by ions in the kev region. *Phys. Rev. B*, 124:128, 1961.

* E-mail: boris.weidtmann@uni-due.de

STUDY ON OXIDATION OF NiAl(110) VIA ELECTRON EMISSION DURING GRAZING SURFACE SCATTERING OF FAST HE ATOMS

D. Blauth[1], N. Nilius[2], and H. Winter[1]*

[1]Institute of Physics, Humboldt University Berlin, Newtonstr. 15, D-12489 Berlin-Adlershof, Germany
[2]Fritz-Haber Institute of the MPG, Department of Chemical Physics, Faradayweg 4-6, D-14195 Berlin, Germany

1. INTRODUCTION

Oxidation of a NiAl(110)-surface leads to a defined two monolayer thick alumina film [1] showing an intricate structure for the topmost surface layers which was recently revealed in a combined effort of experimental STM-work and DFT-calculations [2]. A major interest of such a defined oxide layer is based on its properties to serve as an oxide substrate for studies making use of established surface spectroscopic tools, as e.g. STM. For the work reported here, the attractive aspect lies in the feature to study electron emission for impact of fast atoms on surfaces for the gradual change of the target from a pure metal to an insulator surface.

2. EXPERIMENT AND RESULTS

In the experiment we have scattered He atoms with energies in the keV domain from clean and oxidized NiAl(110) under a grazing angle of incidence of 1° to 2°.

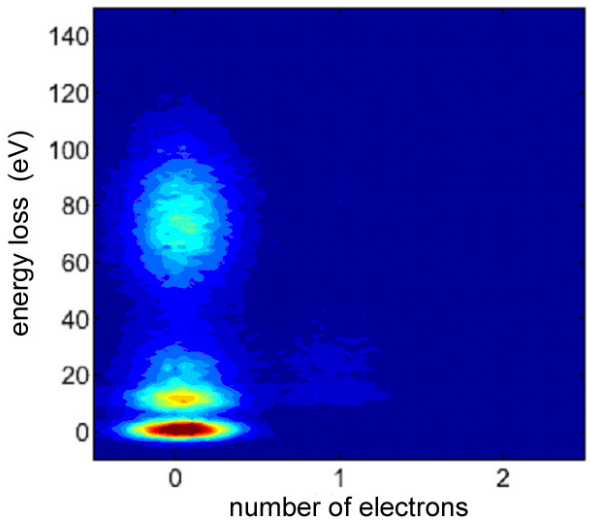

Figure 1: Coincident energy loss and electron number for scattering of 3 keV He atoms from partially oxidized NiAl(110) surface under grazing angle of 1.7°.

The energy loss of the chopped and neutralized He^+ ion beam is measured via a time-of-flight method in coincidence with the number of emitted electrons during the scattering event [3]. As an example we show in Figure 1 a 2D-representation of electron loss vs. electron number where the discrete peaks with low energy loss can be attributed to the interaction of atoms with an insulator surface, whereas the broad distribution with an energy loss around 80 eV is typical for scattering from a metal surface.

Thus our observation shows for a partially oxidized metal surface that the scattering proceeds from patches of the clean metal and of the alumina film. This interpretation is supported by STM-studies where island of closed alumina films can be found as well as domains of the clean metal. In addition, our energy spectra demonstrate that already for an incomplete alumina film on the NiAl-substrate a band gap close to the value of bulk alumina is developed. In a controlled variation of the amount of oxygen dose of the metal we find that already for an alumina coverage of a few percent of a monolayer the signature of the oxide can be identified in the energy loss spectra. In this respect our technique is more sensitive to the presence of oxygen on the surface than conventional Auger spectroscopy.

3. REFERENCES

[1] R.M. Jaeger, H. Kuhlenbeck, H.J. Freund, M. Wuttig, W. Hoffmann, R. Franchy, and H. Ibach, Surf. Sci. **259**, 235 (1991).
[2] G. Kresse, M. Schmid, E. Napetschnig, M. Shishkin, L. Kohler, and P. Varga, Science **308**, 1440 (2005).
[3] H. Winter, in “Slow Heavy-Particle Induced Electron Emission from Solid Surfaces”, eds. HP. Winter and J. Burgdörfer, Springer Tracts in Modern Physics **225** (2007), p. 113.

* E-mail: winter@physik.hu-berlin.de

Development of the new MD potentials for metal walls : Li-C-H

Z. C. Yang[1], J. Dadras[2,3], P. R. C. Kent[4], J.P. Allain[1] and P. S. Krstic[2,3]*

[1] Department of Nuclear Engineering, Purdue University, West Lafayette, IN 47907
[2] Department of Physics and Astronomy, University of Tennessee, Knoxville, TN 37996
[3] Physics Division, Oak Ridge National Laboratory, Oak Ridge, TN 37831
[4] Center for Nanophase Materials Sciences, Oak Ridge National Laboratory, Oak Ridge, TN 37831

1. INTRODUCTION

The use of lithium in combination with carbon as a first-wall material in future fusion reactors may suppress or even eliminate problems of tritium retention and surface erosion which degrade reactor performance [1]. However, the behavior of lithium-carbon mixed materials remains poorly understood. The quality of atomistic, molecular dynamic, simulation depends on the quality of the multi-body potential for this mixed material. Here we report on progress towards developing a Li-C-H potential which will be used for simulations of the interaction of hydrogen, lithium, and carbon impact particles with lithiated and hydrogenated carbon surfaces.

2. POTENTIAL DEVELOPMENT

Lithium's significantly smaller electronegativity in comparison to carbon and hydrogen causes a strong polarization of the atoms in their mixtures and requires introduction of the Coulomb interaction terms in potential models. This complicates the standard Brenner-Tersoff covalent form of potentials used for hydrocarbons [2], adding the long-range E_{Coul} terms

$$E_{Coul} = \sum_i \sum_{j>i} \frac{q_i q_j}{r_{ij}} \quad (1)$$

to the bonding and van der Waals terms [3]:

$$E_{tot} = E_{bond} + E_{vdW} + E_{Coul} \quad (2)$$

We are building the Li-C-H potential on the well-tested hydrocarbon AIREBO form [3], where the radial part of the atom-atom pair interactions is given by a weighted sum of attractive and repulsive terms, with addition of the Lenard-Jones and torsion terms. The parameters in E_{bond} and E_{vdW} of Equation (1) are fit to bonding energies, lengths and "harmonic" forces obtained by density functional theory (DFT) calculations and experimental data on small Li-C, Li-H and Li-C-H molecules as well as on experimental data on bulk lithium-carbide materials and large-cluster DFT calculations, for the multibody components. We have recently refitted the hydrocarbon (REBO) potentials to the extended database of hydrocarbon potentials, which is used in this work, too.

Like in the case of improved hydrocarbon potential, we are incorporating universal repulsive "ZBL" potential [4] for Li-H and Li-C binary interactions for close-encounters at higher impact energies (>50 eV). We are attempting to simultaneously fit all target properties which is accomplished by a weighted least squared deviation fitting procedure using the Levenberg-Marquardt method.

Determination of the atomic charges in the Li-C-H material is certainly the key issue of our new potential. One approach is the electron equalization method (EEM) [5,6,7]. Optimization of the initial EEM parameters is made to reproduce the charge distribution of a number of clusters.

The potential parameters are further iterated based on the validation of the potential by the experimental data for the chemical sputtering yields and reflection of the Li-C-H surfaces, as well as on the bulk structural data, as these become available.

We acknowledge support of DoE and Laboratory Directed Research and Development Program of ORNL, under contract No. DE-AC05 00OR 22725 with UT-Battelle, LLC. ZCY acknowledges the ORISE/ORAU program HERE and DoE for support of his research at ORNL.

3. REFERENCES

[1] D. K. Mansfield, et al., Nucl. Fusion **41**, 1823 (2001)
[2] D.W. Brenner, O.A. Shenderova, J.A. Harrison, S.J. Stuart, B. Ni, and S.B. Sinnott, Journal of Physics: Condensed Matter. **14**, 783 (2002).
[3] Stuart, Steven J.; Tutein, A. B.; Harrison, Judith A. J. Chem. Phys. **112**, 6472 (2000).
[4] J. F. Ziegler, J. P. Biersack, and U. Littmark, *The Stopping and Range of Ions in Matter*, Pergamon Press, NY, 1985.
[5] W. J. Mortier, S. K. Ghosh and S. Shankar, J. Am. Chem. Soc. **108**, 4315 (1986).
[6] G. O. Janssens and et al., J. Phys. Chem. **99**, 3251 (1995)
[7] Sang Soo Han, Adri C. T. van Duin, William A. Goddard III, and Hyuck Mo Lee, *J. Phys. Chem. A* **109**, 4575, **(**2005**).**

* E-mail: yang123@purdue.edu

ALKALI ION SCATTERING FROM METAL NANOCLUSTERS ON TiO_2(110)

J.A. Yarmoff[*] *and A.B. Arjad*

Department of Physics and Astronomy, University of California, Riverside, CA 92521 USA

1. INTRODUCTION

The discovery that Au nanoclusters are catalytically active when supported in an oxide matrix [1] has led to an abundance of surface studies, many of which concentrate on metal nanoclusters deposited on single crystal TiO_2. For example, STM showed that Au nanoclusters form spontaneously on TiO_2(110) and that the size of the clusters increases as more metal is deposited [2].

We previously used low energy alkali ion scattering to interrogate Au clusters by measuring the neutral fraction (NF) of backscattered ions with time-of-flight [3]. We also demonstrated a novel method for the production of nanoclusters by Ar^+ sputtering a thin Au film deposited on TiO_2 [4]. This initial work was performed with Au, so it was not clear whether or not ion scattering is sensitive to quantum size effects in clusters fabricated from other materials. In the present work, Ag and Pt are evaporated onto TiO_2(110) and thin films of these metals are sputtered. The resulting materials are then interrogated via the scattering of 2.5 keV Na^+.

2. RESULTS

Figure 1 illustrates our previous results for Au nanoclusters. The left panel shows how the NF for Na^+ scattering from small clusters is surprisingly high (~50%), and that it decreases with cluster size until it reaches ~3% for a Au film [3]. This demonstrates that scattered alkali ions can couple to electronic states specific to the nanoclusters, and that the energy of the states is a function of cluster size. When the Au film is sputtered by 0.5 keV Ar^+, the NF increases again after a threshold fluence until it reaches ~50%, as shown in the right panel [4]. This demonstrates that the ion-induced interplay between curvature dependent roughening and diffusion-induced smoothing produces clusters with quantum confinement.

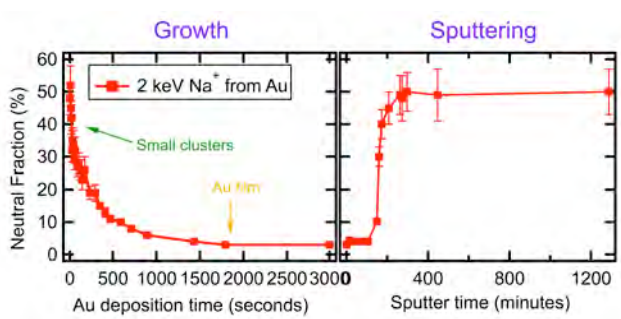

Figure 2 shows data for Pt on TiO_2 during growth and thin film sputtering. There is a clear enhancement of the Na^+ NF for small Pt clusters, but there is no enhancement following sputtering.

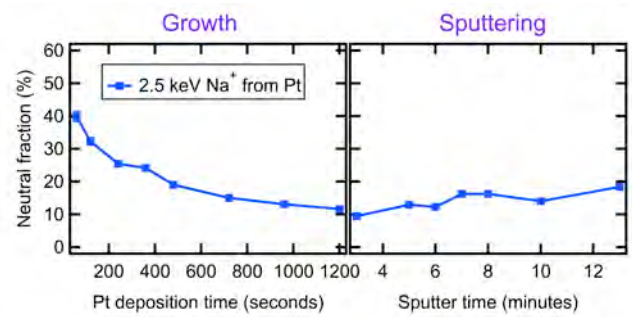

For Ag on TiO_2, there is also an enhancement of the Na^+ NF for small clusters, which is consistent with reports for Li^+ scattering [5]. Similar to Pt, there is no enhancement observed following sputtering.

The lack of enhancement for sputtered Pt or Ag, as is seen for Au, may be due to differences in the surface free energy of the metals or in the propensity of Pt and Ag to oxidize.

3. CONCLUSIONS

Scattered alkali ions can couple directly to electronic states in nanoclusters. Calculations of ion neutralization that specifically consider the cluster states need to be developed in order to understand this process and to enable the nanoparticle electronic structure to be determined directly from a measured NF. Future efforts will expand this technique to other supported nanocrystals, chemically synthesized nanoparticles, and nanomaterials in diverse media.

4. REFERENCES

[1] M. Haruta, Catal. Today **36**, 153 (1997).
[2] M. Valden, X. Lai and D.W. Goodman, Science **281**, 1647 (1998).
[3] G.F. Liu, Z. Sroubek and J.A. Yarmoff, Phys. Rev. Lett. **92**, 216801 (2004).
[4] P. Karmakar, G.F. Liu, Z. Sroubek and J.A. Yarmoff, Phys. Rev. Lett. **98**, 215502 (2007).
[5] A. R. Canario and V. A. Esaulov, J. Chem. Phys. **124**, 224710 (2006).

[*] E-mail: `yarmoff@ucr.edu`

THE FORMATION OF LUMINESCENT SIC NANOCLUSTERS WITHIN ION-IMPLANTED SIO_2 FILMS

A.F. Zatsepin[1,*], *E.A. Buntov*[1], *V.S. Kortov*[1], *A.N. Mihailov*[2], *A.I. Belov*[2], *D.I. Tetelbaum*[2]

[1] Ural Federal University, Ekaterinburg
[2] Physico-Technical Research Institute of University of Nizhny Novgorod

1. INTRODUCTION

The ability of silicon nanocrystals and complex nanoclusters to emit intensive visible light is of interest for combined electro-optical circuits design [1]. During the development of high-speed networks one must consider both spectral and kinetic properties of light-emitting elements. Intentional modification of nanostructures functional properties may be realized by varying their synthesis conditions through size effects. In particular, one can successively control the size of SiC and CdS nanocrystals within ion-implanted silica by means of intermediate annealing that stimulate the nucleation process [2,3].

2. EXPERIMENTAL

The present work we use photoluminescence (PL) spectroscopy techniques to study the influence of intermediate and post-implantation annealing on the formation of silicon-carbon nanoclusters inside 800 nm thick amorphous SiO_2 films grown on silicon wafers. The samples were sequentially implanted by Si^+ (100 keV, $7\cdot10^{16}$ cm^{-2}) and C^+ (50 keV, $7\cdot10^{15}$-$1.5\cdot10^{17}$ cm^{-2}) ions. In order to synthesize the nanoclusters of implanted ions two samples sets were annealed at 1100ºC during two hours: either only after implantation or both between silicon and carbon implantations and after them. PL measurements were carried out on the SUPERLUMI station of DESY (Hamburg) under selective excitation within 65-200 nm range.

3. RESULTS AND DISCUSSION

Sequential implantation of silicon and carbon ions leads to the appearance of several luminescent bands of Si and SiC nanoclusters (Fig. 1). The PL (650-680 nm) of amorphous Si clusters undergoes a red shift during the intermediate annealing of implanted SiO_2 films. PL bands at 504 nm and 405 nm demonstrate high-energy shift with the rise of carbon concentration. The fact points out their connection to carbon-containing clusters. A distinctive feature of SiO_2 films under study is the effective PL excitation in the self-trapped and bound excitons region, as well as at the interband transitions of SiO_2 matrix (90-140 nm). At high implantation doses we observe a nonradiative excitation energy transfer from matrix radiation defects to luminescing clusters. The nanosecond PL kinetics (1÷16 ns) under indirect excitation of clusters through defects shows a possibility of their applications in micro- and optoelectronics.

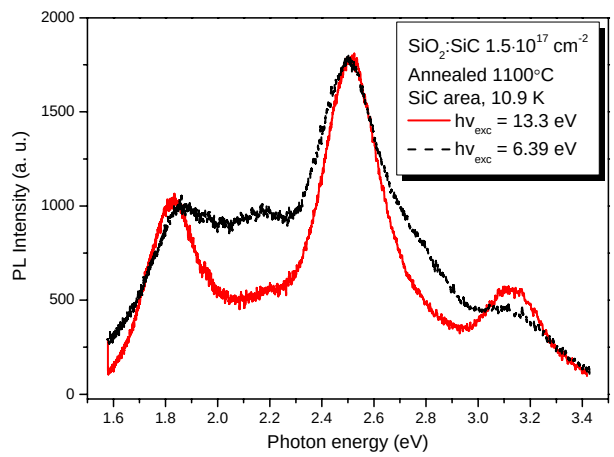

Figure 1: PL spectra of SiC-implanted samples.

The work is performed under support of Russian Foundation for Basic Research, projects No. 08-03-00105, 08-02-01072.

4. REFERENCES

[1] A.F. Zatsepin et al. Journal of Non-Crystalline Solids. **355** (2009) P.1119–1122.
[2] B.G. Potters, J.H. Simmons. Phys. Rev. B. **37** (1988) P.10838.
[3] D.I. Tetelbaum et al. Surf. Coat. Technol. **203** (2009) P.2658.

* E-mail: zats@dpt.ustu.ru

Wednesday, September 29, 2010

Sources of highly charged ions

for materials science and nano-structuring

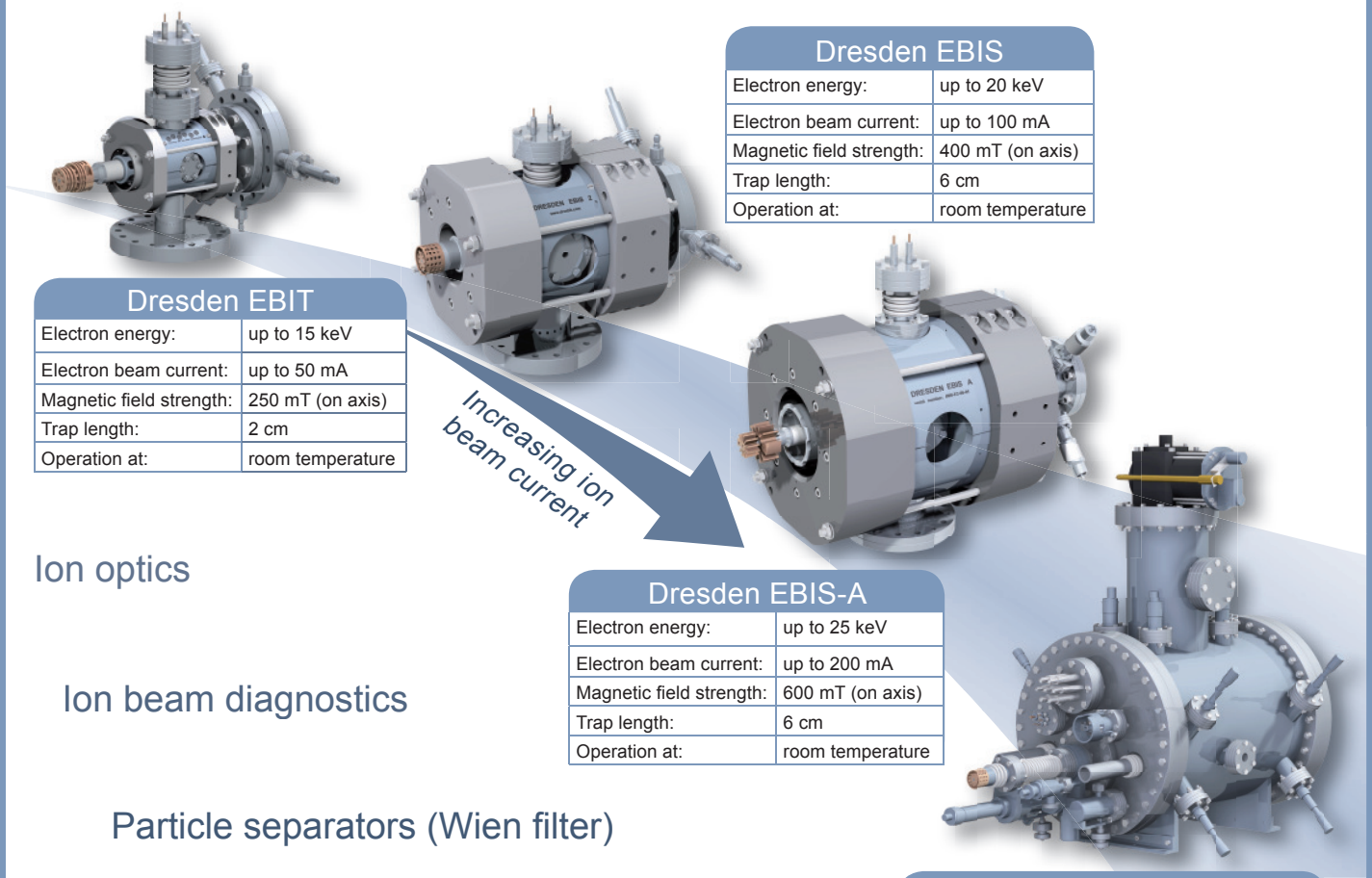

Dresden EBIT	
Electron energy:	up to 15 keV
Electron beam current:	up to 50 mA
Magnetic field strength:	250 mT (on axis)
Trap length:	2 cm
Operation at:	room temperature

Dresden EBIS	
Electron energy:	up to 20 keV
Electron beam current:	up to 100 mA
Magnetic field strength:	400 mT (on axis)
Trap length:	6 cm
Operation at:	room temperature

Dresden EBIS-A	
Electron energy:	up to 25 keV
Electron beam current:	up to 200 mA
Magnetic field strength:	600 mT (on axis)
Trap length:	6 cm
Operation at:	room temperature

Dresden EBIS-SC	
Electron energy:	up to 30 keV
Electron beam current:	up to 1 A
Magnetic field strength:	6 T (on axis)
Trap length:	20 cm
Operation at:	4.2 K (Liquid helium-free magnet cooling)

Ion optics

Ion beam diagnostics

Particle separators (Wien filter)

Individual solutions for ion beamlines and ion irradiation facilities

Example:

Compact beam line with an Dresden EBIS2 and Wien filter

S-Line: charge state separation by a Wien Filter.

M-Line: charge state separation by an analysis magnet.

The following specifications are available:

- Continuous ion beams
- Pulsed ion beams (FWHM from 10 ns up to 100 µs)
- Ion beams with diameter of 500 µm and larger
- On request with electron beam charging by external ion injection

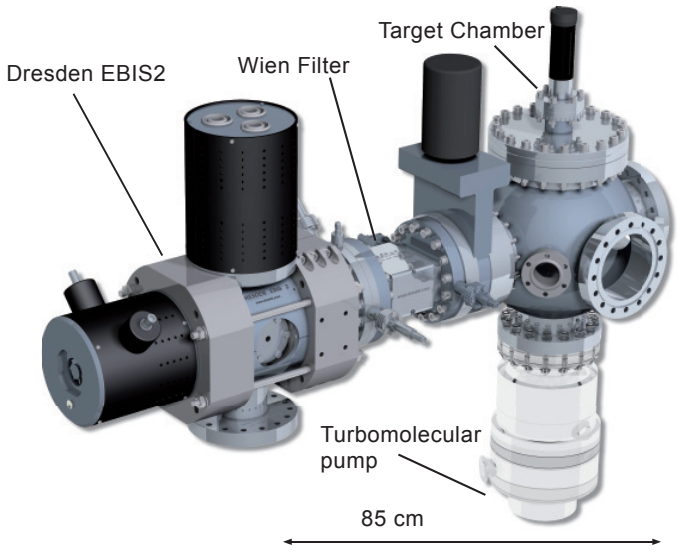

www.dreebit.com

DREEBIT Electron & Ion Beam Technologies

DREEBIT GmbH Zur Wetterwarte 50, Haus 301, 01109 Dresden, Germany
scientific inquiries: +49 (351) 260 2212 (Ass.-Prof. Dr. habil. Günter Zschornack)

TRANSPORT AND GUIDING OF IONS AND ELECTRONS THROUGH NANO-CAPILLARIES

J. Burgdörfer[+,*]

Institute for Theoretical Physics, Vienna University of Technology, A-1040 Vienna, Austria, EU

1. INTRODUCTION

In this talk, we will review our current understanding of transport and guiding phenomena through nano-scale capillaries. This field was initiated by pioneering work on metallic capillaries by Yamazaki et al.[1] and extended to insulating capillaries by Stolterfoht et al.[2] Its initial motivation was the probe of the interaction of highly charged ions with surfaces within meso- or nano-sized structures with the goal to identify similarities and difference to interactions with planar surfaces. More recently, the focus has shifted to transport and guiding of electrons. The theoretical understanding of the underlying processes well as quantitative simulations has remained a challenge. We will illustrate progress as well as open questions within the framework of classical and quantum transport theory with the help of a few examples [3,4]. An outlook to the extension to macroscopic capillaries will be given.

(+) Work in collaboration with Klaus Schiessl, Christoph Lemell, and Karoly Tokesi

2. REFERENCES

[1] Y. Yamazaki et al. J. Phys. Soc. Jpn. **65,** 1199 (1996).
[2] N. Stolterfoht et al. , Phys. Rev. Lett. **88**,133201 (2002).
[3] K. Schiessl et al. Phys. Rev. A **72**, 062902 (2005)
[4] K. Schiessl et al. Phys. Rev. Lett **102**,163201 (2009)

CLOSED-TIP TAPERED GLASS CAPILLARIES AS A NOVEL TOOL FOR MICRO-IRRADIATION OF LIVING CELLS BY MeV ION BEAMS

W. Meissl[1*], *T. Ikeda*[1], *M. Clever*[2], *E. Meissl*[1], *K. Tökesi*[3], *P.H. Schury*[4,b], *K. Maeshima*[2,a], *S. Miyamoto*[1,5], *T. Kobayashi*[1], *T.M. Kojima*[1], *Y. Kanai*[1], *K. Ogiwara*[1], *M. Hamagaki*[1], *M. Wada*[4], *N. Imamoto*[2], *and Y. Yamazaki*[1]

[1] Atomic Physics Laboratory, RIKEN, Wako-shi, Saitama, 351-0198 Japan
[2] Cellular Dynamics Laboratory, RIKEN, Wako-shi, Saitama, 351-0198, Japan
[3] Institute of Nuclear Research of the Hungarian Academy of Sciences, Debrecen 4026, Hungary
[4] SLOWRI team, RIKEN Nishina Center, Wako-shi, Saitama, 351-0198, Japan
[5] Dep. of Physics, Tokyo Univ. of Science, Shinjuku, Tokyo 162-8601, Japan

1. INTRODUCTION

Micro-irradiation of living cells, while being investigated for several decades now, has enabled significant advances in biology over the last 15 years with the reliable production of micrometer sized beams of MeV ions. The relative sensitivity of nucleus and cytoplasm of the cell to ionizing radiation was measured and an effect of targeted irradiation on non-targeted cells was discovered (bystander effect). These findings clearly show that direct damage to the DNA is not the only possible pathway of radiation-induced damage to living cells.

2. FACILITY

We use a completely new approach to creating and delivering an ion microbeam to cell targets by the use of tapered glass capillaries. Apart from their well-known focusing effect on slow highly charged ions, capillaries with end diameters down to below 1 µm have demonstrated their ability to focus and guide MeV beams of protons and helium ions due to small-angle scattering with the walls [1]. We attach thin (1 – 20 µm) end windows to the capillaries which allows their immersion into a liquid environment. Thus we can bring the ion beam extremely close to any biological target in its natural environment [2,3].

Using 2 – 4.5 MeV helium ions with a linear energy transfer between 100 and 240 keV/µm, we can pinpoint the Bragg peak of the transmitted beam to a volume a few µm downstream of the capillary exit, thus achieving full 3D-confinement of an ion beam within a living cell for the first time. Thus we drastically reduce straggling effects which effectively limit the resolution of traditional microbeams. Utilizing a beam chopper with self built fast HV switching electronics (< 200 ns), we can apply pulses containing single ions, although we still lack a method to count the number of transmitted particles.

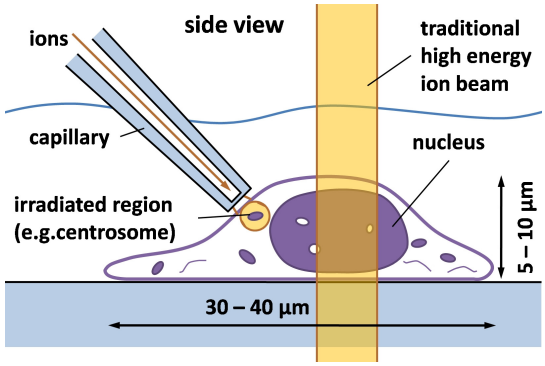

Figure 1: Comparison of traditional microbeam irradiation with beam guiding by glass capillaries. Dimensions of a typical HeLa cell are shown.

This new method is expected to allow a number of novel experiments on living targets. The precise targeting of a selected volume inside the cells allows targeting cell small cell organelles (e.g. the centrosome) without exposing other vital organelles to radiation. Irradiate of a single cell at the top layer of 3-D cell tissue is also possible, without damaging cells in deeper layers, which could be relevant for bystander effect studies.

We show the achievable beam diameters and targeting precision of our setup and analyze the beam density enhancement effect of the capillaries. Finally, we present first preliminary results from the irradiation of human tissue cells using our unique experimental setup.

3. REFERENCES

[1] T. Nebiki *et al.*, J.Vac.Sci.Technol. A **21** (2003) 1671
[2] T. Ikeda *et al.*, J. Phys. Conf. Ser. **88** (2007) 012031.
[3] Y. Iwai *et al.*, Appl. Phys. Lett. **92** (2008) 023509.

[a] Present address: Structural Biology Center, National Institute of Genetics, Mishima, Shizuoka 411-8540 Japan
[b] present address: Institute of Physics, University of Tsukuba, Ibaraki, 305-8571 Japan

[*] E-mail: meissl@riken.jp

TRANSMISSION OF ELECTRONS THROUGH A SINGLE GLASS MACRO-CAPILLARY: ENERGY AND TIME DEPENDENCE

B. S. Dassanayake[1,*], *S. Das*[1,2], *A. Ayyad*[1], *R. J. Bereczky*[3], *K. Tőkési*[3] *and J. A. Tanis*[1]

[1] Department of Physics, Western Michigan University, Kalamazoo, MI, 49008, USA
[2] Manne Siegbahn Laboratory, Stockholm University, Stockholm-11418, Sweden
[3] Institute of Nuclear Research (ATOMKI), H-4001 Debrecen, Hungary

Transmission of slow highly charged ions (HCIs) through various nanoscale channels has been highly investigated both experimentally and theoretically in the recent past [1]. As a result, many viable proposals for the ion transmission mechanism have been put forward and a common ground for the "guiding" mechanism has been reached [1]. Unlike ion guiding, little has been done to investigate electron transmission and its dynamics experimentally or theoretically and consequently many questions regarding its transmission process remain unsolved.

Electron transmission through a single cylindrically-shaped macro glass capillary was investigated for 300-1000 eV electrons at the Van de Graaff accelerator laboratory of Western Michigan University. The Borosilicate glass capillaries of diameter ~0.2 mm and length ~15.0 mm were prepared at the ATOMKI laboratory in Debrecen (Hungary).

The transmitted intensities appear to exhibit two distinct regions with different transmission characteristics. For sample tilt angles $\psi < 2.5^\circ$ (direct region) the transmission falls off with a steeper slope than for $\psi > 2.5^\circ$ (indirect region). In the direct region, the characteristic angle, ψ_c, at which the transmission intensity falls to 1/e is found to be the same for all energies within the experimental uncertainties. In the indirect region, a minimum in ψ_c for 500 eV was observed, contradicting with what has been reported for PET nanocapillary foils [2]. Rutherford scattering was found to be the dominant process at energies ≤ 500 eV, whereas charge buildup and subsequent Coulombic repulsion takes over at higher energies [3].

The process of charge deposition was found to be time dependent. Centroid energies and full width-half-maximum (FWHM) values of the transmitted spectra were analyzed to understand their correlation with the transmitted intensity variations. As seen in Figure 1, when the transmitted intensity goes to "equilibrium" (after ~ 600 mins), the centroid energies and corresponding values of the FWHM found to vary in phase and out of phase with the transmitted intensity, respectively. The equilibrium state shows sudden oscillations caused by charge up and

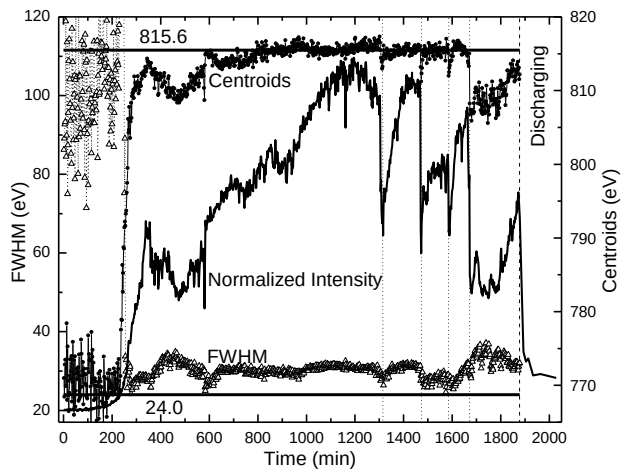

Figure 1: Comparison of the variation in centroid energy (hollow triangles), transmitted beam intensity (solid line), and FWHM value (black circles) with time for 800 eV at $\psi = 2^\circ$. The top horizontal solid line is the bare beam centroid (815.6 eV), whereas the bottom one is the bare beam FWHM (24.0 eV).

discharge of the inner capillary surface, as shown by the dotted vertical lines. The actual discharging of Borosilicate in the absence of the beam was found to be a rapid process as seen in the figure (after ~1900 mins).

These results reveal that Rutherford scattering and Coulombic repulsion govern the electron transmission, depending on incident beam energy range. Stable transmission equilibrium is never reached due to repeated sudden partial discharge of the inner capillary from time to time. Such nonequilibrium has not been previously observed for electron or ion transmission in capillaries.

Acknowledgement: This work was supported by an award from Research Corporation.

REFERENCES

[1] P. Skog, H. Q. Zhang, and R. Schuch, Phys. Rev. Lett. **101**, 223202 (2008), and references therein.

[2] S. Das, B. S. Dassanayake, M. Winkworth, J. L. Baran, N. Stolterfoht, and J. A. Tanis, Phys. Rev. A **76**, 042716 (2007).

[3] B. S. Dassanayake, S. Das, R. J. Bereczky, K. Tőkési, and J. A. Tanis, Phys. Rev. A **81**, 020701(R) (2010).

* E-mail: b5senarathda@wmich.edu

CONTROLLING THE GUIDING PROPERTIES OF MESOSCOPIC GLASS CAPILLARIES FOR SLOW HIGHLY CHARGED IONS

G. Kowarik[1], R. J. Bereczky[2], F. Ladinig[1], A. Macé[1], K. Tőkési[2], and F. Aumayr[1]

[1] Institute of Applied Physics, TU Wien - Vienna University of Technology, 1040 Vienna, Austria, EU
[2] Institute of Nuclear Research of the Hungarian Academy of Sciences (ATOMKI) Debrecen 4001, Hungary, EU

1. INTRODUCTION

Investigations of the interactions of highly charged ions with internal surfaces recently became available due to the advances in the fabrication of nano-, micro-, and mesoscopic-capillaries. In 2002 the effect of capillary-guiding of charged particles through insulating nano-capillaries was discovered [1]. The basic concept is the transmission of charged particles through insulating nano-sized capillaries under incident angles much larger than the geometrical limitation due to the self-organized formation of charge-patches at the inner wall [2, 3].
Since then, the transmission of highly charged ions through insulating linear nanostructures has been investigated from the view point of the fundamental understanding of ion insulator interactions [2 - 4], as well as due to its potential applications [5].
Recently, we were able to show the validity of this so-called guiding effect up to a meso- and even macroscopic length-scale of straight glass capillaries [6, 7].

2. EXPERIMENT

In this work we have studied the transmission of highly charged ions through a single, high aspect ratio glass capillary (length about 1cm, aspect ratio about 80) made of Pyrex (borosilicate glass). As a novel feature we have developed and built a temperature regulated sample holder (fig. 1), which utilizes surrounding copper parts to assure a uniform temperature over the capillary. By changing the temperature of the glass capillary we are - for the first time - able to manipulate the electrical conductivity of the Pyrex by several orders of magnitude. In this way we can study the effect of conductivity on the build-up and removal of charge patches in the capillary.
The measurements were carried out using beams of 4.5 keV Ar^{9+} ions produced by the Vienna 14.5 GHz electron cyclotron resonance ion source. In order to avoid strong fields and to assure rotational symmetry as well as proper charge transport, the capillary‘s outside is covered by graphite. Approximately 18 cm behind the entrance of the capillary, a position sensitive detector mainly consisting of a Chevron-type micro-channel-plate and a wedge-and-strip-anode is used to record the transmitted ions.
Our experiments show that the glass temperature (i.e. conductivity) can be used to control the guiding properties of the Pyrex glass capillary and adjust the conditions from "guiding" at room temperature to "non-guiding" (simple geometrical transmission) at elevated temperatures.

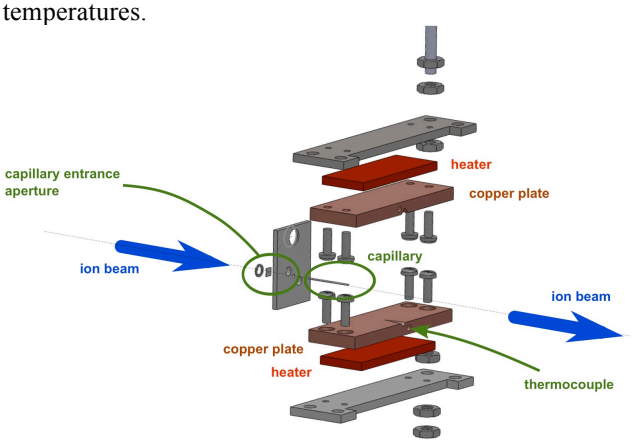

Fig. 1: Temperature regulated capillary holder developed in order to study the effect of electrical conductivity on guiding of slow highly charged ions through mesoscopic glass capillaries.

3. REFERENCES

[1] N. Stolterfoht, et al., Phys. Rev. Lett. 88, 133201 (2002).
[2] K. Schiessl, et al., Phys. Rev. A 72, 062902 (2005).
[3] P. Skog, HQ. Zhang, and R. Schuch, Phys. Rev. Lett. 101, 223202 (2008).
[4] N. Stolterfoht, et al., Phys. Rev. A 79, 042902 (2009).
[5] T. Ikeda et al., Appl. Phys. Lett. 89, 163502 (2006).
[6] R. J. Bereczky, et al., Nucl. Instr. and Meth. Phys. B 267, 317 (2009).
[7] G. Kowarik, et al., Nucl. Instr. and Meth. Phys. B 267, 2277 (2009).

* E-mail: aumayr@iap.tuwien.ac.at

Surface study with MEIS and LEEM/PEEM

Takanori Koshikawa

Fundamental Electronics Research Institute,
Osaka Electro-Communication University

1. INTRODUCTION

Medium energy ion scattering (MEIS) is a powerful tool to clarify the surface and interface structures with the precise atomic position by 0.01 nm order and has high resolution of the depth profiling. It has been currently used in the field of the surface and interface structure analysis and recently has been a well-established way to know the film structures analysis of high-k materials which are important in the new LSI technique. We applied it to obtain the high-k film composition change as changing temperature, however the film structure was changed by place to place by changing the temperature. In order to know the more detailed processes it suggests that we need a lateral sensitive tool. LEEM/PEEM (low energy electron microscopy and photo-emission electron microscopy) is a candidate, relatively new technique and attractive to observe dynamic growth processes of the thin films and nano-structures with 10 nm order spatial resolution. We have developed a novel high brightness, highly spin polarized and long life time LEEM (SPLEEM), which has essentially different capability compared from the conventional one and will present the details of it and give some experimental results obtained with it.

2. EXPERIMENTAL RESULTS

2.1. Pb/W(110)

In the present talk, some of the typical examples of the advantage of LEEM/PEEM with dynamic observation will be presented. For instance, the new growth process has been clarified in connection with the anomalous step contrast of Pb/W(110) films, which cannot be explained with the normal interference contrast The step contrast changed two times, dark, bright and dark which is concerned with the situation of Pb atoms on the terrace and the Pb atom density at the step. The analysis results and the diffraction spot intensity of LEED clarified that there is 2D gas of Pb atoms on the terrace and the Pb atom density is lower at the step, which shows the higher intensity. This is the reason why the step contrast changed from dark to bright [1].

2.2. Novel SPLEEM

The novel spin-polarized LEEM has been developed, which has very high brightness ($1.3 \times 10^7 A/cm^2 sr$, four order higher than the commercial one), high spin polarization (90%, the commercial one: 20%.) and very long life time (over 2 months, the commercial one: 3-4 hours.) [2-5]. Some new ideas and technique have been adopted. The back side illumination of the laser beam makes us high brightness because the laser beam can be finely focused at the cathode (about 1.3μm) after putting the optical lens just behind the cathode. The strain supper lattice thin film [GaAsP/GaAs] which can make us the high spin polarization has been adopted. The new design of the electron optics has been carried out, which makes us 100% electron transfer to the next optics. The dynamically observed images are shown in Fig. 1 Co/W(110). The magnetic images can be seen even with 0.02ms/frame, which is several hundreds times faster than that of the commercial one.

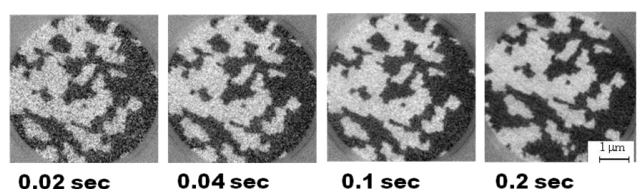

Fig.1 Dynamic magnetic domain observation of Co/W(110) with novel SPLEEM

The work was supported by a Grand-in-Aid for Creative Scientific Research (No.13GS0022) from JSPS and the Technology Development Program for Advanced Measurement and Analysis of JST.

3. REFERENCES

[1] T.Yasue, R.Amakawa, H.Shimizu, A.Nakaguchi, T.Koshikawa and E.Bauer; J. Phys. Condens. Matter **21**, 314024 (2009).
[2] X. G. Jin et al.; Appl. Phys. Express **1,** 045002 (2008).
[3] N. Yamamoto et al.; J. Appl. Phys. **103,** 064905 (2008).
[4] X. G. Jin et al.; J. Cryst. Growth **310,** 5039 (2008).
[5] M.Suzuki et al.; Appl. Phys. Express **3,** 026601 (2010).

* E-mail: kosikawa@isc.osakac.ac.jp

COMPUTING DISSOCIATIVE ADSORPTION PROBABILITIES FROM GRAZING INCIDENCE COLLISIONS OF LIGHT MOLECULES WITH METAL SURFACES

C. Díaz[1,*], *D. Stradi*[1,2], *and F. Martín*[1,2]

[1] Departamento de Química Módulo 13, Universidad Autónoma de Madrid, 28049 Madrid, Spain
[2] Instituto Madrileño de Estudios Avanzados en Nanociencias (IMDEA-Nanociencia), Cantoblanco 28049 Madrid, Spain

During the last few years, the study of the interaction of fast (0.1-2.0 keV) atoms and molecules with metal surfaces under grazing incidence (θ=0.1°-4.0°) has received and important impulse thanks to experiments showing diffraction [1, 2, 3, 4, 5]. Diffraction under these *extreme* conditions is proposed as a very promising tool to determine surface properties with unprecedented accuracy [6]. The physical phenomenon behind these striking experimental results is the strong decoupling between the fast motion along the incidence direction, parallel to the surface, and the slow motion perpendicular to the surface. Along the incidence direction the projectile moves in a periodic potential, and therefore the momentum change along this direction (Δk_x) is zero. Thus, any momentum change in the projectile is due to momentum transfer from the slow motion perpendicular to the surface (k_z) to the motion parallel to the surface and perpendicular to the incidence direction (k_y). The de Broglie wavelength associated to this slow motion is comparable to the surface lattice constant, which leads to out-of-plane diffraction according to Bragg's law when Δk_x coincides with a reciprocal lattice vector. It is noteworthy to point out that this mechanism was proposed by Martín and co. [7] to explain experimental results obtained for H_2/Pd(111) diffraction at thermal energy.

Very recently we have shown [8] that molecular dissociative adsorption (1-reflectivity) probabilities, of H_2 on metal surfaces, for low incidence energies can be obtained from total reflectivity probabilities resulting from fast grazing incidence, for molecules on their rovibrational ground state. This result has been shown to be independent of the total incidence energy (for a wide range of incidence energies) [8]. We show now that grazing incidence results also reproduce thermal sticking results for rotationally and/or vibrationally excited molecules (see Fig. 1), including the surprising non-monotonic behavior for sticking probabilities observed at thermal energies, on activated systems, for vibrationally excited molecules [9]

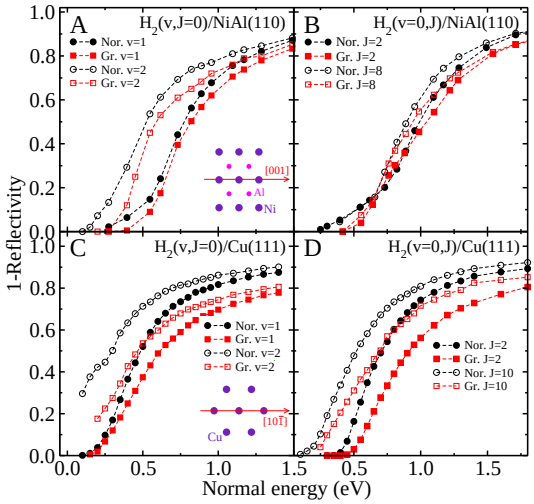

Figure 1: 1-Reflectivity as a function of the normal incidence energy for H_2/NiAl(110) and H_2/Cu(111) at normal incidence and fast grazing incidence, for E_i=400 eV and several initial molecular vibrational state (A) and (C) and several initial molecular rotational states (B) and (D). Quasi-classical calculations

1. REFERENCES

[1] A. Schüller, et al, Phys. Rev. Lett. **98**, 016103 (2007).

[2] P. Rousseau, et al, Phys. Rev. Lett. **98**, 016104 (2007).

[3] A. Schüller, et al, Phys. Rev. Lett. **100**, 097602 (2008).

[4] N. Bundaleski, et al, Phys. Rev. Lett. **101**, 177601 (2008).

[5] A. Schüller, et al, Phys. Rev. Lett. **102**, 017602 (2009).

[6] F. Aigner, et al, Phys. Rev. Lett. **101**, 253201 (2008).

[7] D. Farías, et al, Chem. Phys. Lett. **390**, 250 (2004).

[8] C. Díaz, et al, Phys. Rev. Lett. **103**, 013201 (2009).

[9] G. Laurent, et al, Phys. Rev. B **81**, 161404(R) (2010).

* E-mail: cristina.diaz@uam.es

Thursday, September 30, 2010

MULTI-COMPONENT PLASMA INTERACTIONS WITH ELEMENTAL AND MIXED-MATERIAL SURFACES

R.P. Doerner *

Center for Energy Research, University of California at San Diego, La Jolla, CA. 92093-0417

While significant advances in the understanding of PMI have occurred in recent years, much of this understanding concerns the interaction of a single-component plasma with an elemental material surface. This should be contrasted to ITER where material migration from the differing plasma-facing surfaces will lead to the formation of mixed-material surfaces interacting with the incident plasma. In addition, burning plasma will generate helium ash that will be included in the plasma reaching the surfaces surrounding the plasma. In present and proposed confinement devices, radiating species (such as argon, neon or nitrogen) are intentionally added to the divertor plasma and these radiating species will affect the PMI.

This talk summarizes results from the PISCES steady-state plasma sources at UCSD showing that plasma-surface interactions (both erosion and retention properties) cannot easily be predicted by the superposition of results from pure, single-component plasma interacting with elemental surfaces. Small amounts of condensable impurities in the incident plasma can have dramatic consequences to the erosion behavior of the surface (for example, beryllium carbide surface layer formation on carbon samples exposed to beryllium containing plasma), whereas small amounts of non-condensable impurities (such as helium) have been observed to dramatically alter the retention of fuel species within the plasma-exposed material. The simulation plasma used to investigate plasma-material interactions, therefore, must be configured to conform as closely as possible to the conditions expected in confinement devices, both with respect to composition of materials in a surface, as well as constituents of the impinging plasma, to understand the evolution of surfaces and the feedback of the resultant surfaces to the incident plasma.

HYDROGENIC RETENTION IN TUNGSTEN EXPOSED TO HIGH-FLUX PLASMAS

P.A. Zeijlmans van Emmichoven[1,*], *M.H.J. 't Hoen*[1], *G.M. Wright*[2], *M. Mayer*[3], *K. Ertl*[3], *A.W. Kleyn*[1,4], *and J. Rapp*[1]

[1] FOM-Institute for Plasma Physics Rijnhuizen, EURATOM Association, Trilateral Euregio Cluster, PO Box 1207, 3430 BE Nieuwegein, The Netherlands
[2] Plasma Science and Fusion Center, MIT, Cambridge, USA
[3] Max-Planck-Institut für Plasmaphysik, EURATOM Association, Garching, Germany
[4] Leiden Institute for Chemistry, Leiden University, PO Box 9502, 2300 RA Leiden, The Netherlands

In future magnetic fusion devices as ITER, plasma facing materials will be exposed to very high ion and neutron fluxes. The properties of materials under such extreme conditions are largely unknown. High-flux linear plasma generators are presently used to study plasma-surface interactions under these conditions. This means hydrogenic ion fluxes of ~10^{24} $m^{-2}s^{-1}$ and low electron temperatures below 10 eV. One important issue for future fusion devices is the retention of tritium in the wall of the reactor. For safety reasons and since tritium is one of the components of the reactor fuel, this should be as low as possible.

Tungsten is foreseen as the material of choice for large parts of the ITER diverter. The mechanisms for hydrogenic retention in tungsten are not understood very well. It is known that hydrogenic retention is low for tungsten with a small number of defects. However, in a fusion reactor, the plasma facing materials will continuously be bombarded with energetic neutrons from the fusion process. These neutrons create additional defects thereby increasing hydrogenic retention.

Results will be presented for hydrogenic retention in tungsten exposed to high-flux hydrogenic plasmas. MeV tungsten ions have been used as proxy for neutrons to create defects. The effect on the retention properties of tungsten of the amount of defects, their depth profile, and the growth of voids will be discussed.

[*] E-mail: P.A.Zeijlmans@rijnhuizen.nl

RETENTION AND RELEASE MECHANISMS OF DEUTERIUM IMPLANTED INTO BERYLLIUM AS A FUSION FIRST WALL MATERIAL

M. Oberkofler[*], *and Ch. Linsmeier*

Max-Planck-Institut für Plasmaphysik, EURATOM Association, Boltzmannstraße 2, 85748 Garching b. München, Germany

Beryllium is planned as a plasma-facing material for the international nuclear fusion experiment ITER currently under construction in Cadarache, France [1]. Most of the inner wall of the plasma vessel of this facility will be covered by metallic Be. In the nuclear phase of the experiment the plasma will consist mainly of deuterium and tritium. The Be surface is thus subjected to intense fluxes of these hydrogen isotopes escaping from the magnetically confined plasma. Parallel to erosion, hydrogen is implanted and retained in the plasma-facing material. The radioactive isotope tritium poses a safety issue: An in-vessel tritium inventory of 700 g has been defined as the maximum acceptable level for ITER. Therefore, the fraction of hydrogen atoms retained upon implantation into Be as well as the temperature dependence of the release is of great concern and has been the subject of numerous investigations.
The tendency of Be to oxidise quickly even under very good vacuum conditions often affects the results of dedicated experiments by influencing the observed retained fractions and release temperatures. This makes the investigation of the mechanisms governing retention and release by modelling of experimental results very challenging. Improvements have been made in understanding the underlying mechanisms through experiments on atomically clean metallic Be surfaces [2, 3, 4].

Be samples of various structure (single and polycrystalline) are implanted with a monoenergetic deuterium ion beam at selected implantation energies to various fluences. The retained fraction is measured with nuclear reaction analysis and the temperature dependent release is monitored in temperature programmed desorption (TPD) experiments.
At low fluences, the implanted D atoms are trapped at defect sites that originate from the collision cascades initiated by the impinging atoms themselves. Release from these traps occurs at temperatures around 700 to 800 K. The implantation depth is varied by varying the implantation energy. Higher energies lead to implantation at greater depths and to shifts in the observed desorption peaks towards higher temperatures. This indicates that additionally to the detrapping from binding sites (effective) diffusion affects the desorption temperatures in TPD experiments. Comparison of desorption spectra from samples with different crystal structure (single and polycrystalline) leads to the conclusion that also the anisotropy of the diffusion of vacancies, self interstitials and D impurities in the hexagonal Be lattice plays a role and has to be accounted for when trying to simulate experimental observations on the basis of atomistic models.
While at low fluences the retained fraction of implanted D is close to 100 %, above fluences of 10^{21} m^{-2} "supersaturation" of the samples with D becomes manifest: The retained fraction is reduced and a second sharp desorption peak appears in the TPD spectra at a temperature around 450 K. Desorption in this temperature range is attributed to the release of D from regions in the implanted volume that have been structurally modified due to the irradiation. Release from beryllium surfaces implanted at room temperature to fluences above 10^{21} m^{-2} occurs mainly in this low-temperature desorption stage.

Once the retention and release mechanisms of D in metallic Be with a clean surface have been reasonably well understood these results can be compared to D implantation into a delibertely oxidised Be surface. It is observed that the low temperature stage does not dominate the desorption from BeO. Instead, D is released at a low rate over the whole temperature range from 450 to 1000 K. At this temperature about 20 % of the retained D have still not desorbed. The high affinity of Be towards oxygen - although leading to lower oxygen impurities in the plasma and therefore being a desirable property of a first wall material - might pose problems for the thermal recycling of hydrogen isotopes if very thick oxide layers are formed.

REFERENCES

[1] M. Shimada, et al., Nuclear Fusion **47** (2007) S1.
[2] M. Reinelt, A. Allouche, M. Oberkofler, and Ch. Linsmeier, New J. Phys. **11** (2009) 043023.
[3] M. Oberkofler, M. Reinelt, S. Lindig, and Ch. Linsmeier, NIMB **267** (2009) 718.
[4] M. Oberkofler, M Reinelt, A Allouche, S Lindig, and Ch Linsmeier, Physica Scripta **T138** (2009) 014036.

[*] E-mail: martin.oberkofler@ipp.mpg.de

In-situ elemental and chemical state characterization of lithiated surfaces under energetic singly-charged particle bombardment.

C.N. Taylor[1], *B.Heim*[1,2], *D. Zigon*[1], *M Gonzalez*[1], *J.P Allain*[1,2,*]

[1] Purdue University, West Lafayette, 400 Central Drive, IN 47907, USA
[2] Birck Nanotechnology Center, Discovery Park, Purdue University, West Lafayette, IN 47907, USA

1. INTRODUCTION

Lithium has been considered a potentially viable plasma-facing surface enhancing the operational performance of fusion devices such as: TFTR and NSTX [1]. Lithium conditioning and lithium-based surfaces are gaining unprecedented ground as plasma-facing interfaces and are now used in many current international magnetic thermonuclear experimental reactors including: FTU, T-11M, TJ-II, EAST, and LTX. Solid and liquid lithium surfaces have been studied extensively both in their erosion and hydrogen-retaining properties [2-5]. However, questions still remain on the role of lithiated surfaces and multi-material interactions at the plasma edge [6]. Lithiated surfaces include: liquid Li on metal substrates, Li alloys and Li coatings. The main processes studied here (e.g. erosion, H-retention, HD and D2 recombination, Li, He and D2 ion scattering) consist of spatial scales from a few monolayers at the vacuum/film interface to 10's nm deep.

2. PARTICLE-SURFACE INTERACTIONS

The particle-surface interactions that govern the interface between the fusion plasma and the material surface are strongly dependent on how the plasma modifies that particular surface. Chargled-particle interactions with fusion materials are also driven by surface chemistry evolution, morphology evolution and irradiation-driven mechanisms (e.g. ion-induced diffusion). One critical interaction at the surface involves the particle balance of hydrogen species in and out of the plasma. Incident particle energies vary between a few eV in the private-flux region of fusion tokamak plasma to several 100's eV. At the plasma-material interface the magnetic sheath dictates both the incident particle energy and angle.

3. EXPERIMENTAL SETUP

Processes at the surface and near-surface are studied *in-situ* under energetic particle irradiation [7]. Techniques include: low-energy ion scattering spectroscopy (LEISS), direct recoil spectroscopy, X-ray photoelectron spectroscopy and in-situ erosion diagnosis. LEISS results in elemental information at the first 2-3 monolayers. XPS gives chemical state data 10-nm into the lithiated surface. Three cases are presented: 1) liquid Li response to energetic D, 2) lithium alloy behavior under particle irradiation and 3) lithium coatings on various substrates including: C, W and Mo.

4. RESULTS AND FUTURE DIRECTIONS

Lithium has been introduced as an attractive material for the PMI due to its compatible properties with hydrogen and its isotopes (e.g. secondary ion sputtered fraction, high affinity for O, C impurities and tunability of hydrogen bonding.

Fig.1 shows the physical sputter yield of lithium and lithium-based surfaces. Irradiation at energies between 50-5000 eV at 45-degree incidence with He singly-charged ions. Lithium-based surfaces are treated with D energetic particles emulating conditions in tokamak edge plasmas (e.g. energies 10-100 eV). Lithiated graphite surfaces show over 8-10x decrease in sputter yield mainly due to the inherent binding of lithium atoms with oxygen in the lithium matrix. Li atoms readily intercalate into the graphite basal planes. However, studies presented here show the role of surface morphology is critical in determining effective hydrogen pumping and recycling.

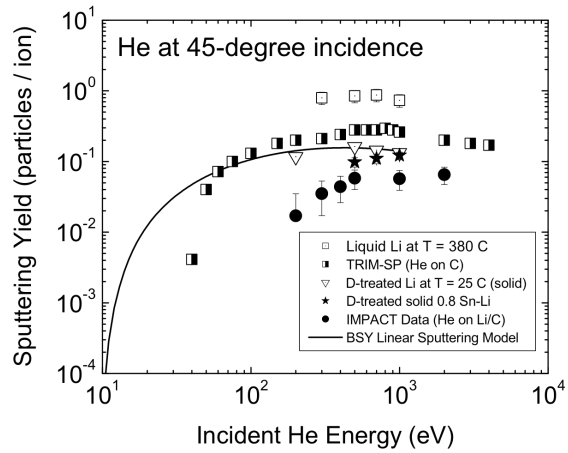

Figure 1: O1s spectrum for 2-µm lithium evaporated polycrystalline graphite with corresponding deuterium fluency.

5. REFERENCES

[1] D.K. Mansfield, et al, Nucl. Fusion, 41 (2001) 1823
[2] J.P. Allain, J. Nucl. Mater. 390-391 (2009) 942
[3] J.P. Allain, Phy. Rev. B 76 (2007) 205434
[4] J.P. Allain, J. Nucl. Mater. 290-293 (2001) 180
[5] J.P. Allain, Nucl Fusion 42 (2002) 202
[6] S.S. Harilal, Appl. Surf. Sci. 255 (2009) 8539
[7] J.P. Allain, Rev. Sci. Instrum. 78 (2007) 113105

* E-mail: allain@purdue.edu

STUDYING SYNERGISTIC EFFECTS IN CHEMICAL SPUTTERING USING DUAL BEAM IRRADIATION

T. Schwarz-Selinger , *C. Hopf, M. Schlüter, and W. Jacob*

Max-Planck-Institut für Plasmaphysik, EURATOM Association, Boltzmannstr. 2, D-85748 Garching, Germany

1. INTRODUCTION

Plasma-facing components in nuclear fusion devices are exposed to large fluxes of ions and neutrals with energies ranging from fractions of eV to keV. Physical sputtering of surfaces by energetic particles is unavoidable but very well understood. For carbon the chemical reactivity of the fuel hydrogen and possible impurities such as oxygen and nitrogen brings about additional erosion processes that are not yet fully understood such as chemical erosion and chemical sputtering. To predict component lifetime as well as retention of the fuel in the material it is essential to understand the microscopic processes involved. Here we present a model experiment to study the plasma-wall–interactions involved.

2. EXPERIMENT

One attempt to study individual processes and synergistic effects between the species is to conduct experiments with multiple quantified particle beams. The experiment MAJESTIX will be introduced that allows to study the interaction of mass selected low energetic ions (energies ranging from 20 eV to 1 keV with ion fluxes of 10^{12} cm^{-2}s^{-1}) and hyperthermal hydrogen atoms (energies 0.25 eV, fluxes of up to 10^{16} cm^{-2}s^{-1}). Film growth, erosion and modification is monitored on a sub-monolyer scale in-situ and in real time with ellipsometry. As a model system for carbon surfaces exposed to large hydrogen fluxes as well as for co-deposited carbon films plasma–deposited amorphous hydrogenated carbon thin films (a-C:H) are used.

3. RESULTS

Bombarding the a-C:H surface with rare gas ions and hydrogen atoms simultaneously allows to separate kinematic from chemical effects in the erosion process. It will be shown that the sputtering yield per impinging ion is significantly higher than the sum of the individual processes – chemical erosion and physical sputtering. The process is termed *chemical sputtering*. Besides this synergistic effect, this process occurs also at energies below the threshold for physical sputtering. A microscopic reaction mechanism for chemical sputtering is presented. It is based on C-C bond braking within the collision cascade and the subsequent reaction of the broken bonds with atomic hydrogen leading to volatile reaction products. A model based on this reaction mechanism is able to quantitatively reproduce the energy dependence of chemical sputtering by atomic hydrogen and argon ions at room temperature using just one free parameter [1]. Model calculations and recent experimental data will be shown for the chemical sputtering of carbon by atomic hydrogen and different rare gas ions (He^+, Ne^+, Ar^+) as a function of energy and substrate temperature [2]. An extension of the model is also capable of quantitatively explaining the experimentally observed isotope effect in the erosion of carbon by hydrogen ions (H^+, D^+) and allows extrapolation to Tritium [3]. In addition, recent results for the simultaneous bombardment of a-C:H surfaces with rare gas ions and molecular oxygen are presented as a function of ion energy and substrate temperature [4]. Finally interaction of molecular nitrogen ions [5] and simultaneous interaction of these low-energy ions with atomic hydrogen will be presented as a function of energy and substrate temperature.

4. REFERENCES

[1] C. Hopf, A. von Keudell, W. Jacob, J. Appl. Phys. **94**, 2373 (2003).

[2] M. Schlüter, C. Hopf, T. Schwarz-Selinger, W. Jacob, Journal of Nuclear Materials **376** 33-37 (2008).

[3] C. Hopf and W. Jacob, J. Nucl. Mater. **342**, 141-147 (2005).

[4] C. Hopf, M. Schlüter, T. Schwarz-Selinger, U. von Toussaint and W. Jacob, New Journal of Physics **10** 093022 (2008).

[5] M. Schlüter, C. Hopf and W. Jacob, New Journal of Physics **10** 053037 (2008).

* E-mail: Thomas.Schwarz-Selinger@ipp.mpg.de

MOLECULAR SIZE EFFECT IN THE CHEMICAL SPUTTERING OF a-C:H THIN FILMS BY LOW ENERGY H^+, H_2^+, and H_3^+ IONS[&]

P. R. Harris[1,*], *F. W. Meyer*[1], *W. Jacob*[2], *T. Schwarz-Selinger*[2] *and U. von Toussaint*[2]

[1] Physics Division, Oak Ridge National Laboratory, P.O. Box 2008, Oak Ridge, TN 37831-6372
[2] Max-Planck-Institut für Plasmaphysik, EURATOM Association, Boltzmannstr. 2, 85748 Garching, Germany

1. INTRODUCTION

We report a molecular size effect in the chemical sputtering of amorphous hydrogenated carbon (a-C:H) thin films by H^+, H_2^+, H_3^+ in the energy range 30-400 eV/H. By molecular size effect we mean that the sputtering yield (per atomic constituent) for molecular incident projectiles at energy E is greater than that for atomic projectiles incident at the same velocity. These observations are in contrast to the commonly made assumption that, normalized to the incident H count, yields from equal velocity H^+, H_2^+, and H_3^+ should be the same when compared at the same velocity. We determine yields from data acquired both in-situ, via mass spectrometry and ex-situ, via ellipsometry. We compare our data to sputtering yields obtained from total mass loss measurements by Balden & Roth [1].

2. EXPERIMENT

We employ an Electron Cyclotron Resonance (ECR) ion source to produce 10 keV atomic and molecular hydrogen ions. The ions are mass analyzed and then transported to a floating surface scattering end station at the entrance to which efficient deceleration prior to impact onto our a-C:H sample occurs.

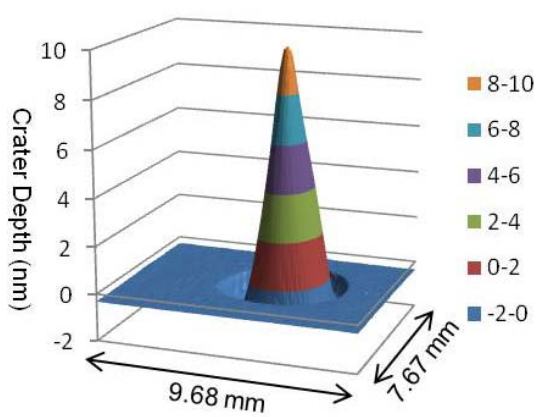

Figure 1: Pre- and post-exposure 2-D ellipsometry scan difference for H_3^+ @ 300eV/H incident on a-C:H to a fluence of 1.5 x 10^{19} H/cm^2.

A UTI-100 quadrupole mass spectrometer monitors the partial pressures of hydrocarbons produced by exposure to the incident H beam. We use the QMS to acquire both transient (immediately after beam turn-on and turn-off) and steady-state spectra. Through the use of cracking pattern matrices and calibrated leaks we obtain quantitative hydrocarbon yields for the dominant species, whose sum provides an estimate of the total carbon yields [2]. We use 2-D ellipsometry to measure the volume of the erosion craters by comparing scans taken pre- and post- beam exposure, as shown in Figure 1. The crater volumes, together with the measured integrated sample current, and the known carbon density of the thin film samples, are used to deduce total carbon yields for each incident beam species/energy.

3. RESULTS

In 2-D ellipsometry measurements we observe a molecular size dependence of total erosion yields on the incident projectile, as we have previously reported for atomic and molecular D beams incident on a-C:D [3]. The yields for H_3^+ agree with previous measurements reported for this ion [1], while yields for atomic ions are systematically lower at energies below 140eV/H. Additionally, the transient measurements gave insight into the fluences required to reach steady state conditions from an unexposed (but hydrogenated to ~35%) surface. These measurements confirmed that the total erosion seen by ellipsometry occurs predominantly at steady state. In the future we plan to employ direct line of sight mass spectrometry techniques to obtain improved total and partial hydrocarbon yields.

[&]This work was supported by the Office of Fusion Energy Science and the Office of Basic Energy Science of the U.S. Department of Energy under Contract No. DE-AC05-00OR22725 with UT-Battelle, LLC.

4. REFERENCES

[1] M. Balden and J. Roth, J. Nucl. Mater. 280, (2000) 39.
[2] L. I. Vergara, F. W. Meyer, and H. F. Krause, J. Nucl. Mater. 347 (2005) 118.
[3] F. W. Meyer, P. R. Harris, W. Jacob, T. Schwarz-Selinger, U. von Toussaint, Proceedings of the 19th International Conference on Plasma Surface Interactions, San Diego, May 24-28, 2010, to be published, J. Nucl. Mater.

AN OVERVIEW OF NUCLEAR MICRO-PROBE APPLICATIONS FOR CHARACTERISATION OF PLASMA-FACING MATERIALS FROM TOKAMAKS

M. Rubel[1,*], *P. Petersson*[2], *G. Possnert*[2] *and A. Kreter*[3]

[1] Alfvén Laboratory, Royal Institute of Technology (KTH), Association EURATOM – VR, 100 44 Stockholm, Sweden
[2] Ångström Laboratory, Uppsala University, Association EURATOM – VR, Uppsala, Sweden
[3] Institute for Energy Research, IEF-4, Plasma Physics, Forschungszentrum Jülich, Germany

1. INTRODUCTION

Plasma-facing components (PFC) in controlled fusion devices undergo severe modification by processes of plasma-wall interactions (PWI). They cause the change of structure, composition and thermo-mechanical properties of materials irradiated by particles escaping the hot plasma. Material erosion, transport in the plasma and re-deposition of eroded species also lead to the accumulation of hydrogen isotopes in PFC, so-called fuel inventory. It is one of key issues decisive for safety and economy of a tokamak operation [1-3].

Examination of PFC is carried out by means of a large number of material research techniques. Accelerator-based ion beam analysis (IBA) methods play here crucial role because of their sensitivity and selectivity in quantification of light isotopes and, unique possibility for analyzing and depth profiling of deuterium by nuclear reaction analysis (NRA) using a $^3He^+$ beam: $^3He(d,p)\alpha$ [4]. In most studies a standard broad beam (spot of 0.5 – 1 mm in diameter) has been used, but such measurement could not reflect details of fuel distribution on surfaces and in the bulk of PFC; the latter is studied on cleaved samples.

The aim of this work is to provide an overview of high-resolution NRA measurements with a ^3He micro-beam [5] on PFC made of carbon-fibre composites (CFC) which were exposed to deuterium plasma in tokamaks or simulators of PWI. Secondly, a comparison is also made between results obtained using a standard and μ-NRA.

2. SUMMARY OF RESULTS

Figure 1 shows maps of deuterium and carbon distribution on the surface of CFC (NB41 produced by SNECMA) exposed to fusion plasma in the TEXTOR tokamak. The deposition pattern is highly non-uniform on a micro-scale. The preferential fuel retention has been correlated with surface topography of that region. Moreover, the result corresponds to previous findings regarding the micro-scale distribution of re-deposited plasma impurities.

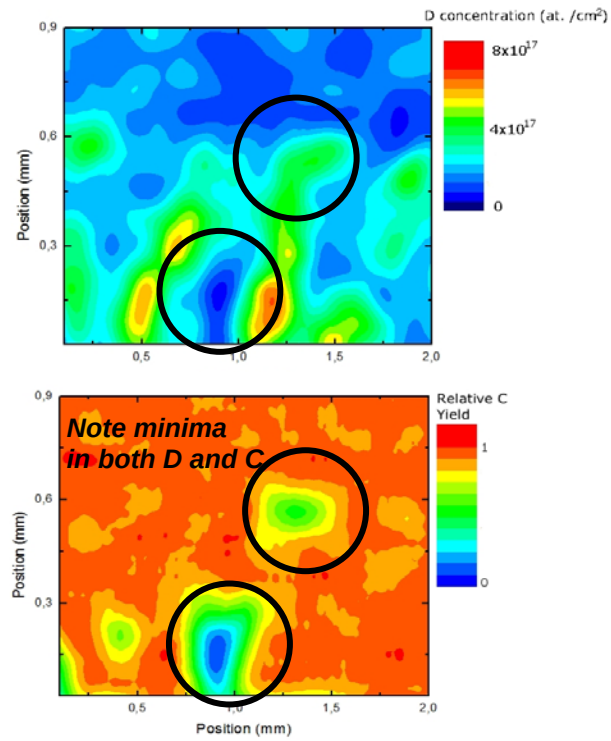

Figure 1: μ-NRA maps of deuterium and carbon.

The relation between the deuterium concentration, the content and distribution of other elements and, the CFC structure will be discussed. A reference to results obtained by microscopy and other techniques will be made. Results of quantitative analysis of deuterium migration into the bulk of carbon composites will also be presented.

3. REFERENCES

[1] G. Federici et al., Nucl. Fusion **41**, 1697 (2001).
[2] V. Philipps eta al., Vacuum **70**, 399 (2002).
[3] M. Rubel et al., J. Nucl. Mater. **290-293**, 473 (2001).
[4] M. Rubel et al., Nucl. Instr. Meth. **B267**, 711 (2009).
[5] P. Petersson et al., Nucl. Instr. Meth. B, in press.

E-mail: rubel@kth.se

DECOHERENCE IN FAST ATOM DIFFRACTION FROM SURFACES

N. Bundaleski[1, 2*], *P. Soulisse*[1], *A. Momeni*[1,3], *H. Khemliche*[1], *P. Roncin*[1]

[1] ISMO, CNRS, Univ. Paris-Sud, F-91405 Orsay cedex, France
[2] FCT, Universidade Nova de Lisboa, 2829-516 Caparica, Portugal
[3] LERMA, CNRS, Univ. Cergy Pontoise, F-95031 Cergy Pontoise Cedex, France

Diffraction of fast atoms from crystal surfaces at grazing incidence has been observed on all types of materials, from wide band gap insulators [1,2] to metals [3,4], including semiconductors [5]. In spite of the much reduced de Broglie wavelength associated to the fast atoms (e.g. 0.45 pm for 1 keV He), very nice diffraction patterns are observed that are comparable to those obtained at thermal energies. This is because at very grazing incidence, only the (slow) motion normal to the surface is important for the diffraction process. Furthermore, the decoherence phenomena related to thermal vibrations are still much less pronounced than for the equivalent thermal particle impinging on the surface because of the large number of scatterers inherent to the grazing geometry. This effect is well taken into account by a modified Debye-Waller factor [6, 7]. With respect to electronic excitations, though partially quenched on insulators and semiconductors because of the band gap, they are unavoidable on metals because excitation of Fermi electrons requires very little energy. Yet, although present and measurable, electronic excitations do not prevent coherent scattering even at 2 keV energy. The reason is that electrons responsible for the inelastic scattering usually have a preferred momentum normal to the surface, thus leading to a very limited momentum exchange in the surface plane.

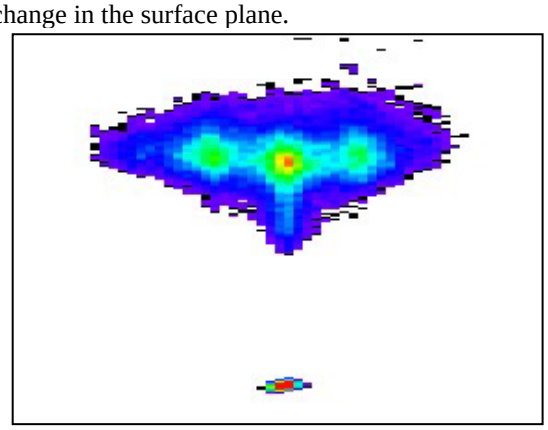

Figure 1: scattered profile of a 500 eV He on Ag(110); beam is along the <001> direction

Experimentally, the primary ion beam is pulsed prior to neutralization, and the inelastic energy loss is measured from the time-of-flight of the scattered atoms, while the diffraction profile is recorded on a position sensitive detector.

We have developed a simple model that describes the atom-electron scattering process; the results are in good agreement with the observed energy loss spectra.

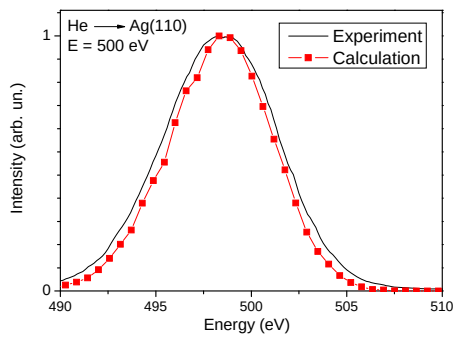

Figure 2: Energy distribution of 500 eV He scattered on Ag(110) at grazing incidence.

REFERENCES

[1] A. Schuller, S. Wethekam, and H. Winter, Phys. Rev. Lett. **98**,016103 (2007).
[2] P. Rousseau, H. Khemliche, A.G. Borisov, and P.Roncin, Phys. Rev. Lett. **98**, 016104 (2007)
[3] N. Bundaleski, H. Khemliche, P. Soulisse, and P. Roncin, Phys. Rev. Lett. **101**,177601 (2008).
[4] A. Schüller, M. Busch, S. Wethekam, and H. Winter, Phys. Rev. Lett. **102**, 017602 (2009)
[5] H. Khemliche, P. Rousseau, P. Roncin, V. H. Etgens, and F. Finocchi, Appl. Phys. Lett. **95**, 151901 (2009)
[6] J. Manson, H. Khemliche, and P.Roncin, Phys. Rev. B. **78**, 155408 (2008).
[7] P. Rousseau, H. Khemliche, N. Bundaleski, P. Soulisse, A. Momeni, and P. Roncin, Journal of Physics: Conference Series **133**, 012013 (2008)

He-LiF SURFACE INTERACTION POTENTIAL FROM FAST ATOM DIFFRACTION

A. Schüller[1], *H. Winter*[1], *M.S. Gravielle*[2,*], *J.M. Pruneda*[3] *and J.E.Miraglia*[2]

[1]Institut für Physik, Humboldt Universität zu Berlin, Newtonstrasse 15, D-12489 Berlin-Adlershof, Germany.
[2] Instituto de Astronomía y Física del Espacio, CONICET, and Depto de Física, FCEN, UBA, Buenos Aires, Argentina.
[3] Centre d'Investigació en Nanociència i Nanotecnología-CIN2 (CSIC-ICN), Campus UAB 08193 Bellaterra, Spain.

Recently new experiments [1,2] have shown interference effects for grazing scattering of fast atoms from surfaces, where classical mechanics was supposed to be adequate. This unexpected diffraction phenomenon was found to be very sensitive to the projectile-surface interaction, which opens the way for a method to probe surface potentials with high accuracy.

The aim of this work is to find out to what extent surface potentials derived from state-of-the-art ab-initio methods are capable of reproducing experimental diffraction patterns for grazing scattering of swift He atoms from a LiF(001) surface [3]. The He-LiF surface interaction is derived here by using the SIESTA [4] implementation of the density-functional theory (DFT), which is a self-consistent method for performing first-principles calculations on systems with a large number of atoms.

For the description of the collision process we employ the surface-eikonal approximation [5], which takes into account quantum interference between different projectile paths. The dependence of projectile spectra on the parallel and perpendicular incident energies is experimentally and theoretically analyzed, demonstrating the range of applicability of the proposed model.

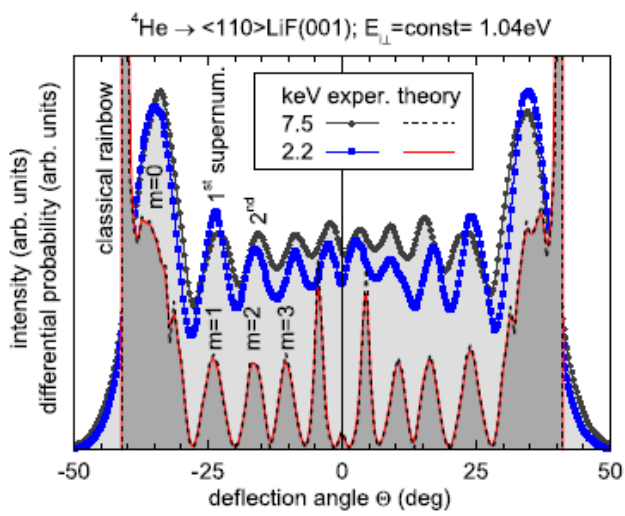

Figure 1: Projected intensities, as a function of the deflection angle Θ, for E_i=7.5 keV (gray circles) and 2.2 keV (blue squares) and corresponding differential probabilities derived from the surface-eikonal approach (black dashed and red full curves). *m* denotes the order of the supernumerary rainbow.

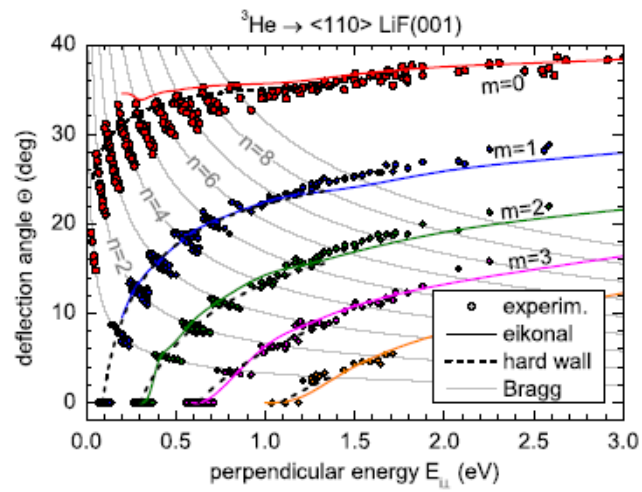

Figure 2: Deflection angles Θ corresponding to maxima of angular distributions, as a function of the perpendicular energy $E_{i\perp}$, for ^{3}He atoms scattered from LiF(001) along the direction ⟨110⟩. Full colored curves, quantum rainbow *m*=0 and supernumerary rainbows *m*=1 to 4 derived within the surface-eikonal approximation based on the present DFT potential; dashed curves, positions of supernumerary rainbows in hard wall approximation using the effective corrugation of the DFT potential across the ⟨110⟩ channel; thin grey curves, theoretical positions of maxima of order *n* from Bragg condition.

[1] A. Schüller *et al.*, Phys. Rev. Lett. **98**, 016103 (2007).
[2] P. Rousseau *et al.*, Phys. Rev. Lett. **98**, 016104 (2007).
[3] A. Schüller *et al.*, Phys. Rev. A **80**, 062903 (2009).
[4] J.M. Soler *et al.*, J. Phys.: Condens. Matter **14**, 2745 (2002).
[5] M.S. Gravielle *et al.*, Phys. Rev. A **78**, 022901 (2008).

* E-mail: msilvia@iafe.uba.ar

RECENT PROGRESS IN STUDIES ON FAST ATOM DIFFRACTION DURING GRAZING SURFACE SCATTERING

H. Winter[*], *J. Seifert, U. Specht, M. Busch, S. Wethekam, A. Schüller*

Institute of Physics, Humboldt University Berlin, Newtonstr.15, D-12489 Berlin-Adlershof, Germany

1. INTRODUCTION

Recently it was demonstrated that fast atoms and molecules with energies up to some keV show diffraction effects during scattering from surfaces under axial channeling conditions [1-3]. This at first glance surprising finding can be understood by specific features of scattering of fast atoms from surfaces under glancing angles of incidence with respect to the surface plane. Key issues in this respect are (1) the slow motion of projectiles normal to the surface plane so that the associated de Broglie wavelength is about two orders of magnitude larger compared to the free motion of the particles and (2) the suppression of excitations for electrons and atoms of the target which preserves quantum coherence in the scattering process. In basic features, the method is closely related to the scattering of thermal atoms (TEAS), however, it has the advantage of a simple tuning of the projectile energy by the acceleration voltage and the angle of incidence and of a highly efficient detection of the diffraction pattern by means of a position sensitive detector.

2. STUDIES ON SURFACE STRUCTURES

In terms of Bragg scattering, the diffraction pattern contains information on the width of axial channels formed by strings of topmost surface atoms. Furthermore the Bragg peaks of given orders reveal an intensity modulation with the projectile energy for the motion normal to the surface plane caused by the corrugation of the interaction potential across axial channels. These features can be exploited for studies on the structure of surfaces and on the interaction potentials of atoms in front of surfaces. It turns out that – aside from insulator surfaces - well defined diffraction patterns can also be observed for structures of adsorbed atoms and ordered ultrathin films on metal surfaces.

As first examples we present studies on the adsorption of O and S atoms on clean Fe(110) and Ni(110) surfaces. From the analysis of the diffraction patterns for scattering along different low indexed axial channels in the surface plane we derive the ordered structure of adsorbed atoms. For O/Fe(110) forming a c(2x2) structure we deduce from the intensity modulations of diffraction spots the corrugation of the interaction potential and the height of adsorbed O atoms with respect to substrate atoms.

We have also investigated the surface structure of a monolayer film of silica on Mo(112) where two conflicting structural models were proposed: an arrangement of Si and O atoms in terms a 2D-network [4] or in terms of SiO_4 clusters [5]. The analysis of angular distributions reveals already in the regime of classical (rainbow) scattering a clear cut evidence for the 2D network model which is supported by the results for atom diffraction. The data for diffraction of fast He atoms during axial surface channeling from the film surface are compared with semi-classical calculations based on a DFT-potential for He atoms in front of the film surface. The calculations are in good accord with the experiment.

In detailed studies on the quantum coherence in the scattering process, we have correlated via a time-of-flight technique the shape of diffraction peaks to the energy loss of H atoms scattered from a LiF(001) surface and find that the coherence is closely and predominantly related to electronic excitations of the target surface.

3. REFERENCES

[1] A. Schüller, S. Wethekam, and H. Winter, Phys. Rev. Lett. **98**, 016103 (2007).
[2] P. Rousseau, H. Khemliche, A.G. Borisov, and P. Roncin, Phys. Rev. Lett. **98**, 016104 (2007).
[3] A. Schüller and H. Winter, Phys. Rev. Lett. **100**, 097602 (2008).
[4] M. Sierka et al., Chem. Phys. Lett. **424**, 115 (2006).
[5] M.S. Chen and D.W. Goodman, J. Phys.: Condens. Matter **20**, 264013 (2008).

[*] E-mail: winter@physik.hu-berlin.de

ATOM-AL SURFACE SCATTERING POTENTIALS FROM AB-INITIO CALCULATIONS

P. Tiwald, C. Lemell, and J. Burgdörfer

Inst. f. Theoretical Physics, Vienna Univ. of Technology, Wiedner Hauptstr. 8-10, A–1040 Vienna, Austria, EU

1. INTRODUCTION

Atom-surface potentials entering the calculations of atom scattering at surfaces are often taken to be purely repulsive with a parametrization of the form

$$V_j(R) = \frac{Z_t Z_p}{R} \sum_i a_i \exp(-b_i R/a_s), \qquad (1)$$

where Z_t and Z_p are the core charges of the target and projectile atoms, respectively, and $\{a_i\}$ and $\{b_i\}$ are model dependent parameter sets (e.g. [1, 2]).
However, surface potentials derived from such pairwise superpositions of binary potentials fail to reproduce recent results of rainbow scattering measurements performed for various atomic projectiles above different faces of atomically flat single crystal Al surfaces. It was found that the dependence of the rainbow angle θ_{rb} on the kinetic energy component normal to the surface for the projectile motion perpendicular to the surface $E_\perp$ varies with the electronic structure of the projectile as well as the crystallographic face of the aluminum surface. Modeling the atom-surface interaction by ab-initio methods, we determine atom-surface potentials which yield satisfactory agreement with experiment.

2. MODEL AND RESULTS

We calculate the electronic structure of the complex (atom + crystal surface) using the ABINIT code [3]. The combined system is represented by a supercell with periodic boundary conditions of sufficient size in order to avoid interaction of the projectile atom with its replicas in neighboring cells. The resulting potentials were taken as input to classical trajectory Monte-Carlo (CTMC) calculations for the transport of atomic projectiles through channels of various faces of the Al surfaces. Beam parameters (energy, direction, and divergence) were chosen to match the experiment. The final angular distribution was extracted from the receding trajectory recorded at a distance z=8 a.u. above the surface.
Fig. 1 clearly demonstrates the necessity to go beyond binary pair potentials in slow atom-surface scattering simulations. While pair potentials fail to even qualitatively reproduce the energy dependence of the rainbow angle θ_{rb}, we find good agreement for potentials from ab-initio calculations. Since pair potentials depend on the nuclear charges only, they cannot account for the electronic rearrangement near the metal surface which is important in this case. The difference in the dependence of θ_{rb} on $E_\perp$ can be traced back to the different corrugations above the wide and narrow channels above Al(111). The potential corrugation above the latter even features a change in sign at a distance of about $z_c \approx 1.9$ a.u. leading to the zero of θ_{rb} at $E_\perp \approx 20$ eV.

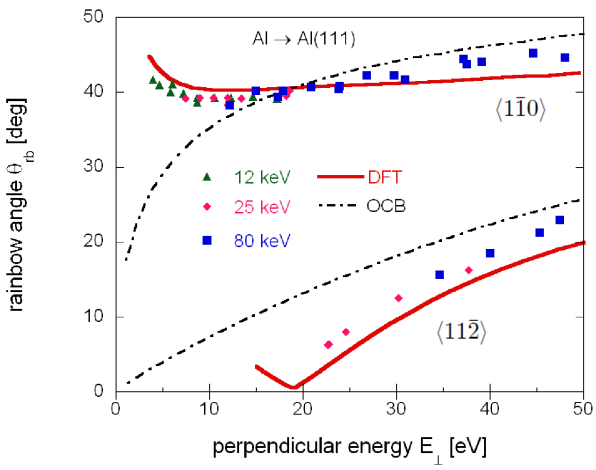

Figure 1: Rainbow angles of Al atoms scattered off an Al(111) surface along the $\langle 1\bar{1}0\rangle$ and $\langle 11\bar{2}\rangle$ directions. Symbols: experimental results for different total energies E_0, black dashed lines: simulations using the OCB potential [2], and red solid curves: simulations based on complete Al–Al(111) ab-initio DFT surface-potentials.

3. REFERENCES

[1] J.F. Ziegler, J.P. Biersack, U. Littmark, *The stopping and ranges of ions in solids*, (Pergamon Press, New York, 1985).

[2] D.J. O'Connor and J.P. Biersack, NIM B **15**, 14 (1986).

[3] X. Gonze et al., Comp. Mat. Science **25**, 478 (2002).

* E-mail: paul@dollywood.itp.tuwien.ac.at

PROBING STRAY ELECTRIC FIELDS AT SURFACES WITH RYDBERG ATOMS

D. D. Neufeld,* *Y. Pu, and F. B. Dunning*

Department of Physics and Astronomy, Rice University MS 61, Houston, Texas 77005-1892, USA

The presence of stray electric "patch" fields at conducting surfaces is important in studies of short-range surface phenomena such as the Casimir-Polder force and non-contact friction, or when trapping atoms and ions near a surface. Because of their large physical size and weak binding, high-*n* Rydberg atoms are strongly perturbed by the presence of nearby surfaces. Even relatively far from the surface the motion of the excited electron can be strongly affected by image charge interactions and by stray fields. Furthermore, ionization can occur through resonant tunneling of the excited electron into a vacant level in the metal. Here we show how studies of Rydberg atom surface ionization can be used to examine stray fields present at surfaces.

In the present experiments thermal-energy xenon Rydberg atoms are directed at near-grazing incidence onto a Au(111) target surface. Ions formed by tunneling are attracted to the surface by their image charge fields which are large and rapidly accelerate them to the surface where they are lost through Auger neutralization. To prevent this, an ion collection field is applied perpendicular to the surface. The initial image charge field, and hence the external field required to overcome it, depends on the atom-surface separation at which ionization occurs. In principle, the ionization distance can then be inferred from measurements of the surface ionization signal as a function of applied field such as presented in Fig. 1.

The onsets in the surface ionization signals in Fig. 1 are much broader than those anticipated for a truly equipotential conducting surface. This can be attributed to the presence of stray fields at the surface which modify the height of the potential barrier between the atom and surface, i.e., the atom-surface separation at which ionization occurs, and the ion collection efficiency.[1,2] While the stray fields will have a range of magnitudes and directions, an estimate of their typical upper limit can be obtained by considering the ion collection fields at which a surface ion signal is first detected, i.e., the threshold fields. To this end it is assumed that the stray fields act perpendicular to the surface and exhibit a multi-exponential decay with distance from the surface. A simple over-the-barrier model of ionization is then used to select those field parameters that provide the optimum fit to the various thresholds measured using different values of *n* and angles of incidence θ. Preliminary results show

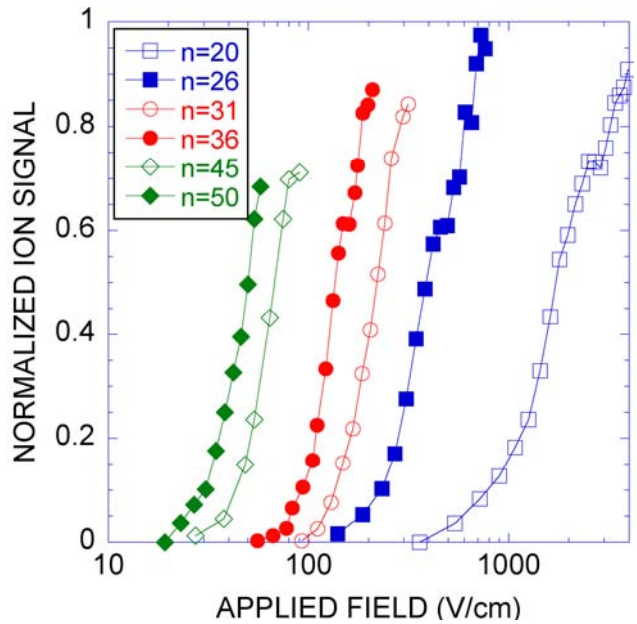

Figure 1: Dependence of surface ion signal (normalized to the number of incident Rydberg atoms) on applied ion collection field for the values of *n* indicated and an angle of incidence θ~4°.

the stray fields required to explain the positions of the onsets are sizeable, decreasing from ~ 10^3 V cm^{-1} 100 nm from the surface to ~ 10 V cm^{-1} 1 μm from the surface. These fields are similar in magnitude to those deduced from direct measurements of potential variations across a Au(111) surface using Kelvin force probe microscopy[1] and are sufficient to influence the outcome of many particle-surface interactions.

Research supported by the NSF and the Robert A. Welch Foundation.

REFERENCES

[1] H. R. Dunham, S. Wethekam, J. C. Lancaster, and F. B. Dunning, Nucl. Instrum. Meth. Phys. Res. B **256**, 46-49 (2007)

[2] Y. Pu, D. D. Neufeld, and F. B. Dunning, Phys. Rev. A, **81**, 042904 (2010)

* E-mail: dneuf2@rice.edu

EVOLUTION OF CARBON-BASED SURFACES USING DEUTERIUM BOMBARDMENT: CHARACTERISTICS OF THE STEADY STATE

M. Fallet[1,*] *and S. J. Stuart*[1]

[1] Department of Chemistry, Clemson University, Clemson, SC 29634, USA

1. ABSTRACT

Chemical sputtering and erosion at carbon-based surfaces is important for many applications such as astrophysics and plasma-surface interactions. We use molecular dynamics (MD) simulations to investigate the bombardment of carbon-based surfaces by deuterium (D) at conditions relevant for modeling the plasma-facing components in fusion devices.

Past MD simulations have examined chemical sputtering phenomena and have been compared to molecular beam and plasma experiments. The models have agreed with experiment, reproducing sputter yields for specific ejecta, and variation of sputter yields with impact energy. The total sputter yield, however, is often too large in simulations, particularly for ejecta containing three or more carbons.

Most of these simulations have modeled the sputtering of amorphous carbon (a-C:D) in an attempt to reproduce the steady-state surface conditions achieved in experiment after starting with graphite. We explicitly modeled the sputtering of both a-C:D and graphite, and find that the modified surface evolves differently in both cases.

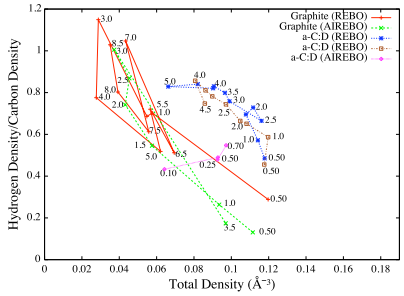

Figure 1: Evolution of the modified surface for graphite and a-C:D surfaces with the REBO and AIREBO potentials under bombardment by 20 eV D. Points are labeled by fluence in units of 1 x 10^{20} D m^{-2}

These differences are both structural and dynamic, and are observed in the depth of the modified surface, its composition, sputter yields and rates of erosion. The erosion of graphite at 20 eV occurs in a distinctly cyclic pattern, modifying and eroding successive layers rather than creating a modified surface which maintains a steady-state composition.

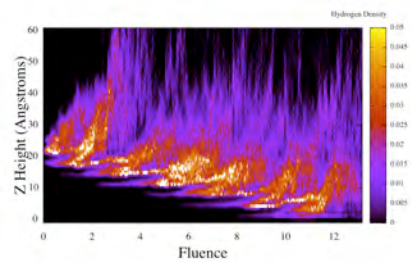

Figure 2: Evolution of hydrogen density in graphite impacted by 20 eV D with REBO.

We also test the assumption in most previous simulations that weak non-bonded interactions are not critical in modeling chemical sputtering in hard materials at energies of 20 eV and above. To this end, the sputtering behavior obtained using the chemically reactive REBO potential[1] is compared with that obtained using the related AIREBO potential[2], which includes non-bonded dispersion and repulsive interactions, but requires more computational effort. We find the composition of the surface as well as the sputtering behavior depend strongly on the model potential employed. The repulsive interactions in the AIREBO potential result in much higher scattering cross sections, as previously observed[3]. This leads to lower total sputtering yields with the AIREBO potential, in closer agreement with experiment. The structure of the modified surface is also different, with the higher cross sections under AIREBO leading to shallower modifications.

2. REFERENCES

[1] D.W. Brenner *et al.*, J. Phys.: Cond. Matt. **14**, 783 (2002).

[2] S.J. Stuart, A.B. Tutein, and J.A. Harrison, J. Chem. Phys. **112**, 6472 (2000).

[3] C.O. Reinhold *et al.*, J. Nucl. Mater. **401**, 1 (2010).

* E-mail: mfallet@clemson.edu

Electronic Interaction of Highly Charged Ions with Dielectric Covered Metal Surfaces

R. E. Lake[1,2,*], J. M. Pomeroy[1,2], and C. E. Sosolik[2]

[1] National Institute of Standards and Technology (NIST), Gaithersburg, MD USA 20899
[2] Department of Physics & Astronomy, Clemson University, Clemson, SC USA 29634

We present data and modeling for neutralization of highly charged ions (HCIs) on a metal surface covered with an ultrathin dielectric film. Besides being of interest in solid state device technology [1], studying HCI neutralization on a thin film/metal composite system may provide a more refined understanding of the electronic relaxation processes at surfaces [2].

To form the samples, amorphous aluminum oxide (a-Al_2O_3, thickness s = 1.5 nm) films were produced on Co and exposed to a total number of ions N of a single charge state of Xe^{q+} ($26 \leq q \leq 44$) with "slow" perpendicular velocities. The HCI irradiated surfaces were subsequently integrated into tunnel junction devices by depositing another Co electrode on top of the area bombarded with HCIs. This formed a crossed wire junction with the irradiated area sandwiched between two Co electrodes. The electrical conductance G through each tunnel junction was measured with a four point technique. $G(N)$ plots were made for each q, where $G(N) = \sigma_c N + G_0$ and G_0 is the undosed conductance of a device. The slope σ_c is interpreted as the average contribution from each ion of charge state q to the total increase in conductance. Within this $G(N)$ model, σ_c was found to increase by nearly four orders of magnitude for q values of 26 to 44 and ion potential energy was identified as the most important parameter in this observed trend.

To determine how the ion potential energy couples to the electronic system of the metal/insulator during neutralization, relative transfer probabilities for electrons originating from both the metal and dielectric thin film were calculated as a function of ion distance from the surface R over the range of q used in this study. The electrostatic potential for an "active electron" was constructed and the effect of image forces for the surface covered with a thin dielectric film were taken into account through the dielectric continuum model [3]. Within our model, the dielectric layer is parameterized by thickness, dielectric constant, band gap, and conduction and valence band minimum and maximum. Electron potential energies for two ion positions, R' and R'', are plotted in Figure 1. At R' the bands in the dielectric have been perturbed so that metal electrons at E_F can transport classically over the dielectric and vacuum potential barriers. There is still a significant tunnel barrier for valence band electrons with energy E'_{vbm}. At ion position R'', the electron's self-image has further decreased the vacuum barrier, but E''_{vbm} remains below the vacuum barrier peak. This indicates that neutralizing electrons originate preferentially from the metal.

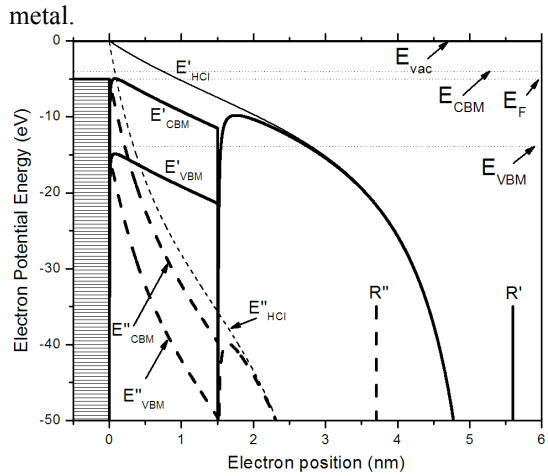

Figure 1: Potential energies for electrons when the HCI is at positions R'=5.6 nm (solid) and R''=3.7 nm (dashed) outside a dielectric covered metal surface.

Effective critical distances for the onset of neutralization in our calculation are presented and compared to the classical-over barrier [4] scenario for neutralization above clean metals. Surface modifications, as seen in our device conductance measurements (σ_c) are analyzed based on the prediction that the metal below the dielectric layer is the dominant source of electrons contributing to the neutralization.

REFERENCES

[1] J. M. Pomeroy, H. Grube, A. C. Perrella, J. D. Gillaspy, Appl. Phys. Lett. **91**, 073506 (2007).
[2] H. Khemliche, T. Schlathölter, R. Hoekstra, R. Morgenstern, S. Schippers, Phys. Rev. Lett. **81**, 1219 (1998).
[3] C. B. Harris, N.-H. Ge, R. L. Lingle, Jr., J. D. McNeill, Annu. Rev. Phys. Chem. **48**, 711 (1997).
[4] J. Burgdörfer, in *Review of Fundamental Processes and Applications of Atoms and Ions*, edited by C. D. Lin (World Scientific, New Jersey 1993), Ch. 11, p. 517.

* E-mail: russell.lake@nist.gov

Friday, October 1, 2010

VACUUMUNIVERSITY.COM

UNIVERSITY & NON-PROFIT VACUUM EXCLUSIVES!

LDS VACUUM PRODUCTS Longwood, Florida 32750
Phone: (407)862-4643 E-Mail: info@ldsvacuum.com

PARTICLE-INDUCED SURFACE PROCESSES IN THE SOLAR SYSTEM

T. M. Orlando[1,2*], *G. A. Grieves*[1] *and J. McLain*[1]

[1] School of Chemistry and Biochemistry and [2] School of Physics, Georgia Institute of Technology
Atlanta, Georgia 30332-0400 USA

Material degradation (i.e. space weathering) in our solar system is known to involve the interaction of solar-wind and magnetospheric particles (ions and electrons) with the surfaces of airless bodies. Since high energy particles create low-energy electrons, most non-thermal degradation/transformations result from the inelastic scattering of secondary electrons. Therefore the damage is inherently due to electronic excitations and the chemical products formed are often exotic and not easily produced under normal thermal conditions. This is true for complex targets such as minerals on planet, lunar and asteroid surfaces, as well as mixed low-temperature ices on outer solar system grains or within comets.

The role of electronic excitations in processing/weathering surfaces in the solar system and interstellar media are often examined directly using controlled low-energy electron-beam bombardment of complex targets under ultrahigh vacuum conditions. Since electronic excitations are known to localize at surfaces and lead to stimulated desorption, such events could be involved in forming tenuous atmospheres in the Jovian system, at Mercury and near asteroids. As an example, an overlooked and perhaps important mechanism for releasing material to Mercury's neutral and ionized exosphere and near-space environment is electron-stimulated desorption (ESD) [1]. This well known process involves excitation (often with ionization) of a surface target followed by charge ejection, bond breaking, and ion expulsion due to the resultant Coulomb repulsion.

Results from the Moon Mineralogy Mapper (M^3) on the Chandrayaan-1 spacecraft, the Visual and Infrared Mapping Spectrometer (VIMS) on Cassini during its flyby of the moon in 1999, and the extended mission for the Deep Impact Spacecraft (EPOXI) have recently implicated the existence of hydroxyl and water on the Moon [2-4]. More recently, the potential presence of water on and within the surface regolith material of the Moon was further validated by the Lunar Crater Observation and Sensing Satellite (LCROSS) impact event. LCROSS examined ejecta from a permanently-shadowed crater in the southern polar region, whereas the spacecraft observations characterized optical features in the 2-3.5 micron region throughout the polar and equatorial regions on the sunlit side. These optical features are thought to be indicative of hydroxyl and/or water-bearing materials with concentrations between 10 – 1000 parts per million and possibly higher. Though the source(s) of the hydroxyl and water is (are) not known, their formation via solar wind proton irradiation has been strongly suggested. There is precedent in the literature for proton irradiation-induced defect production and hydroxyl formation in silicates and some minerals. However, ***there are actually no reports that clearly indicate that proton irradiation leads to the formation of molecular water***.

Finally, for mixed ices found in the outer solar system, complicated chemistry occurs such as the formation of CO, CO_2, CH_3OH as well as the formation of complex hydrocarbons. The sources of these molecules are not known and the chemistry is too complicated to occur via simple addition reactions. The spatial deposition of energy and the transport of this energy to trapped molecules and buried interfaces during irradiation must be considered. CO and CO_2 are likely formed by proton- or electron-beam induced production of reactive O atoms at the graphite grain interface. Water is the source of the atomic oxygen and the presence of even sub-monolayer quantities of water greatly enhances the stimulated removal of hydrocarbons from these grains.

Experimental activities in low-energy (5-50 eV) electron and 5 keV proton induced processes on minerals characteristic of Mercury and Earth's moon will be emphasized. Specifically, we examine i) the role of ESD in contributing to the formation of Mercury's exosphere, ii) the stimulated removal of water and the purported formation of lunar water via ion-beam impact of lunar simulants, and iii) the formation of H_2,[5] O_2,[6] CO_2, CO and hydrocarbon fragments during the irradiation of nanoscale ice films on graphitic surfaces reminiscent of interstellar grains.

[1] J. McLain, G. A. Grieves, A. Sprague, D. Schriver, P. Travinicek. and T. M. Orlando, submitted *J. Geophys. Res*.
[2] C. M. Pieters, et. al., *Science*, **326**, 568 (2009).
[3] R. N. Clark, *Science*, **326**, 562 (2009).
[4] J. Sunshine, et. al., *Science*, **326**, 565 (2009).
[5] G.A. Grieves and T.M. Orlando, *Surf. Sci.* **593**, 180 (2005), M.T. Sieger, W.C. Simpson, and T.M. Orlando, *Nature* **394**, 554 (1998).

* E-mail: thomas.orlando@chemistry.gatech.edu

SOLAR WIND SPUTTERING OF LUNAR SURFACE MATERIALS: Role and Some Possible Implications of Potential Sputtering

A.F. Barghouty[1,], J.H. Adams, Jr. [1], F.W. Meyer[2], P.R. Harris[2], and H.M. Meyer II[2]*

[1]NASA-Marshall Space Flight Center, Huntsville, AL 35812
[2]Oak Ridge National Laboratory, Oak Ridge, TN 37831

1. INTRODUCTION

Lunar surface sputtering yields are important as they affect the compositional changes in the lunar surface, its erosion rate, as well as its contribution to the exosphere. They can also affect estimates of the hydrogen and water contents on the lunar surface.

Solar-wind induced sputtering of the lunar surface includes both kinetic and potential sputtering. Role of potential sputtering (associated more with heavy ions) in has not been properly ascertained. This is partly due to lack of data, but it can also be attributed to the assertion that the contribution of solar-wind heavy ions to the total sputtering yield is expected to be quite low due to their low number densities compared to solar-wind protons. Limited laboratory measurements [1], however, show marked enhancements in the sputter yields of slow-moving, highly-charged ions impacting oxides.

The typical range of solar-wind ions at ~1 keV/amu is a few tens of nm, which is comparable to the thickness of the amorphous rim found on lunar soil grains [2]. Most laboratory studies of potential sputtering were carried out in single crystal targets, which are quite different from the rim's amorphous structure. It is critical to measure potential sputter yields from lunar regolith analogs with this structure.

2. POTENTIAL vs. KINETIC SPUTTERING

The enhancements seen in the laboratory can be orders of magnitude for some surfaces and highly charged incident ions, but they depend sensitively on the properties of the impacted surface in addition to the fluence, energy and charge of the impacting ions [1]. For oxides, potential sputtering yields are markedly enhanced and sputtered species, especially hydrogen and light ions, show marked dependence on both charge and dose.

Potential sputtering data for lunar regolith simulant JSC-1A – AGGL from ongoing experiments [3,4] at ORNL's MIRF facilities are expected to be available soon.

In anticipation of these new measurements, this talk explores possible implications to lunar surface and exosphere compositions due to enhanced sputter yields associated with potential sputtering. It will also allude to implications of preferential sputtering, characteristic of potential sputtering.

3. POSSIBLE IMPLICATIONS

Since the penetration depth of solar-wind ions is comparable to the thickness of the vapor-deposited layer found on lunar regolith particles, the properties and composition of this layer is expected to play a critical role in how the solar-wind ions couple to the lunar surface, dynamically and at various scales.

For certain lunar surface constituents, sputtering may change their stoichiometry and/or chemical composition. Depending on the sputtered species energy and charge state, some are lost to space, while others become part of the lunar exosphere or return to the lunar surface.

A possible implication of this coupling along with potential sputtering [1] is that the surface erosion rate [5] would increase proportionally leading to efficient mixing.

Also, if sputtering selectivity is dominated by potential sputtering, surface composition may have mineral depletions or enrichments that are difficult to reconcile with estimates based on kinetic sputtering alone.

Other implications of enhanced sputtering relate to hydrogen and ice deposits on the moon. Such estimates have been shown [5] to depend sensitively on both efficient erosion and preferential sputtering.

4. REFERENCES

[1] F. Aumayr and H. Winter, Phil. Trans. R. Soc. (London) A 362, 77-102 (2004).
[2] L.P. Keller and D.S. Mckay, Geochimica et Cosmochimica Acta, 61, 2331-2341 (1997).
[3] P.R. Harris et al., SELAC Workshop, Dust & Ice: Their Roles in Astrophysical Environments March 2010, Athens, Georgia.
[4] F.W. Meyer et al., these proceedings.
[5] L.V. Starukhina, Sol. Phys. Res. 37, 36-50, (2003).

* E-mail: abdulnasser.f.barghouty@nasa.gov

STEREODYNAMICAL CONTROL OF SURFACE CHEMISTRY WITH ORIENTED MOLECULAR BEAMS

Michio Okada[*]

Renovation Center of Instruments for Science Education and Technology, Osaka University,
Mihogaoka 8-1, Ibaraki, Osaka 567-0047 and 1-2 Machikaneyama-cho, Toyonaka, Osaka 560-0043, JAPAN

One of the ultimate goals of surface science is to be able to design surfaces with particular catalytic reactivity. This entails a need for an atomic-level understanding of the fundamental principles (elementary processes) underlying the bond-making and bond-breaking at surfaces. It is expected that the orientation of a molecule incoming on the surface may play an important role in such elementary processes. We have been developing new machines with ultra-high-vacuum (UHV) compatible oriented-molecular beam apparatuses [1, 2] in order to investigate for the initial molecular-orientation effects of an incoming molecule on the surface chemical reactions, as shown in Fig. 1. Here, we introduce the steric effects, especially on Si surfaces, recently observed with these new machines.

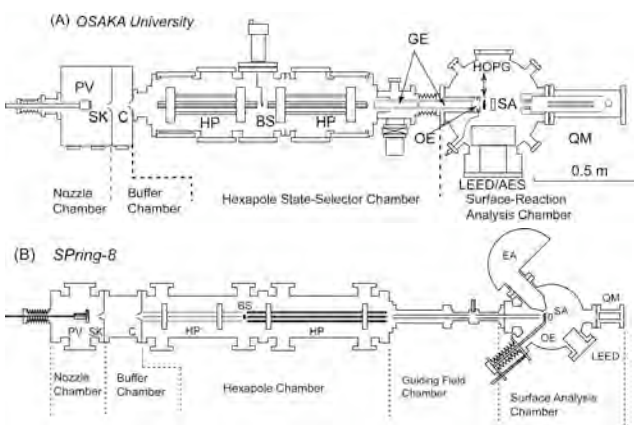

Figure 1: Oriented molecular beam at (A) Osaka University and (B) SPring-8.

We report results of a study on the incident-energy and the surface-temperature dependence of the steric effects in the dissociative adsorption of CH_3Cl on a Si(100) surface. The initial sticking probability of CH_3Cl on Si(100) was measured by the King-Wells method [1, 3]. Data presented in Fig. 2 show that the initial sticking probability for the Cl-end collision is larger at an incident energy of 120 meV than that in the CH_3-end collision. Furthermore, the observed steric preference is quite sensitive to the kinetic energy, the rotational state of CH_3Cl and the surface temperature. This study demonstrates that the transient surface trapping plays a

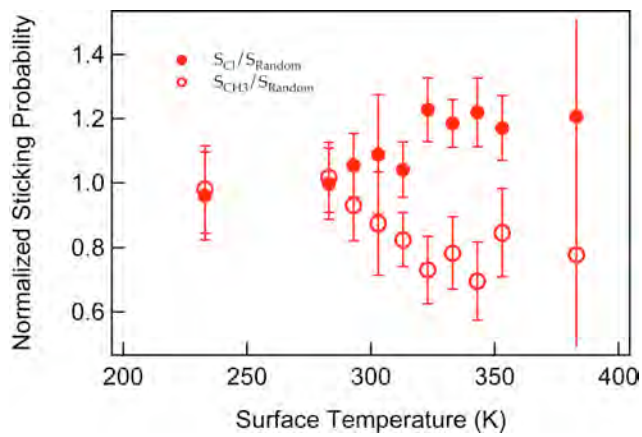

Figure 2: Molecular orientation dependence of the initial sticking probability of CH_3Cl on Si(100)

key role in the initial step of the decomposition of CH_3Cl on Si(100). The scattering experiments on oriented CH_3Cl from HOPG and Si(111) (weakly bound systems) also demonstrate the importance of such transient surface trapping in the observed steric effects [4, 5].

We also introduce the experiments using apparatus (Fig. 1(B)) equipped with the oriented-molecular beam line and the reaction chamber for X-ray photo-emission spectroscopy [2, 6]. In the reaction of oriented NO molecules with Si(111), we found that the N-end collision is more effective in the dissociative adsorption than the O-end collision.

REFERENCES

[1] M. Okada et al., Japanese Journal of Applied Physics, **44**, 8580 (2005).
[2] M. Okada et al., Japanese Journal of Applied Physics, **47**, 3686 (2008).
[3] M. Okada et al., Physical Review Letters, **95**, 176103 (2005).
[4] T. Fukuyama, M. Okada et al., Journal of Physical Chemistry A, **113**, 14749 (2009).
[5] H. Ito, M. Okada et al., Journal of Physical Chemistry A, **114**, 3080 (2010).
[6] M. Hashinokuchi, M. Okada, et al., Physical Review Letters, **100**, 256104 (2008).

[*] E-mail: `okada@chem.sci.osaka-u.ac.jp or mokada@cw.osaka-u.ac.jp`

Determining Concentration Depth Profiles in Thin Foam Films with Neutral Impact Collision Ion Scattering Spectroscopy

*C. Ridings and G. Andersson**

Centre for NanoScale Science and Technology, Flinders University, SA, 5001, Australia

1. INTRODUCTION

Understanding the structure and dynamics of foam films is of interest in flotation, producing emulsions and in food processing. Self supported foam films are stabilised through the adsorption of surfactants at the surface of the foam films. The stability is given by the equilibrium of the internal and external pressure [1]. The internal pressure is the sum of repulsive electrostatic forces, attractive van-der-Waals forces and steric forces. The van-der-Waals forces can be described through empirical models based on measurements with the surface force apparatus. Describing the electrostatic forces is based on standard models in colloid science. Describing steric forces no agreement has yet been achieved in the scientific community though they are of importance.

All three forces depend on the concentration depth profiles of the constituents. However, so far concentration depth profiles in foam films at equilibrium could not be measured directly and thus have been approximated with models. However, so far it was not possible to proof, whether these models describe the structure in foam films. Here we show how the vacuum based method Neutral Impact Collision Ion Scattering Spectroscopy (NICISS) can be used to determine the concentration depth profiles directly.

2. Experimental Work

Concentration depth profiles of the elements in a thin foam film made from a solution of glycerol and the cationic surfactant hexadecyltrimethylammonium bromide (C16TAB) were measured. The measured concentration depth profiles are used to compare the charge distribution in foam films with the charge distribution at the surface of a bulk solution. A greater charge separation was observed at the films' surface compared to the bulk surface which implies a greater electrostatic force contribution to the stabilisation of thin foam films. This feature of foam films could not yet be derived from the existing models for foam films.

We have developed a film holder based on the design of those used for TFPB measurements [2]. The film holder consists of a micro-porous glass disc with a glass capillary fused to one side such that the solution is able to flow from the capillary into the disc. Additionally, a small aperture (of radius, r = 2 mm) is drilled through the disc. The solution is filled through the capillary, upon which it soaks through the disc. When removing the film holder from the solution, a foam film is formed over the aperture.

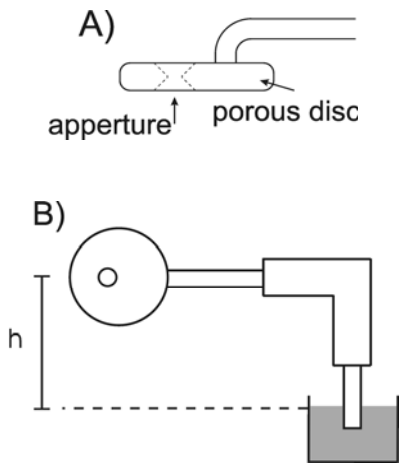

Figure 1: Figure 1A shows the schematic of the film holder viewed from top with the glass capillary fused to the back of the porous disc. Figure 1B is a front view and details the schematic for applying an underpressure over the film. The filled capillary is connected to a beaker. The difference between the level of solution in the beaker and the height of the film is proportional to the pressure applied.

In order to reduce the evaporation from the film, the film holder is placed in a pressure cell. The pressure cell is designed to hold the film holders while reducing the amount of evaporation of solvent from the film holders.

3. REFERENCES

1 V. Bergeron, J. Phys Condens. Matter 11 (1999) R215.
2 C. Stubenrauch and R. v. Klitzing, Journal of Physics: Condensed Matter (27), R1197 (2003).

* E-mail: gunther.andersson@flinders.edu.au

CHARACTERIZATION OF SURFACE STRUCTURE IN REAL SPACE USING LOW ENERGY ION SCATTERING AND RECOIL MAPS

R. D. Kolasinski[*], *J. A. Whaley*, *R. A. Karnesky*, *C. San Marchi*, and *R. Bastasz*

Sandia National Laboratories, Hydrogen and Metallurgical Science Department, Livermore, CA 94550

1. INTRODUCTION

Low energy ion scattering (LEIS) and direct recoil spectroscopy (DRS), because of their high surface specificity, are well suited for characterizing the behavior of atoms adsorbed on surfaces. Of particular interest is how hydrogen binds to single crystal surfaces, where LEIS and DRS often are the only practical methods of directly detecting the adsorbate configuration. A necessary first step in this process includes characterizing the complex collision processes which contribute to the detected scattering and recoil intensities. We have previously developed techniques for accomplishing this task by constructing maps of scattering intensity and making quantitative comparisons with modeling results [1]. Such maps are also particularly useful for elucidating local atomic surface structure. In this work, we describe how these techniques can be used to examine a variety of single crystal surfaces, particularly the Al(111)+H system which is emphasized herein.

2. EXPERIMENTAL AND SIMULATION RESULTS

In this study, low energy (500 eV - 3 keV) Ne^+ and He^+ ion beams were used to probe the surface. Using an angle-resolved ion energy spectrometer (ARIES), forward-scattered and recoiled ions were collected using a hemispherical energy analyzer. We have found the binary collision code MARLOWE to be particularly effective for simulating complex surface scattering processes. As discussed in Ref. [1], we developed a modified version of this program specifically suited for LEIS and DRS simulations.

Ion scattering maps were compiled from scattering data acquired for a wide range of incidence angles (α) and azimuths (φ). (See Fig. 1 inset.) Under appropriate conditions, these maps can be rendered in real-space by taking into account shadow cone intersections with neighboring atoms [2].

Consider Fig. 1(a), which shows a quadrant from an experimental scattering map constructed by monitoring the energy associated with a single elastic collision of Ne^+ from Al. The scattering intensity patterns produced by this process are roughly parabolic in shape, and are reproduced well by the MARLOWE simulations shown in Fig. 1(b). The regions of highest scattering intensity correspond largely to the atom positions indicated by the circular markers and the calculated curves shown in the overlay of Fig. 1(c). Near the periphery of the maps, scattering is enhanced indicating conditions are favorable for focusing along atom rows.

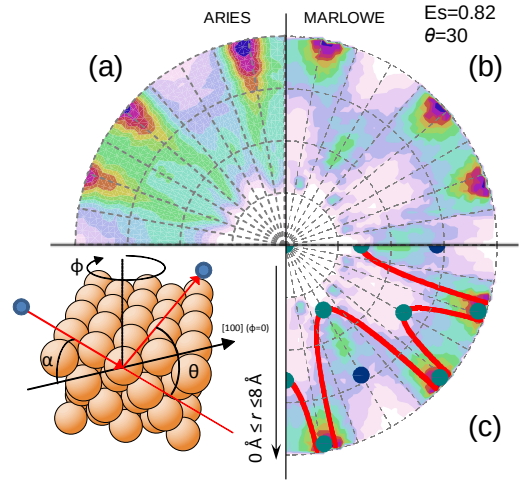

Figure 1: Experimental (a) and simulated (b) real-space ion scattering maps of the Al(111) surface. The predicted intensity patterns and corresponding atom positions are indicated in (c).

Scattering maps therefore provide a wealth of information on the surface structure, as well as prominent focusing effects. We expect that such techniques can be readily extended to examining the configuration of adsorbates and compound surfaces.

3. REFERENCES

[1] R. D. Kolasinski, J. A. Whaley, and R. Bastasz, Phys. Rev. B **79**, 075416 (2009).

[2] R. G. Agostino, P. Aebi, J. Osterwalder, J. Hayoz, and L. Schlapbach, Surf. Sci. **384**, 36 (1997).

Sandia is a multiprogram laboratory operated by Sandia Corporation, a Lockheed Martin Company, for the United States Department of Energy's National Nuclear Security Administration under Contract DE-AC04-94AL85000.

[*] E-mail: rkolasi@sandia.gov

STRUCTURE AND COMPOSITION OF HIGH-K MATERIALS ON NOVEL SUBSTRATES

Torgny Gustafsson

Department of Physics and Astronomy, Rutgers University, Piscataway, NJ 08854, USA

Medium Energy Ion Scattering (MEIS) has been very successfully applied to the study of oxidation and interface structure of silicon. This topic was of central importance for understanding the performance of microelectronic devices as silicon oxide is used as an insulator in such circuits. As the size of these devices was scaled down, these insulating SiO_2 layers became too thin, and the focus for the microelectronics industry is therefore changing to materials with higher dielectric constant ("high-k") that could be made thicker. MEIS results have made major contributions in making high-k materials a commercial reality. In the ever increasing push towards even smaller devices, this community is now directing its attention in part to substrate materials with better performance (higher channel mobilities) than Si, such as Ge, GaAs and InGaAs. The removal of native oxides and the growth an ideal dielectric layer on these materials remain serious challenges. It is known that chemical cleaning and subsequent passivation of the interface prior to dielectric deposition can greatly reduce the interface state density (D_{it}). We have used atomic layer deposition (ALD) to obtain detailed structural and chemical information about the interface and reduction processes when high-k materials are deposited on GaAs and Ge. We have determined depth profiles of the elements with an integrated tool that enables ALD growth with *in situ* characterization by MEIS. Films were also analyzed by x-ray photoelectron spectroscopy (XPS). Our results show the existence of a preferential interface reduction of native oxides (especially AsO), which helps create a higher capacitance, lower interface defect density CMOS gate stack.

We will also present results on the interface structure of an epitaxial layer of $AlLaO_3$ on $SrTiO_3$. Others have shown that this combination of two insulators surprisingly exhibits a free electron-like interface layer of charge, giving rise to various unexpected phenomena such as superconductivity. Our data show that this system exhibits massive interdiffusion, which helps to elucidate the origin of these spectacular properties. It also serves as a nice example of the importance of sub-nanometer level depth profiling.

Acknowledgments

Work done with L. Goncharova, T. Feng, H. D. Lee, D. Mastrogiovanni, A.Wan, L. Yu, E. Garfunkel and S. Chambers and supported by the National Science Foundation and the Semiconductor Research Corporation.

A PASSION FOR PERFECTION

PFEIFFER VACUUM

Perfect vacuum solutions

Leading. Dependable. Customer Friendly.

Pfeiffer Vacuum stands for innovative custom vacuum solutions worldwide.
Well renowned German engineering, competent advice, and reliable service and support.
Ever since we invented the turbopump, we've been setting industry standards.

Are you looking for a perfect vacuum solution?
Please contact us:

Pfeiffer Vacuum Inc.
24 Trafalgar Square · Nashua · NH 03063
Phone: 800-248-8254 · Fax: 603-578-6550
contact@pfeiffer-vacuum.com
www.pfeiffer-vacuum.com

AUTHOR INDEX

Abufager, P.N. 48
Acuña, M. A. 38
Adams Jr., J.H. 90
Alducin, M. 43
Allain, J.P. 40, 52, 59, 76
Álvarez Soria, H.L. 47, 48
Amekura, H. 6
Andersson, G. 92
Andrzejewski, R. 50
Araujo, L.L. 6
Archubi, C. 39
Arjad, A.B. 60
Aumayr, F. 4, 23, 29, 68
Ayyad, A. 67
Baragiola, R.A. 54
Barghouty, A.F. 90
Bastasz, R. 93
Bauer, P. 13, 36, 44, 50, 51, 53
Bekker, H. 23
Belov, A.I. 61
Bereczky, R.J. 67,68
Bernard, A. 41
Björkas, C. 19
Blauth, D. 58
Bobisch, C. 41
Bocán, G. 37
Bodewits, E. 23
Briner, C.A 21, 24, 30
Buchsbaum, A. 10
Bundaleski, N. 31, 80
Buntov, E.A. 61
Burgdörfer, J. 65, 83
Busch, M. 20, 82
Busnengo, H.F. 48
Byrne, A.P. 6
Cederquist, H. 20
Chakraborty, P. 25
Chen, L. 16
Clever, M. 66
Cook, E.L. 24, 32
Crespo López-Urrutia, J.R. 4
Dadras, J. 33, 35, 59
Daniel, B. 23
Das, S. 67
Dassanayake, B.S. 34, 67
de Nijs, A.J. 23
De Silva, G.G. 34
Diaz, C. 70
Diesing, D. 11, 41
Díez Muiño, R. 37, 43
Dobes, K. 23
Doerner, R.P. 73
Dufour, C. 4
Dukes, C.A. 8
Dunning, F.B. 84
Duvenbeck, A. 57
Efrosinin, D.V. 50
Ehemann, R.C. 35
El-Atwani, O. 52
El-Said, A.S. 29
Entani, S. 9
Ertl, K. 74
Esaulov, V.A. 16
Fallet, M. 85
Fascko, S. 29
Ferrón, J. 8
Fhur, J. 16
Fichtner, P.F.P 6
Garrison, B.J. 24, 30, 32
Geethalakshmi, K.R. 43
Ghosh, B. 25
Ginzel, R. 4
Giulian, R. 6
Göbl, D. 13, 36
Gonzalez, M. 76
Gravielle, M.S. 37, 38, 39, 81
Grieves, G.A. 89
Grube, H. 12
Giulian, R. 6
Gustafsson, T. 94
Gutierrez, F.A. 15
Hamagaki, M. 66
Hanke, S. 57
Harris, P.R. 49, 78, 90
He, X. 26
Heim, B. 40, 52, 76
Heller, R. 29
Heuser, C. 41
Hoekstra, R. 23
Hoen, M.H.J. ‘t 74
Hopf, C. 77
Ikeda, T. 66
Imamoto, N. 66
Irle, S. 42
Ivanović, N. 31
Jacob, W. 77, 78
Jakowski, J. 42
Jouin, H. 55
Juaristi, J.I. 43
Kanai, Y. 66
Karlusić, M. 15
Karnesky, R.A. 93

AUTHOR INDEX

Keerthisinghe, D. 34
Kent, P.R.C. 59
Khalal-Kouache, K. 44
Khemliche, H. 80
Kimura, K. 7, 45
Kirschner, J. 56
Klein, Ch. 10
Kleyn, A.W. 74
Kluth, P. 6
Kobayashi, T. 66
Kojima, T.M. 66
Kolasinski, R.D. 93
Köppen, M. 46
Kortov, V.S. 61
Koshikawa, T. 69
Kowarik, G. 4, 23, 68
Krantzman, K.D. 21, 24, 30, 32
Krasheninnikov, A.V. 14
Kremer, F. 6
Kreter, A. 79
Krstić, P.S. 33, 35, 59
Kucher, A. 21
Kurahashi, M. 9
Ladinig, F. 68
Lake, R.E. 12, 86
Lasa, A. 19
Lebius, H. 3, 4
Lemell, C. 83
Linsmeier, Ch. 20, 46, 75
Llewellyn, D.J. 6
Macé, A. 68
Maekawa, S. 45
Maeshima, K. 66
Markin, S.N. 13, 50, 53
Marpe, M. 41
Martiarena, M.L. 16, 47, 48
Martin, F. 70
Maunoury, L. 4
Mayer, M. 74
McLain, J. 89
Medvedev, N. 5
Mehine, M. 19
Meinander, A. 19
Meissl, E. 66
Meissl, W. 66
Merck, J. 20
Meyer, F.W. 49, 78, 90
Meyer III, H.M. 49, 90
Mihailov, A.N. 61
Miraglia, J.E. 81
Miskovic, Z.L. 22
Miyamoto, S. 66
Möller, R. 41
Momeni, A. 80
Monreal, R.C. 36
Morokuma, K. 42
Nakajima, K. 7, 45
Neufeld, D.D. 84
Nilius, N. 58
Nordlund, K. 19
Oberkofler, M. 46, 75
Ogiwara, K. 66
Okada, M. 91
Orlando, T.M. 89
Ortoleva, S. 40, 52
Osmani, O. 5
Pagura, C. 31
Papaléo, R.M. 4
Peters, T. 55
Petersson, P. 79
Phan, T.-V. 46
Platzgummer, E. 10
Pomeroy, J.M. 12, 86
Possnert, G. 79
Pratt, A. 9
Primetzhofer, D. 13, 36, 44, 50, 51, 53
Pruneda, J.M. 81
Pu, Y. 84
Radisavljević, I. 31
Rapp, J. 74
Rethfeld, B. 5
Reuter, K. 48
Ridgway, M.C. 6
Ridings, C. 92
Ritter, R. 4, 10
Rizza, G. 6
Rokusek, D.L. 52
Roncin, P. 80
Ruano, G. 8
Rubel, M. 79
Rund, S. 13, 53
Rupp, W. 4, 10
Ruth, M. 55
San Marchi, C. 93
Scheer J.A. 8
Schleberger, M. 3, 5, 15
Schlüter, M. 77
Schmid, M. 10
Schüller, A. 81, 82
Schury, P.H. 66
Schwarz-Selinger, T. 77, 78
Seifert, J. 82

AUTHOR INDEX

Sha Zaman, S. 10
Shen, Q. 4
Silkin, V.M. 39
Sosolik, C.E. 12, 86
Soulisse, P. 80
Specht, U. 20, 82
Spitz, M. 13
Sprouster, D.J. 6
Steinbauer, E. 50
Stradi, D. 70
Stuart, S.J. 85
Sun, X. 9
Suzuki, M. 7, 45
Suzuki, T. 7, 9
Takagi, S. 45
Tanis, J.A. 34, 67
Taylor, C.N. 40, 49, 76
Teichert, C. 4
Tetelbaum, D.I. 61
Tiwald, P. 83
Tökési, K. 66, 67, 68
Tolstogouzov, A. 31
Toulemonde, M. 4, 6
Trautmann, C. 29
Tusche, C. 56
Ullrich, J. 4
Valdés, D. 36
Varga, P. 10
Vasko, C. 4
Vidal, R.A. 8
von Toussaint, U. 78
Vörtler, K. 19
Wada, M. 66
Weidtmann, B. 57
Wethekam, S. 20, 82
Whaley, J.A. 93
Winklehner, D. 23
Winograd, N. 21
Winter, H. 20, 58, 81, 82
Wright , G.M. 74
Wucher, A. 21, 24, 32, 41, 57
Wurz, P. 54
Yamauchi, Y. 9
Yamazaki, Y. 66
Yang, Z.C. 59
Yarmoff, J.A. 26, 60
Zatsepin, A.F. 61
Zeijlmans van Emmichoven, P.A. 74
Zettergren, H. 20
Zigon, D. 40, 76

18th International Workshop on Inelastic Ion-Surface Collisions

September 26 – October 1, 2010

List of Participants and accompanying persons

Allain, Jean Paul	United States	allain@purdue.edu
Andersson, Gunther	Australia	gunther.andersson@flinders.edu.au
Aumayr, Friedrich	Austria	aumayr@iap.tuwien.ac.at
Barghouty, Abdulnasser	United States	abdulnasser.f.barghouty@nasa.gov
Baragiola, Raul	United States	raul@virginia.edu
Baragiola, Beatriz	United States	
Bauer, Peter	Austria	peter.bauer@jku.at
Bodewits, Erwin	Netherlands	ebodewits@kvi.nl
Briner, Clarissa	United States	cabriner@edisto.cofc.edu
Bundaleski, Nenad	Portugal	n.bundaleski@fct.unl.pt
Burgdoerfer, Joachim	Austria	burg@concord.itp.tuwien.ac.at
Chakraborty, Purushottam	India	purushottam.chakraborty@saha.ac.in
Cook, Edward	United States	elcook@edisto.cofc.edu
Dadras, Mostafa	United States	jonny@utk.edu
Dassanayake, Buddhika	United States	b5senarathda@wmich.edu
Diaz, Cristina	Spain	cristina.diaz@uam.es
Diesing, Detlef	Germany	detlef.diesing@uni-due.de
Doerner, Russell	United States	rdoerner@ucsd.edu
Ehemann, Robert	United States	rcehemann@gmail.com
Fallet, Marcel	United States	mfallet@clemson.edu
Giulian, Raquel	Australia	raq109@physics.anu.edu.au
Gšbl, Dominik	Austria	dominik.goebl@jku.at
Gravielle, Maria	Argentina	msilvia@iafe.uba.ar
Gustafsson, Torgny	United States	gustaf@physics.rutgers.edu
Gustafsson, Ingrid	United States	
Harris, Peter	United States	harrispr@ornl.gov
Havener, Charles	United States	havenercc@ornl.gov
Heim, Bryan	United States	bheim@purdue.edu
Heuser, Christian	Germany	Christian.Heuser@uni-due.de
Hillis, Donald	United States	hillisdl@ornl.gov
Hoekstra, Ronnie	Netherlands	hoekstra@kvi.nl
Jakowski, Jacek	United States	jjakowsk@utk.edu
Jouin, Herve	France	herve@celia.u-bordeaux1.fr
Juaristi, Joseba	Spain	josebainaki.juaristi@ehu.es
Khalal-Kouache, Karima	Algeria	kkouache@yahoo.fr
Kimura, Kenji	Japan	kimura@kues.kyoto-u.ac.jp
Kolasinski, Robert	United States	rkolasi@sandia.gov
Koshikawa, Takanori	Japan	kosikawa@isc.osakac.ac.jp
Krantzman, Kristin	United States	krantzmank@cofc.edu

Krasheninnikov, Arkady	Finland	akrashen@acclab.helsinki.fi
Krause, Herbert	United States	krausehf@ornl.gov
Krstic, Predrag	United States	krsticp@ornl.gov
Lake, Russell	United States	russell.lake@nist.gov
Lebius, Henning	France	lebius@ganil.fr
Linsmeier, Christian	Germany	christian.linsmeier@ipp.mpg.de
Martiarena, Maria	Argentina	mlmartiarena@gmail.com
Meissl, Walter	Japan	meissl@riken.jp
Meyer, Fred	United States	meyerfw@ornl.gov
Miskovic, Zoran	Canada	zmiskovi@uwaterloo.ca
Murphy, Michael	United States	michael.murphy@oerlikon.com
Nakajima, Kaoru	Japan	kaoru@kues.kyoto-u.ac.jp
Neufeld, Dennis	United States	dneuf2@rice.edu
Nordlund, Kai	Finland	kai.nordlund@helsinki.fi
Oberkofler, Martin	Germany	martin.oberkofler@web.de
Okada, Michio	Japan	okada@chem.sci.osaka-u.ac.jp
Orlando, Thomas	United States	thomas.orlando@chemistry.gatech.edu
Osmani, Orkhan	Germany	orkhan.osmani@uni-due.de
Ownby, Fay	United States	ownbyfm@ornl.gov
Pomeroy, Joshua	United States	joshua.pomeroy@nist.gov
Primetzhofer, Daniel	Austria	daniel.primetzhofer@jku.at
Reinhold, Carlos	United States	reinhold@ornl.gov
Ritter, Robert	Austria	ritter@iap.tuwien.ac.at
Rokusek, Dan	United States	drokusek@purdue.edu
Rubel, Marek	Sweden	rubel@kth.se
Rund, Stefanie	Austria	stefanie.rund@jku.at
Saddiq, Lynda	United States	saddiqlh@ornl.gov
Scheer, Juergen	Switzerland	jscheer@space.unibe.ch
Schleberger, Marika	Germany	marika.schleberger@uni-due.de
Schwarz-Selinger, Thomas	Germany	Thomas.Schwarz-Selinger@ipp.mpg.de
Sosolik, Chad	United States	sosolik@clemson.edu
Stroetenga, Suzanne	Netherlands	
Stuart, Steven	United States	ss@clemson.edu
Tanis, John	United States	john.tanis@wmich.edu
Taylor, Chase	United States	jones41@purdue.edu
Tiwald, Franz Paul	Austria	paul@dollywood.itp.tuwien.ac.at
Tusche, Christian	Germany	tusche@mpi-halle.mpg.de
Varga, Peter	Austria	varga@iap.tuwien.ac.at
Weidtmann, Boris	Germany	boris.weidtmann@uni-due.de
Wells, Jack	United States	wellsjc@ornl.gov
Wethekam, Stephan	Germany	stephan.wethekam@physik.hu-berlin.de
Winter, Helmut	Germany	winter@physik.hu-berlin.de
Wucher, Andreas	Germany	andreas.wucher@uni-due.de
Yamauchi, Yasushi	Japan	yamauchi.yasushi@nims.go.jp
Yang, Zhangcan	United States	yang123@purdue.edu
Yarmoff, Jory	United States	yarmoff@ucr.edu
Zatsepin, Anatoly	Russia	zats@dpt.ustu.ru
Zeijlmans van Emmichoven, Pedro	Netherlands	p.a.zeijlmans@rijnhuizen.nl

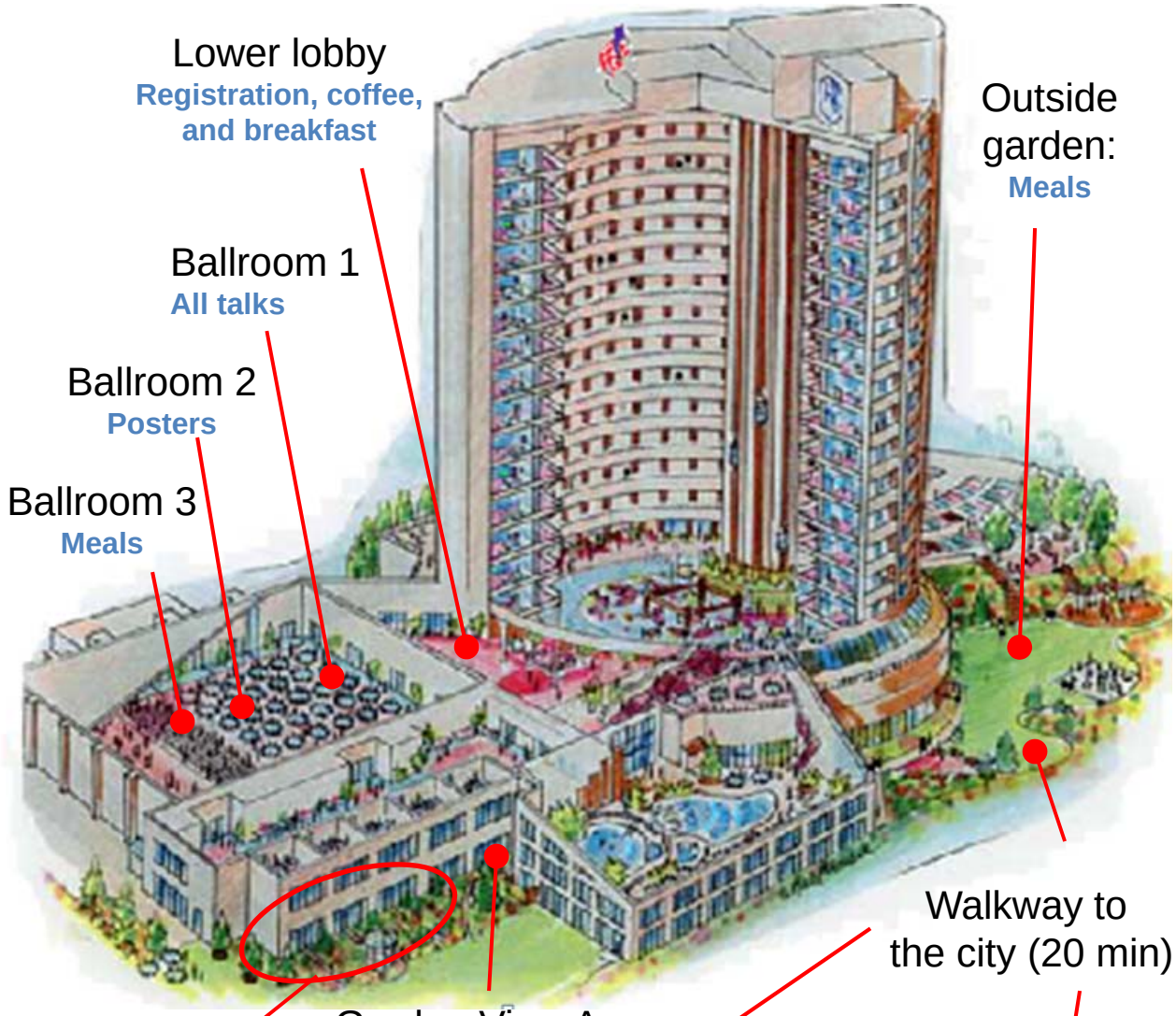

Walkway to the city (20 min)

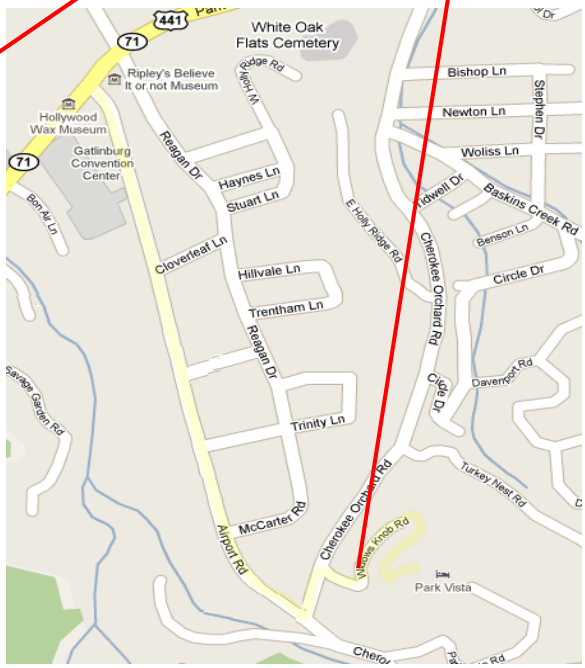

18th International Workshop on Inelastic Ion-Surface Collisions (IISC-18)

September 26 – October 1, 2010

Gatlinburg, Tennessee, USA

(S) Selected Contrib.: 15 + 5 min
(R) Progress Report: 25 + 5 min
(P) Plenary: 40 + 5 min

Sunday Sept. 26, 2010

14:00 Registration

19:00 Welcome Dinner (Outside garden)
Speakers: Reinhold, Meyer, Krstic

Monday Sept. 27, 2010

7:30 Breakfast

08:30–08:45 Opening
08:45–09:30 Lebius (P)
09:30–10:00 Ritter (R)

10:00 – Coffee Break

10:30–11:00 Osmani (R)
11:00–11:30 Giulian (R)
11:30–12:00 Nakajima (R)
12:00–12:20 Scheer (S)

12:20 – Lunch (Garden View)

14:20–14:50 Yamauchi (R)
14:50–15:10 Varga (S)
15:10–15:40 Diesing (R)
15:40–16:00 Pomeroy (S)

16:00 – Coffee Break

16:30–17:00 Bauer (R)
17:00–17:30 Krasheninnikov(R)
17:30–17:50 Schleberger (S)
17:50–18:10 Martiarena (S)

20:00 Committee Meeting

Tuesday Sept. 28, 2010

7:30 Breakfast

08:30–09:15 Nordlund (P)
09:15–09:45 Wethekam(R)
09:45–10:05 Wucher (S)

10:05 – Coffee Break

10:30–11:00 Miskovic (R)
11:00–11:30 Bodewits (R)
11:30–11:50 Krantzman(S)

11:50 – Lunch (Garden View)

14:00–14:20 Chakraborty(S)
14:20–14:40 Yarmoff (S)
14:40 Poster Introduction

Poster Session (Ballroom 2)

Wednesday Sept. 29, 2010

7:30 Breakfast

08:30– 09:15 Burgdorfer(P)
09:15– 09:45 Meissl (R)
09:45–10:05 Dassanayake(S)

10:05 – Coffee Break

10:30–10:50 Aumayr (S)
10:50–11:20 Koshikawa (R)
11:20–11:50 Diaz (R)

11:50 – Lunch (Garden View)

13:00 – 18:30 Conference Excursions

19:30 Dinner (Garden View)
Speaker: J. Wells

Thursday Sept. 30, 2010

7:30 Breakfast

08:30–09:15 Doerner (P)
09:15–09:45 Zeijlmans (R)
09:45–10:15 Oberkofler (R)

10:15 Coffee Break

10:45–11:15 Allain (R)
11:15–11:45 Schwarz-S. (R)
11:45–12:05 Harris (S)
12:05–12:25 Rubel (S)

12:25 – Lunch (Outside garden)

14:30–15:00 Bundaleski (R)
15:00–15:20 Gravielle (S)
15:20–15:40 Winter (S)
15:40–16:00 Tiwald (S)

16:00 – Coffee Break

16:30–16:50 Neufeld (S)
16:50–17:10 Fallet (S)
17:10–17:30 Lake (S)

19:00 Conference Dinner (Ballroom 3)
Speaker: D. Hillis

Friday Oct. 1, 2010

7:30 Breakfast

08:30–09:15 Orlando (P)
09:15–09:35 Barghouty (S)
09:35–10:05 Okada (R)

10:05 – Coffee Break

10:30–10:50 Andersson (S)
10:50–11:20 Kolasinski (R)
11:20–11:50 Gustafson (R)
11:50-12:00 Closing

12:00 – Lunch (Ballroom 2)

Departure